VOL. 5 NO. 2 FEBRUARY 1963

Journal of

ELECTROANALYTICAL CHEMISTRY

International Journal Dealing with all Aspects of Electroanalytical Chemistry, Including Fundamental Electrochemistry

E L S E V I E R

GENERAL INFORMATION

Types of contributions

(a) Original research work not previously published in other periodicals.
(b) Reviews on recent developments in various fields.
(c) Short communications.
(d) Bibliographical notes and book reviews.

Languages

Papers will be published in English, French or German.

Submission of papers

Papers should be sent to one of the following Editors:

Professor J. O'M. Bockris, John Harrison Laboratory of Chemistry, University of Pennsylvania, Philadelphia 4, Pa., U.S.A.
Dr. R. Parsons, Department of Chemistry, The University, Bristol 8, England.
Professor C. N. Reilley, Department of Chemistry, University of North Carolina, Chapel Hill, N.C., U.S.A.

Authors should preferably submit two copies in double-spaced typing on pages of uniform size. Legends for figures should be typed on a separate page. The figures should be in a form suitable for reproduction, drawn in Indian ink on drawing paper or tracing paper, with lettering etc. in thin pencil. The sheets of drawing or tracing paper should preferably be of the same dimensions as those on which the article is typed. Photographs should be submitted as clear black and white prints on glossy paper.
All references should be given at the end of the paper. They should be numbered and the numbers should appear in the text at the appropriate places.
A summary of 50 to 200 words should be included.

Reprints

Twenty-five reprints will be supplied free of charge. Additional reprints can be ordered at quoted prices. They must be ordered on order forms which are sent together with the proofs.

Publication

The *Journal of Electroanalytical Chemistry* appears monthly and has six issues per volume and two volumes per year, each of approx. 500 pages.

Subscription price (post free): £ 10.15.0 or $ 30.00 or Dfl. 108.00 per year; £ 5.7.6 or $ 15.00 or Dfl. 54.00 per volume.
Additional cost for copies by air mail available on request.
For advertising rates apply to the publishers.

Subscriptions

Subscriptions should be sent to:

ELSEVIER PUBLISHING COMPANY, P.O. Box 211, Spuistraat 110-112, Amsterdam-C., The Netherlands.

THE POLAROGRAPHY OF COPPER(II) IN ORTHOPHOSPHATE MEDIUM*

GARY D. CHRISTIAN AND WILLIAM C. PURDY

Department of Chemistry, University of Maryland, College Park, Md. (U.S.A.)

(Received July 12th, 1962)

The polarography of copper(II) has been extensively investigated in a variety of supporting electrolytes[1]. Some recent work in this laboratory has employed orthophosphate as the supporting electrolyte[2]. In particular for our determination of the apparent instability constants of copper complexes orthophosphate buffers were chosen as the supporting electrolytes[3,4,5].

The polarographic method for the determination of the instability constant of a metal complex is based upon the measurement of the shift of the half-wave potential of the metal ion with the addition of the complexing agent. The equation employed for the determination of the apparent instability constant, K_c, of the complex metal ion at 25° is:

$$(E_{\frac{1}{2}})_c - (E_{\frac{1}{2}})_s \sim \frac{0.0591}{n} \log K_c - \frac{0.0591}{n} p \log C_x \qquad (1)$$

where $(E_{\frac{1}{2}})_c$ is the half-wave potential for the complex metal ion at concentration, C_x, of complexing agent, $(E_{\frac{1}{2}})_s$ is the half-wave potential of the simple metal ion, n is the number of faradays of electricity required per mole of electrode reaction, and p is the number of moles of complexing agent reacting with one mole of the metal ion[6]. In order to employ eqn. (1) it is necessary to know $(E_{\frac{1}{2}})_s$ and n. The value of p can be determined from the following equation:

$$\frac{\Delta (E_{\frac{1}{2}})_c}{\Delta \log C_x} = \frac{-0.0591}{n} p \qquad (2)$$

$(E_{\frac{1}{2}})_s$ and n are obtained from a polarogram of the simple metal ion in the supporting electrolyte chosen for the investigation.

Several investigators have used orthophosphate buffers as the supporting electrolytes in their studies of copper complexes. LAITINEN *et al.*[7], studying copper–glycine complexes, reported a two-electron reduction for copper in a buffer consisting of 0.05 *M* monopotassium phosphate plus sodium hydroxide. On the other hand, MALIK AND KHAN[8] in their polarographic study of copper–biuret complexes in phosphate medium found a one-electron transfer for copper over the pH range of 10.97–12.04.

In the present paper the current–voltage curves for copper(II) in orthophosphate

* This paper was presented in part at the 140th National Meeting of the American Chemical Society, September 3 through 8, 1961, Chicago, Ill., U.S.A.

medium, obtained over a pH range of 2.6–10.1, are presented. Polarographic results are compared with those obtained by constant potential coulometry, hanging-drop studies and wave-height measurements.

EXPERIMENTAL

Reagent chemicals were used without further purification. All studies were conducted in buffer solutions of an ionic strength of 0.2 *M*. The composition of the buffers employed has been described elsewhere[2].

All polarographic measurements were made with a Leeds and Northrup Electro-Chemograph, Type E. A Lingane H-cell fitted with a saturated calomel reference electrode and a 3% agar-saturated potassium chloride salt bridge was employed. The solution of copper(II) in the supporting electrolyte was placed in the sample compartment of the H-cell and flushed with nitrogen gas for 15 min prior to the running of the polarogram. During the course of the polarographic measurements a nitrogen atmosphere was maintained above the sample solution. The nitrogen gas employed was deoxygenated by passage through two solutions of chromous sulfate and one of the supporting electrolyte before entrance into the H-cell. All polarograms were obtained on a sample thermostatted at 25 $\pm$ 0.2°.

Reversibility of the electrode reactions was tested by determining the slopes of the log $(i_d - i)/i$ *vs.* E plots. Values for the half-wave potentials were taken from these logarithmic plots. Data for these plots were taken by manual operation of the polarograph. Applied voltages were determined by measurement with a Rubicon Model 2730 Potentiometer.

The controlled potential for the coulometric analyses was supplied by a Greenough-Williams-Taylor Potentiostat[9]. Coulombs were measured with a titration coulometer[10]. A known amount of copper(II) was electrolyzed for 15 minutes in a cell consisting of a mercury-pool cathode and a saturated calomel anode. After electrolysis the copper remaining in solution was determined iodometrically.

The electrode for the hanging-drop studies was prepared according to the directions of ROSS, DEMARS, AND SHAIN[11]. Copper(II) was reduced at the hanging-drop electrode by the five minute application of a potential 100 mV more negative than the polarographic half-wave potential. The potential was then scanned in the positive direction and the anodic stripping curves were plotted on the Electro-Chemograph.

DISCUSSION OF RESULTS

In Fig. 1 are shown the polarograms for the reduction of copper(II) in orthophosphate medium. The polarographic data for these waves are collected in Table I. These data indicate a shift in the half-wave potential to more negative values with an increase in the pH of the supporting electrolyte. The polarographic half-wave potentials were compared with the peak potentials obtained by studying the reduction at the hanging mercury drop electrode. These data are tabulated in Table II. At pH values greater than 6.5, the peak potentials of both the hanging mercury drop electrode (HMDE) and the anodic stripping curves were found to become more negative at a greater rate than the half-wave potential for the dropping mercury electrode (DME).

The number of electrons involved in the reduction of copper(II) in orthophosphate medium was determined by constant potential coulometry and wave-height measure-

TABLE I

POLAROGRAPHIC DATA FOR COPPER(II) AT 25°. SUPPORTING ELECTROLYTE, 0.2 *M* ORTHOPHOSPHATE BUFFER

pH	$m^{2/3}t^{1/6}$ ($mg^{2/3}sec^{-1/2}$)	$E_{1/2}$ (*vs.S.C.E.*)	*Conc. Cu(II)* (*mM*)	i_d (*μA*)	$i_d/Cm^{2/3}t^{1/6}$
2.60	2.18	−0.138	0.100	0.620	2.84
3.48	2.20	−0.136	0.100	0.720	3.27
4.60	2.20	−0.144	0.100	0.720	3.27
5.40	2.20	−0.158	0.100	0.760	3.46
6.50	2.20	−0.177	0.100	0.360	1.64
7.40	2.20	−0.178	0.100	0.360	1.64
8.00	2.20	−0.197	0.100	0.340	1.55
9.00	2.20	−0.198	0.200	0.480	2.18
10.00	2.22	−0.206	0.200	0.560	2.52

TABLE II

COMPARISON OF DATA OBTAINED BY POLAROGRAPHIC, HANGING-DROP, AND COULOMETRIC STUDIES. SUPPORTING ELECTROLYTE, 0.2 *M* ORTHOPHOSPHATE BUFFER

pH	$E_{1/2}$ *DME*	*Slope*	E_p *HMDE*	E_p *Strip*	*n(Coulometric)*	*Wave height DME (mm)*	*Conc. Cu(II) (Conc. M)*
2.60	−0.138	0.0344	−0.155	−0.128	2.52	15.5	$1\cdot10^{-4}$
3.48	−0.136	0.0381	−0.162	−0.120	2.32	18.0	$1\cdot10^{-4}$
4.60	−0.144	0.0367	−0.173	−0.128	2.02	18.0	$1\cdot10^{-4}$
5.40	−0.158	0.0431	−0.185	−0.142	—	19.0	$1\cdot10^{-4}$
6.50	−0.177	0.0622	−0.210	−0.162	1.01	9.0	$1\cdot10^{-4}$
7.50	−0.178	0.0597	−0.240	−0.183	—	9.0	$1\cdot10^{-4}$
8.00	−0.197	0.0597	−0.252	−0.190	—	8.5	$1\cdot10^{-4}$
9.00	−0.198	0.0748	−0.275	−0.212	—	12.	$2\cdot10^{-4}$
10.00	−0.206	0.0509	−0.311	−0.260	—	14.	$2\cdot10^{-4}$

TABLE III

WAVE-HEIGHT COMPARISONS IN ORTHOPHOSPHATE BUFFERS. ALL SOLUTIONS MEASURED WERE 10^{-4} *M* IN THE METAL ION

pH	*Metal ion*	*Wave-height (mm)*	*Sensitivity (μA/mm)*
3.0	Cadmium	29	0.020
3.0	Copper(II)	30	0.020
7.4	Cadmium	64	0.010
7.4	Cobalt(II)	63	0.010
7.4	Iron(II)	55	0.010
7.4	Manganese(II)	57	0.010
7.4	Zinc	54	0.010
7.4	Copper(II)	26	0.010

ments. Coulometric studies indicated that at pH values less than 6 a two-electron reduction took place; at pH values greater than 6 copper(II) underwent a one-electron reduction. These coulometric results were supported by wave-height measurements for copper(II) and for several other divalent cations (see Table III). Coulometric studies could not be carried out in solutions more basic than pH 8.0 due to the appear-

ance of a copper precipitate. This would suggest that in the basic pH region the depolarization of the dropping mercury electrode was caused by a reducible copper phosphate suspension. MICKA[12] has shown that suspensions of HgS, PbS, CuS and Ag_2O yield polarographic curves.

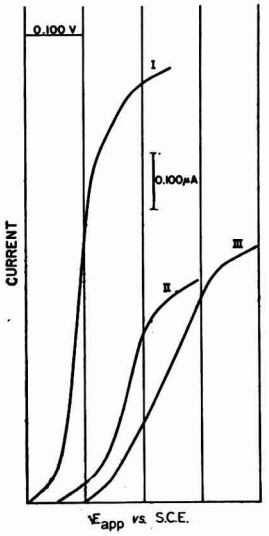

Fig. 1. Polarograms for the reduction of copper(II) in orthophosphate medium. All polarograms begin at a potential of −0.050 V. *vs.* S.C.E.: curve I, pH 4.60, 10^{-4} *M* Cu(II); curve II, pH 7.40, 10^{-4} *M* Cu(II); curve III, pH 9.00, $2 \cdot 10^{-4}$ *M* Cu(II).

The slopes of the log $(i_d - i)/i$ *vs.* E plots for copper(II) in various orthophosphate buffers indicated that the reduction of copper is reversible only over the narrow pH range of 6.5–8.0. At pH values on either side of this range the value of the slope was significantly different from the reversible value.

These data suggest that as the concentration of the HPO_4^{2-} species increased (pH > 6), the copper(I) formed by the electrode reduction was stabilized by formation of a HPO_4^{2-} complex so stable or so insoluble that its further reduction was not readily observed. The fact that hanging-drop and anodic stripping results start deviating at pH 7 from those obtained at the dropping mercury electrode leads one to believe that either kinetics are involved or else that there is actual solid formation. The coulometric runs at pH values greater than 8.0 seem to suggest the latter.

SUMMARY

The polarographic reduction of copper(II) in orthophosphate medium yields a single wave. In solutions more acidic than pH 6 the wave represents a two-electron reduction. At pH values greater than 6 the wave corresponds to a one-electron reduction. These results were obtained by coulometric and wave-height measurements. The reduction of copper(II) is reversible only over the narrow pH range of 6.5–8.0. These data suggest the formation of a highly stable insoluble copper(I)–HPO_4^{2-} complex in solutions more basic than pH 6.

REFERENCES

1 I. M. KOLTHOFF AND J. J. LINGANE, *Polarography*, 2nd ed., Vol. II, Interscience Publishers, Inc., New York, 1952, p. 493.
2 G. D. CHRISTIAN AND W. C. PURDY, *J. Electroanal. Chem.*, 3 (1962) 363.
3 E. C. KNOBLOCK AND W. C. PURDY, *Radiation Res.*, 15 (1961) 94.
4 E. C. KNOBLOCK AND W. C. PURDY, *J. Electroanal. Chem.*, 2 (1961) 493.
5 G. D. CHRISTIAN AND W. C. PURDY, *Biochim. Biophys. Acta*, 54 (1961) 587.
6 I. M. KOLTHOFF AND J. J. LINGANE, *Polarography*, 2nd ed., Vol. I, Interscience Publishers, Inc., New York, 1952, p. 214.
7 H. A. LAITINEN, E. I. ONSTOTT, J. C. BAILAR, JR. AND S. SWANN, JR., *J. Am. Chem. Soc.*, 71 (1949) 1550.
8 W. U. MALIK AND A. A. KHAN, *Naturwiss.*, 46 (1959) 378.
9 M. L. GREENOUGH, W. E. WILLIAMS, JR. AND J. K. TAYLOR, *Rev. Sci. Instr.*, 22 (1951) 484.
10 J. J. LINGANE AND L. A. SMALL, *Anal. Chem.*, 21 (1949) 1119.
11 J. W. ROSS, R. C. DEMARS AND I. SHAIN, *Anal. Chem.*, 28 (1956) 1768.
12 K. MICKA, *Collection Czech. Chem. Commun.*, 21 (1956) 647.

ELECTROCHEMICAL CHARACTERISTICS OF MANGANESE IN CYANIDE SOLUTIONS

I. POLAROGRAPHY OF MANGANESE(I), (II), and (III)

STEPHEN A. MOROS*† AND LOUIS MEITES

Department of Chemistry, Polytechnic Institute of Brooklyn, Brooklyn, N.Y. (U.S.A.)

(Received June 26th, 1962)

The polarographic reduction of manganese(II) in cyanide media was first studied by VERDIER[1], who reported its half-wave potential to be -1.33 V *vs.* S.C.E. in 1.5 *F* sodium cyanide and stated that the half-reaction involved was a reversible two-electron reduction to the metal. As this value is about 0.1 V more *positive* than the standard potential of the manganese(II)–manganese(0) couple[2], it appeared more probable that the reduction actually proceeds only to the $+1$ state, whose existence in cyanide media was demonstrated by TREADWELL AND RATHS[3]. Indeed, shortly after this investigation was begun, SIEKIERSKI AND SIEKIERSKA[4] asserted that this was in fact the case. The work described below confirms this conclusion, identifies and characterizes a new hydroxocyano complex of manganese(II) formed in alkaline cyanide solutions, shows that the polarographic characteristics of manganese(I) and (II) in cyanide media are largely affected by a chemical decomposition of manganese(I) cyanide solutions at a rate proportional to the square root of the manganese(I) concentration, and briefly describes the polarographic behavior of manganese(III) in these media.

EXPERIMENTAL

Polarograms were obtained with a locally constructed and carefully calibrated pen-and-ink recording instrument. Due attention was paid to the application of the various corrections appropriate in precise work. A conventional dropping-electrode assembly was used. All values of m and t were obtained under the conditions employed for the related diffusion-current measurements.

A modified H-cell[5] was used in most of the work with manganese(II) and (III) solutions. The potential of its saturated calomel electrode was checked frequently, and the electrode and agar-saturated potassium chloride bridge were replaced whenever necessary. For work with manganese(I), which is extremely readily air-oxidized, a double-diaphragm controlled-potential electrolysis cell[6] was modified by sealing a vertical 10-mm i.d. tube to the horizontal cross-member between the body

* This paper is based on a thesis submitted by STEPHEN A. MOROS to the Faculty of the Polytechnic Institute of Brooklyn in partial fulfillment of the requirements for the Ph. D. degree, June, 1961.
† Present address: Research Department, American Cyanamid Company, Bound Brook, N.J.

of the working-electrode compartment and the fritted disc leading to the central compartment. After a solution of manganese(I) had been prepared in this cell by the controlled-potential electroreduction of manganese(II), the insertion of a dropping electrode into this tube permitted polarograms to be recorded while minimizing the danger of air-oxidation. A silver–silver chloride electrode of the type previously described[7] was used in obtaining such polarograms and in all controlled-potential electrolyses. This electrode was prepared with sodium chloride because difficulties would have been caused by the precipitation of $K_5Mn(CN)_6$[3] had potassium chloride been used. Numerous measurements showed that the potential of the electrode Ag/AgCl (satd.), NaCl (satd.) is -0.047 ± 0.003 V *vs.* S.C.E. at $25 \pm 1°$. When due care was taken to change the saturated sodium chloride solution in the bridge compartment of this electrode frequently, its potential remained constant for many months despite its exposure to concentrated cyanide solutions.

All potentials are referred to the customary saturated calomel electrode.

The potentiostat and current integrator were obtained from Analytical Instruments, Inc. (Wolcott, Conn.). Because very small currents often had to be integrated with the highest possible accuracy, another input resistance network was added to the integrator and was carefully trimmed to give a sensitivity of 0.01000 microfaraday (μF) per count, which is one-tenth of the lowest sensitivity figure of the instrument as received from the manufacturer. Whenever necessary, corrections were applied for the change of sensitivity at very low counting rates[6].

All electrolyses and all electrometric measurements were carried out at $25.00 \pm 0.02°$. Deaeration was effected with pre-purified nitrogen which had been freed from oxygen, either by passage through one or more efficient gas-washing bottles containing chromous chloride solution or [in work with manganese(I)] by passage over copper gauze at 450°; it was then pre-saturated with water vapor and equilibrated with respect to hydrogen cyanide by passage through a gas-washing bottle immersed in the thermostat, containing a portion of the supporting electrolyte being used.

The procedure for the purification of mercury in this work has been described elsewhere[7]. All other chemicals were ordinary reagent grade and were not further purified, except where pre-electrolyses at controlled potential are mentioned below. Stock solutions of manganese(II) sulfate were standardized by the method of LINGANE AND KARPLUS[8]. Sodium cyanide was assayed by potentiometric titration with standard silver nitrate, using a silver indicator electrode, and the result was employed in preparing the sodium cyanide solutions used as supporting electrolytes.

A few polarograms were obtained with solutions prepared from water purified by passage through a commercial mixed-bed-ion-exchange unit. However, the chronoamperometric measurements to be described in the following paper, showed that the use of this water led to large and apparently random fluctuations in the measured rates of decomposition of manganese(I) cyanide solutions, presumably because of the presence of traces of acidic or basic materials derived from the resins. Distilled water alone was used, after this source of difficulty was identified.

All pH measurements were made with a Beckman Model G pH meter and Type 1190–72 glass electrodes. These were standardized against saturated potassium hydrogen tartrate[9,10,11] and the alkaline phosphate buffer of BATES AND BOWER[12].

Weights and volumetric apparatus were calibrated by standard techniques.

DATA AND DISCUSSION

Manganese(II) in neutral cyanide solutions*

The addition of a neutral manganese(II) solution to a neutral sodium cyanide solution in the absence of air yields a clear light green solution whose polarogram consists of a single well-defined wave for which $E_{\frac{1}{2}}$ is about -1.3 V. Solutions containing 0.500 mmole of manganese(II) in 100 ml of 1 F sodium cyanide were electrolyzed with a mercury cathode at -1.00 V to reduce any trace of manganese(III) that might have been formed by air-oxidation (*cf.* Fig. 5), then at -1.50 V to produce the reduced species resulting from the electroreduction of manganese(II). The latter electrolysis was terminated as soon as the current had decreased to a small and essentially constant value; the solution then had the characteristic deep yellow color of the manganese(I)–cyanide complex[3], and the mean of the n-values obtained in three experiments was 1.09 ± 0.02. This is conclusive proof that the reduction proceeds to the $+1$ state rather than to the metal.

Separate experiments in which solutions of manganese(II) in 1 F sodium perchlorate were electroreduced to the metal at mercury cathodes, resulted in the formation of a gray turbidity very soon after the beginning of the electrolysis. This reflects the limited solubility of manganese in mercury[13,14]. As no such precipitate was formed during the reduction of manganese(II) in cyanide medium, the discrepancy between the observed n-value of 1.09 and the expected value of 1.00 could not have been due to a partial reduction to the metallic state. Its causes are discussed in detail in a following paper.

Plots of $E_{\text{d.e.}}$ *vs.* $\log i/(i_d - i)$ for this wave had slopes of -58 ± 1 mV over the range $0.04 \leqslant i/i_d \leqslant 0.96$. This is in good agreement with the expected value for a reversible one-electron reduction at 25°. Further proof of the reversibility of the half-reaction is given below.

The half-wave potential becomes more positive as the cyanide concentration increases: it is -1.41 V in 0.3 F, -1.364 ± 0.007 V in 1 F, and -1.25 V in 9 F sodium cyanide. Since $n = 1$, the reversible half-wave potential is given by

$$E_{1/2} = E^0 - 0.0296 \log (D_2/D_1) - 0.0591 \log (f_1/f_2) \qquad (1)$$

where E^0 is the standard potential of the couple, D is a diffusion coefficient, and f is an activity coefficient; the subscript numbers give the oxidation states of the manganese. This may be combined with the extended Debye–Hückel equation in the commonly encountered form

$$-\log f_i = 0.51\, z_i^2 L - B_i \mu \qquad (2)$$

where $L = \mu^{1/2}/(1 + \mu^{1/2})$ and B_i is the salting-out constant. Assuming that B_1 and B_2 are equal and that the ratio D_2/D_1 is not sensibly affected by variations of the ionic strength μ, the result is

$$\Delta E_{1/2}/\Delta L = +0.030 (z_1^2 - z_2^2) \qquad (3)$$

If it is further assumed that the half-reaction is $Mn(CN)_6^{4-} + e = Mn(CN)_6^{5-}$, then the expected slope of a plot of $E_{1/2}$ *vs.* L is $+0.27$. The data are shown in Fig. 1, where the dashed line is drawn with this slope. Except at the highest concentration

* In the sense that no foreign acid or base was added.

of sodium cyanide, where the liquid-junction potential is surely appreciable and is of the proper sign to account for the deviation observed, the agreement is entirely satisfactory.

Extrapolating the plot of Fig. 1 to zero ionic strength ($L=0$) and taking D_2 and D_1

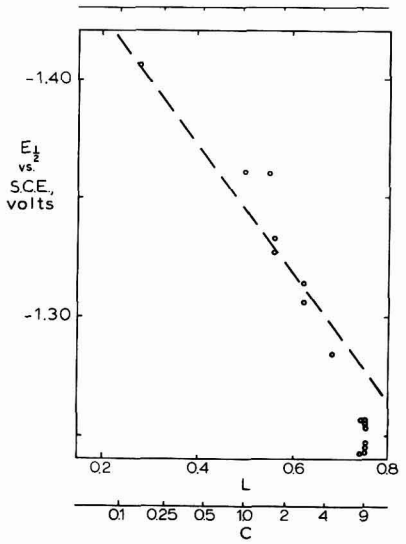

Fig. 1. Effect of sodium cyanide concentration on the half-wave potential of manganese(II). The horizontal axis gives values of both C, the concentration of sodium cyanide in moles/liter, and the parameter L defined in the text.

as equal (the diffusion-current data cited below indicate that the difference between them is at most a few per cent), E° of the manganese(II)–manganese(I) couple in cyanide media is found to be -1.50 V *vs.* S.C.E., or -1.25 V *vs.* N.H.E. TREADWELL AND RATHS[3] reported that the formal potential in 1.5 F sodium cyanide was -1.30 V *vs.* S.C.E.; this is about 30 mV more positive than the value interpolated in Fig. 1. The discrepancy is attributable to the reduction of water or hydrogen cyanide by manganese(I) at the surface of the platinum indicator electrode employed by TREADWELL AND RATHS[3], who indeed noted that the electrode potential became more negative on increasing the stirring rate.

In 1 F sodium cyanide the half-wave potential was not detectably affected by varying the manganese(II) concentration from 0.8–10 mF.

Data to be presented below show that the wave for the reduction of manganese(II) is partially catalytic in character: a slow chemical oxidation of manganese(I) by water or, more probably, hydrogen cyanide is followed by the re-reduction of some of the manganese(II) thus regenerated. The diffusion current constant of such a wave would be expected to vary somewhat with the characteristics of the capillary employed. Data obtained with 1.00 mF manganese(II) solutions, using a capillary for which $m^{2/3}t^{1/6}$ was 1.69 $mg^{2/3}$ $sec^{-1/2}$ at -1.6 V, gave $I(= i_d/Cm^{2/3}t^{1/6}) = 1.65 \pm 0.05$; another capillary, for which $m^{2/3}t^{1/6}$ was 1.88 $mg^{2/3}$ $sec^{-1/2}$ at -1.6 V, gave $I = 1.48 \pm 0.02$ with the same concentration of manganese(II). If the rate of

oxidation of manganese(I) were proportional to its concentration, the value of I would be expected to be independent of the concentration of manganese(II). However, with 9.80 mF manganese(II) the value of I obtained with the first of the above capillaries was only 1.54 $\pm$ 0.04. This suggests that the catalytic step is fractional order with respect to manganese (I). Confirmation of this suggestion is presented below.

Manganese(II) in alkaline cyanide solutions

SIEKIERSKI AND SIEKIERSKA[4] investigated the hydrolysis of $K_4Mn(CN)_6$ in 0.1 F sodium cyanide, and observed waves at -1.10, -1.25, and -1.59 V in addition to the one at about -1.3 V whose characteristics were described above. These additional

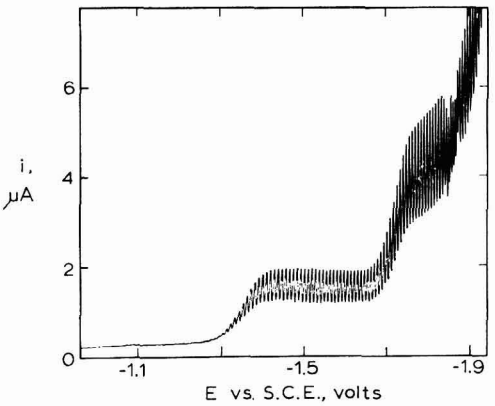

Fig. 2. Polarogram of 0.88 mF manganese(II) in 0.88 F sodium cyanide–0.28 F sodium hydroxide.

waves were ascribed to the formation of various aquocyano complexes of manganese (II).

The addition of sodium hydroxide to 1 F sodium cyanide containing manganese(II) causes a new wave to appear at $E_{1/2} = -1.72$ V; increasing the hydroxide concentration causes the height of this wave to increase while that of the original wave at -1.36 V decreases. A typical polarogram of manganese(II) in alkaline cyanide is shown in Fig. 2. VERDIER[1] observed a wave at -1.80 V in alkaline cyanide solutions of manganese(II) and surmised that it corresponded to the reduction of a hydroxocyano complex. He represented this by the formula Mn(OH)(CN), but gave neither any proof of this improbable formula nor any quantitative information concerning the stability of the complex.

Assuming that the addition of hydroxide brings about the reaction

$$Mn(CN)_6^{4-} + p\,OH^- = Mn(CN)_{6-p}(OH)_p^{4-} + p\,CN^- \qquad (4)$$

and that the diffusion current of the second wave, i_2, is proportional to the concentration of the hydroxocyano complex — *i.e.*, that the equilibrium of reaction (4) is slow — (a similar assumption cannot be justified for the first wave because of its partially catalytic character) and letting $C_1 = [Mn(CN)_6^{4-}]$, $C_2 = [Mn(CN)_{6-p}(OH)_p^{4-}]$,

$C = C_1 + C_2$, and $k_2 = i_2/C_2$, the equilibrium constant of reaction (4) can be written

$$K = \frac{C_2}{C_1}\left(\frac{[CN^-]}{[OH^-]}\right)^p = \frac{i_2/k_2}{C - (i_2/k_2)}\left(\frac{[CN^-]}{[OH^-]}\right)^p$$

or

$$\frac{C}{i_2} = \frac{1}{k_2} + \frac{1}{k_2 K}\left(\frac{[CN^-]}{[OH^-]}\right)^p \qquad (5)$$

A plot of C/i_2 *vs.* $[CN^-]/[OH^-]$ was constructed for data obtained with solutions containing approximately 0.9 M cyanide, 0.9 mF manganese(II), and 0.09–0.25 M hydroxide, and was found to be accurately linear, showing that $p = 1$. From the slope and intercept of this plot, the values $k_2 = 7 \pm 1$ and $K = 2.1 \pm 0.4$ were deduced. The value of k_2 is roughly 2.5 times the average value of the ratio i_1/C_1 calculated from the same data. This indicates that the reduction of the hydroxocyano complex involves two electrons. The slope of a plot of $E_{d.e.}$ *vs.* $\log i/(i_d - i)$ for the wave of the hydroxocyano complex is −34.4 mV, an entirely reasonable value for an irreversible two-electron wave.

It is interesting that the half-wave potential of the hydroxocyano complex should be nearly identical with that (−1.70 V) given by ZUMAN[15] for the reduction of manganese(II) from sodium hydroxide alone. It appears that the rate-determining step in each case may be the addition of a pair of electrons through a hydroxyl group serving as a bridge between the manganese atom and the electrode surface, and that the activation energy for this step is essentially independent of the composition of the remainder of the coordination field of the manganese atom.

Calculating the concentration of the cyano complex present at equilibrium, with the aid of the above value of K for reaction (4), shows that the ratio, i_1/C_1, of wave height to concentration for the cyano complex *decreases* as the hydroxyl-ion concentration increases. With 0.3 M added hydroxide, this ratio is almost 20% smaller than in a neutral cyanide solution. If the only factor operative were the previously mentioned variation of the diffusion current constant of the cyano complex with its concentration, the calculated values of i_1/C_1 should *increase* as the equilibrium concentration of the cyano complex is decreased by the addition of hydroxide. These facts can mean only that the rate of the chemical regeneration of manganese(II) decreases with decreasing concentration of hydrogen cyanide, and thus that the reaction responsible for this regeneration is one in which manganese(I) is oxidized by hydrogen cyanide rather than by water.

Although the height of the wave of the hydroxocyano complex is greater than that of the cyano complex in a solution containing 0.2 M hydroxyl ion and 0.88 M cyanide, no wave at all is observed for the hydroxocyano complex in a solution containing 1 M hydroxide and 4 M cyanide. Very probably the predominating forms of manganese(II) in 0.9 and 4 M cyanide solutions are not the same. It is suggested that the reaction occurring when hydroxide is added to 0.9 F sodium cyanide containing manganese(II) is actually

$$Mn(H_2O)(CN)_5^{3-} + OH^- = Mn(OH)(CN)_5^{4-} + H_2O;\ K = 2.3 \pm 0.4$$

which is consistent with the data described above, but that $Mn(CN)_6^{4-}$ predominates in 4 F sodium cyanide and is relatively inert toward hydroxyl ion. This interpretation cannot be excluded by the data of Fig. 1, and the stepwise formation constants of

the manganese(II)–cyanide complexes, which would serve to settle the question, have not been measured.

The addition of acid to neutral cyanide solutions of manganese(II) appeared to result in a shift of the half-wave potential toward less negative values and in an increase of the diffusion current constant. The latter would, of course, be expected from the partly catalytic nature of the wave, but the decomposition of the cyanide occurred so rapidly and distorted the polarograms so badly that useful data were impossible to obtain.

Manganese(I)

The fact that manganese(I) is chemically reoxidized at an appreciable rate in aqueous cyanide solutions makes its quantitative preparation impossible, and data on its behavior have therefore had to be obtained with solutions containing some manganese(II) as well. These were prepared by subjecting solutions of manganese(II) in freshly prepared neutral 1 F sodium cyanide to controlled-potential electrolysis at -1.50 V until a steady final current was reached, and recording polarograms as rapidly as possible thereafter.

The polarogram of a cyanide solution containing manganese(I) and (II) consists of a composite anodic-cathodic wave whose half-wave potential (-1.36_4 V in 1 F sodium cyanide) and slope [$\Delta E_{d.e.}/\Delta \log i/(i_d - i) = -58$ mV] are identical with those of the cathodic wave obtained with manganese(II) alone. Together with the proof below that the anodic portion of the composite wave does represent the oxidation of manganese(I) to manganese(II), this constitutes definitive proof of the polarographic reversibility of the half-reaction.

The diffusion current constant of manganese(I) was estimated from the recorded polarograms as shown by the following example. The diffusion current, measured at -1.50 V, of 1.33 mF manganese(II) in 1 F sodium cyanide was 3.34 μA; after controlled-potential electroreduction to the steady state the cathodic diffusion current of the composite wave was 0.23 μA. The ratio of these values would indicate that the concentration of unreduced manganese(II) was 0.09 mF; this is fairly uncertain because, as was shown above, the diffusion current of manganese(II) under these conditions is not proportional to its concentration. Neglecting this error on the ground that the manganese(II) concentration is only a small fraction of the whole, one calculates the manganese(I) concentration to be $1.33 - 0.09 = 1.24$ mF. The anodic diffusion current of manganese(I) was -3.52 μA, and $m^{2/3}t^{1/6}$] was 1.71 $mg^{2/3}\,sec^{-1/2}$, both at -1.00 V, and therefore $I = -1.66$. Similar experiments with manganese(I) concentrations ranging from 1–9 mF gave, in mean, $I = 1.6_4 \pm 0.1_6$. The mean deviation is perhaps not unreasonably large in view of the experimental and chemical complexities involved.

When a solution of manganese(I) prepared as described above is allowed to stand, the anodic diffusion current of manganese(I) decreases, and the cathodic diffusion current of manganese(II) increases, even though extreme precautions are taken to exclude atmospheric oxygen. The rate of this process, which is responsible for the partly catalytic nature of the manganese(II) wave, was investigated by measuring the cathodic and anodic diffusion currents at various intervals. The concentrations of manganese(II) and (I) were calculated from these currents by using the concentration–diffusion current ratios obtained with the same solution during the same

experiment. To minimize errors due to the variation of i_d/C for the cathodic wave as the manganese(II) concentration changed, only a very narrow range of manganese (II) concentrations was covered in each experiment.

The *a priori* possibility that the decomposition of manganese(I) consists of a disproportionation into manganese(II) and manganese(0) is excluded by the fact that the sum of the manganese(I) and (II) concentrations always remained constant within experimental error, as the decomposition proceeded. Thus $d[Mn(II)]/dt = -d[Mn(I)]/dt$, whereas the disproportionation hypothesis would require $d[Mn(II)]/dt = -\frac{1}{2}d[Mn(I)]/dt$. Moreover, despite the fact that even very small amounts of metallic manganese could be detected visually during the electroreduction of manganese(II) in perchlorate solutions, cyanide solutions of manganese(I) always remained perfectly clear even after extensive decomposition.

Typical kinetic plots are shown in Fig. 3. To prevent overlapping, the data are taken from different experiments involving slightly different concentrations of

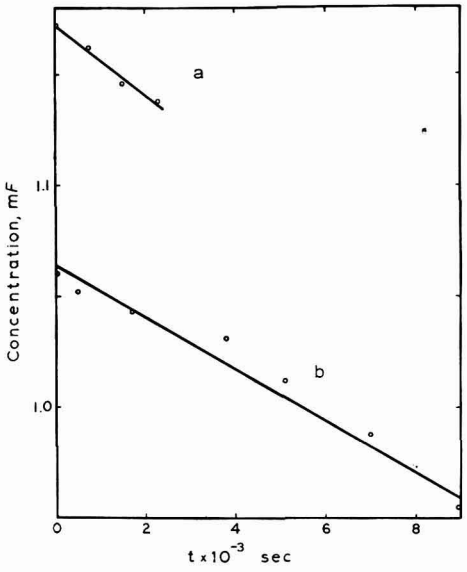

Fig. 3. Decomposition of air-free solutions of manganese(I) in neutral 1 *F* sodium cyanide. The ordinate is the square root of the concentration of manganese(I) remaining, calculated (a) from the cathodic diffusion current of manganese(II) and the known total concentration of manganese, or (b) from the anodic diffusion current of manganese(I).

manganese(I). Curve a is a plot of $(C - [Mn(II)])^{1/2}$ *vs.* time, where C is the total concentration of manganese and [Mn(II)] is calculated from the cathodic diffusion current; curve b is a plot of $[Mn(I)]^{1/2}$ *vs.* time, where [Mn(I)] is calculated from the anodic diffusion current. Each of the experiments shown here covered so narrow a range of concentrations that the data could have been fitted about equally well by pseudo-first-order plots; but the results of similar experiments with different manganese(I) concentrations, the spectrophotometric data described below, and the

amperometric data to be described in a following paper show conclusively that the rate law actually has the form

$$d[Mn(II)]/dt = k\,[Mn(I)]^{1/2} \qquad (6)$$

which is also in accord with the previously mentioned effect of manganese (II) concentration on its diffusion current constant. The cathodic and anodic diffusion current data give $k = 3.1 \cdot 10^{-5}$ and $2.4 \cdot 10^{-5}$ mmole$^{1/2}$ l$^{-1/2}$ sec^{-1}, respectively, in neutral 1 F sodium cyanide.

The decomposition of a manganese(I)-cyanide solution is evinced by a fading of its intense yellow color. A solution of manganese(II) in 1 F sodium cyanide was placed in a small quartz tube stoppered with a rubber serum-bottle cap, and sodium amalgam was added by means of a hypodermic syringe. The color intensity appeared to become constant after about 1 h of occasional shaking, and a portion of the solution was then transferred by means of a syringe to a similarly stoppered 1-cm quartz spectrophotometric cell containing some thoroughly deaerated 1 F sodium cyanide. The absorption spectrum of the resulting solution, obtained with a Cary Model 11 recording spectrophotometer, consisted of a single broad band in the 350–700 mμ region. The absorption peak was at 365 mμ (independent of manganese concentration above 0.04 mF), and the molar absorptivity at this wavelength is approximately $2 \cdot 10^4$ l mole^{-1} cm^{-1}. On standing, the spectrum changes as shown in Fig. 4; not only does the transmittance at the wavelength of maximum absorption

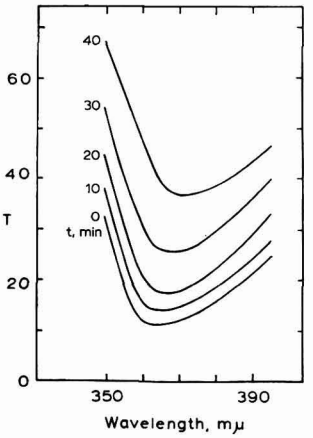

Fig. 4. Absorption spectra of manganese(I) after standing in air-free 1 F sodium cyanide for the numbers of min indicated beside the curves. The initial concentration of manganese(I) was approximately 0.04 mF.

increase as the decomposition proceeds, but the peak also shifts towards longer wavelengths. As manganese(II) shows no detectable absorption in this region, this can only reflect a change in the distribution of manganese(I) between two (or more) absorbing species as its total concentration changes.

Assuming that the peak absorbance is proportional to the total concentration of manganese(I) (which, however, cannot be exactly true), that the reduction by sodium amalgam was essentially complete, and that only an insignificant fraction of the

manganese(I) was air-oxidized during the transfer to the spectrophotometric cell, the data lead to the value $k = 5 \cdot 10^{-5}$ mmole$^{1/2}$ l$^{-1/2}$ sec^{-1} for the rate constant of eqn. (6) at an average manganese(I) concentration of 0.03 mF. This is in acceptable agreement with both the polarographic value given above and the amperometric one to be given in the following paper. On the other hand, the corresponding pseudo-first-order rate constant would have been nearly 12 times as large as that calculated from the polarographic data.

Attempts to determine the value of n for the anodic wave of manganese(I) by coulometry at controlled potential, were undertaken in the realization that they could not provide an accurate and precise value, both because quantitative reduction of the manganese to the +1 state cannot be secured and because some of the manganese (I) would be oxidized chemically while the rest of it was being oxidized electrolytically. A few trials gave, in mean, $n = -0.9$. This is clearly inconsistent with any integral value except −1, and polarograms of the oxidized solutions showed only the characteristic wave of the cyano complex of manganese(II). There is no doubt that the oxidation of manganese(I) at a mercury electrode in a cyanide solution does actually proceed to the +2 state.

Manganese(III)

The instability of cyanide solutions of manganese(I), the ease of air-oxidation of cyanide solutions of manganese(II), and the partly catalytic nature of the manganese-(II) wave all prompted an investigation of the behaviour of manganese(III) in cyanide solutions, in the belief that this might afford a better route to the practical polarographic determination of manganese. For this purpose, cyanide solutions of manganese(II) were oxidized by passing air or oxygen into them for 10–50 min through coarse-porosity sintered-glass gas-dispersion cylinders. This was done in the absence of any metallic mercury, which would also have been air-oxidized if present. The solution was then deaerated and subjected to polarographic or coulometric investigation.

Figure 5 is a typical polarogram of a solution thus prepared. It consists of two waves of approximately equal heights. The first rises from zero applied e.m.f. and

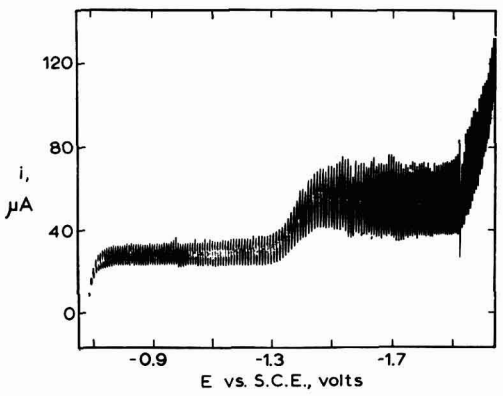

Fig. 5. Polarogram of manganese(III) in neutral 1 F sodium cyanide. A 9.8 mF solution of manganese(II) was treated with oxygen for 30 min prior to deaeration and recording of the polarogram.

represents a 1-electron reduction to the +2 state; the second has a half-wave potential identical with that of the wave for the cyano complex of manganese(II), and represents a further reduction to the +1 state.

The completeness of oxidation by the above treatment was determined by measuring the quantity of electricity consumed in reducing the manganese(III) back to the +2 state in a controlled-potential electrolysis at −1.00 V. The results showed that the oxidation could be considered stoichiometric only to a very rough approximation. With relatively low concentrations of both manganese and cyanide (1–5 mF manganese in 1–1.5 F sodium cyanide), n was found to be 1.06 ± 0.01. This must reflect the formation of some more highly oxidized species, either manganese(IV) or a peroxo-bridged binuclear manganese(III) complex. However, n decreases with increasing concentration of either manganese or cyanide. With 10–25 mF manganese in 1.5 F sodium cyanide, n was 0.965 ± 0.005; with 0.7 mF manganese in 9 F sodium cyanide, n was 0.98; and with 10 mF manganese in 9 F sodium cyanide, n was only 0.70. Appreciable amounts of manganese(II) remain unoxidized under these conditions despite prolonged treatment with air or oxygen.

Corrections based on these data were employed in calculating values of i_d/C for the first wave of manganese(III). This was done by dividing the ratio of the diffusion current of the first wave to the *total* manganese concentration, by the n-value determined coulometrically for an identical solution that had been oxidized under identical conditions. Where n was less than 1, this involved no assumption beyond that of incomplete oxidation; where n exceeded 1, it involved the assumption that the diffusion coefficients of manganese(III) and the more highly oxidized species were the same. Since the proportion of the latter in these experiments never exceeded 7%, this assumption could not have led to a serious error.

In 1 F sodium cyanide the mean values of I thus calculated from data obtained

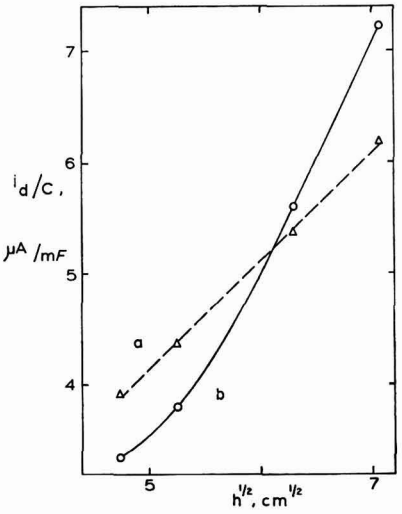

Fig. 6. Effect of mercury pressure on the values of i_d/C for (a) the first and (b) the second wave of manganese(III) in neutral 1 F sodium cyanide. See text for details of calculation. The manganese concentration was 1.0 mF.

with capillaries giving relatively long drop times are 1.68 ± 0.1 for the first wave and 3.38 ± 0.11 for the second. These agree well with the expected ratio (1 : 2) of the overall n-values.

However, as is shown by Fig. 6, their ratio is not independent of the drop time. Curve a in this Figure is a plot of $i_d/[\mathrm{Mn(III)}]$, obtained in the manner just described, *vs.* the square root of the pressure of mercury above the capillary tip. Its linearity indicates that the height of the first wave is diffusion-controlled. Curve b is a similar plot for the second wave, whose diffusion current was obtained by correcting the diffusion current measured at −1.00 V for the decrease in $m^{2/3}t^{1/6}$ between that potential and −1.50 V, and subtracting the result from the total diffusion current measured at −1.50 V. At low pressures of mercury, the value of i_d/C for the second wave is 0.96 ± 0.01 times that for the first wave; this is in exact agreement with the ratio (0.955) of the values of $m^{2/3}t^{1/6}$ at the two potentials employed. But as the pressure of mercury increases, so does the contribution of the chemically regenerated manganese(II) to the height of the second wave, and therefore the latter undergoes an anomalous increase that constitutes still further proof of its partially catalytic nature.

SUMMARY

In neutral sodium cyanide solutions, manganese(II) is reversibly reduced to the +1 state at a dropping mercury electrode. The half-wave potential of the resulting polarographic wave is −1.364 ± 0.007 V *vs.* S.C.E. in 1 F sodium cyanide, and varies with sodium cyanide concentration in a manner that can be ascribed to activity effects. The value of i_d/C for this wave decreases on adding sodium hydroxide, on increasing the manganese(II) concentration, and (at an anomalous rate) on increasing the drop time. These facts indicate that manganese(I) reacts with hydrogen cyanide to regenerate manganese(II), and that this reaction is fractional order with respect to manganese(I). Direct polarographic and spectrophotometric measurements of the rates of decomposition of air-free cyanide solutions of manganese(I) give for the pseudo-half-order rate constant

$$k = \frac{1}{[\mathrm{Mn(I)}]^{1/2}} \frac{\mathrm{d}[\mathrm{Mn(II)}]}{\mathrm{d}t} = (4 \pm 2) \cdot 10^{-5}\ \mathrm{mmole^{1/2}\ l^{-1/2}\ sec^{-1}}$$

The absorption spectra of very dilute (0.02–0.05 mF) solutions of manganese(I) in cyanide media indicate the presence of more than one absorbing species.

Adding sodium hydroxide to a solution of manganese(II) in 1 F sodium cyanide results in a reaction which is probably best represented by the equation

$$\mathrm{Mn(H_2O)(CN)_5^{3-} + OH^- = Mn(OH)(CN)_5^{4-} + H_2O};\ K = 2.3 \pm 0.4$$

and the resulting hydroxocyano complex undergoes an irreversible 2-electron reduction to the metal at $E_{1/2} = -1.72$ V. The data do not appear to confirm the supposition that $\mathrm{Mn(CN)_6^{4-}}$ is the sole important species of manganese(II) in moderately concentrated neutral cyanide solutions.

Manganese(III) is the principal product of the oxidation of manganese(II) with air or oxygen in neutral cyanide media, but the reaction is not stoichiometric. At high concentrations of manganese and/or cyanide, the oxidation is incomplete even

though very prolonged; at low concentrations of both, substantial amounts of a more highly oxidized species are present. Manganese(III) in neutral cyanide media is polarographically reduced to the +1 state in two successive 1-electron steps.

REFERENCES

1 E. T. VERDIER, *Collection Czech. Chem. Commun.*, 11 (1939) 216.
2 W. M. LATIMER, *Oxidation States of the Elements and their Potentials in Aqueous Solutions*, 2nd edn., Prentice-Hall, Inc., Englewood Cliffs, N.J., 1952.
3 W. D. TREADWELL AND W. E. RATHS, *Helv. Chim. Acta*, 35 (1952) 2259.
4 S. SIEKIERSKI AND E. K. SIEKIERSKA, *Roczniki Chem.*, 30 (1956) 399.
5 L. MEITES AND T. MEITES, *Anal. Chem.*, 23 (1951) 1194.
6 L. MEITES, *Anal. Chem.*, 27 (1955) 1116.
7 L. MEITES AND S. A. MOROS, *Anal. Chem.*, 31 (1959) 23.
8 J. J. LINGANE AND R. KARPLUS, *Anal. Chem.*, 18 (1946) 191.
9 J. J. LINGANE, *Anal. Chem.*, 19 (1947) 810.
10 R. G. BATES, *Anal. Chem.*, 23 (1951) 813.
11 R. G. BATES, V. E. BOWER, R. G. MILLER AND E. R. SMITH, *J. Res. Nat. Bur. Std.*, 47 (1951) 433.
12 R. G. BATES AND V. E. BOWER, *Anal. Chem.*, 28 (1956) 1322.
13 G. TAMMAN AND K. KOLLMANN, *Z. Anorg. Allgem. Chem.*, 160 (1927) 242.
14 G. TAMMAN AND J. HINNUBER, *Z. Anorg. Allgem. Chem.*, 160 (1927) 249.
15 P. ZUMAN, *Collection Czech. Chem. Commun.*, 15 (1950) 1107.

ELECTROCHEMICAL CHARACTERISTICS OF MANGANESE IN CYANIDE SOLUTIONS

II. BACKGROUND CORRECTIONS IN THE CONTROLLED-POTENTIAL COULOMETRIC DETERMINATION OF MANGANESE(II). KINETICS OF THE OXIDATION OF MANGANESE(I) BY HYDROGEN CYANIDE

STEPHEN A. MOROS*† AND LOUIS MEITES

Department of Chemistry, Polytechnic Institute of Brooklyn, Brooklyn, N.Y. (U.S.A.)

(Received June 26th, 1962)

The first paper of this series[1] described the polarographic characteristics of manganese (I) and (II) in sodium cyanide solutions, and presented polarographic and spectrophotometric evidence regarding the rate of the spontaneous chemical reoxidation of manganese(I). During a controlled-potential electroreduction of manganese(II), the occurrence of this process leads to the establishment of a steady state in which the rate of the electrolytic reduction of manganese(II) is equal to the rate of its chemical regeneration. The current flowing at this steady state, which, after suitable correction for other contributions, is proportional to the rate of the chemical process, has been termed a "kinetic" current[2]. The present paper is devoted to a detailed examination of this phenomenon and of the various other side reactions that are also involved in this system.

The general theory of background corrections in coulometry at controlled potential has been outlined previously[2]; the terms and symbols used here are identical with those previously defined.

EXPERIMENTAL

The apparatus, techniques, and reagents employed were described in the preceding paper[1].

DATA AND DISCUSSION

The continuous faradaic current

Curve *i* in Fig. 1 is the chronoamperogram** obtained when 100 ml of a neutral 1 *F*

* This paper is based on a thesis submitted by STEPHEN A. MOROS to the Faculty of the Polytechnic Institute of Brooklyn in partial fulfillment of the requirements for the Ph.D. degree, June, 1961.

† Present address: Research Department, American Cyanamid Company, Bound Brook, N.J.

**Chronoamperograms, chronopotentiograms, and voltammograms are commonly encountered in the current literature; the general form "*x*-*y*-ogram" leads immediately to chronocoulograms, coulopotentiograms, couloamperograms, and others. Similarly, the terms "strenoamperogram", "strenopotentiogram" and the like (from Greek στρηνής = strong) might be used to denote plots having concentration as the independent variable.

sodium cyanide solution containing 0.035 mF manganese(II) is electrolyzed at a large stirred mercury cathode at a potential of −1.50 V *vs.* S.C.E. The initial decrease of current reflects the normal exponential decrease of the concentration of manganese-(II) that has not yet undergone reduction. In principle it also includes contributions from the reduction of any impurity that is electroreducible at this potential and

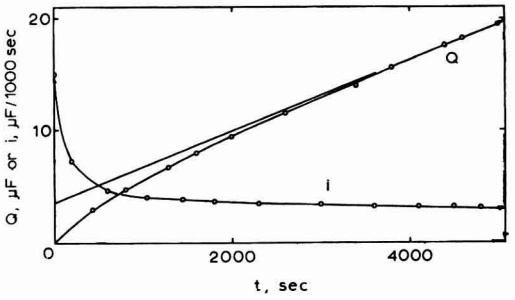

Fig. 1. Variations with time of (i) the current and (Q) the total quantity of electricity accumulated during the electrolysis, at −1.50 V *vs.* S.C.E., of 100 ml of neutral 1 F sodium cyanide solution containing 0.035 mF manganese(II).

from the charging of the electrical double layer around the working electrode; however, the first of these was virtually eliminated by pre-electrolysis and deaeration, while the second consumes too little electricity (at most 10 mμF) to be visible on the scale of this Figure.

The steady final current attained after about 3000 sec is unaffected by even prolonged further electrolysis. In a typical case, it was found to be 0.50 μF/100 sec (approximately 0.50 mA) after electrolysis at −1.7 V for 1 h; after a further 3 h at the same potential it was measured repeatedly during an additional hour and found to remain constant at 0.493 ± 0.003 μF/100 sec.

As is illustrated by Fig. 2, the steady final current obtained in the presence of

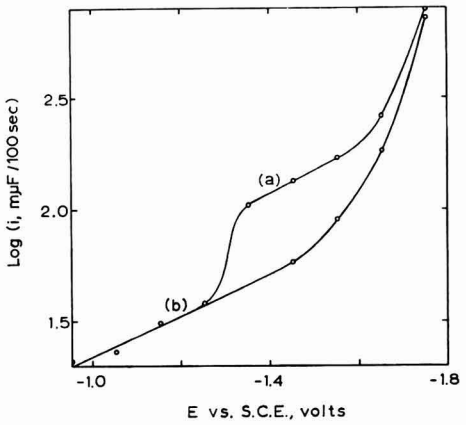

Fig. 2. Steady final electrolysis currents obtained with ((a), upper curve) 0.1 mF manganese in neutral 1 F sodium cyanide, ((b), lower curve) neutral 1 F sodium cyanide alone

manganese can be divided into three components. Curve (a) represents the data obtained in the presence of 0.1 mF manganese; curve (b) is the corresponding curve for a manganese-free solution. The difference between these curves at potentials more negative than about -1.3 V, where manganese(II) is reduced to the $+1$ state, is the kinetic current, which will be discussed in a subsequent section. Curve (b) represents the continuous faradaic current, $i_{f,c}$; its shape shows that this current reflects the rate of two independent processes. The data are reproduced within experimental error by the equation

$$i_{f,c} = 2.14 \cdot 10^{-0.926E_{\text{w.e.}}} + (4.0 \cdot 10^{-12}) \cdot 10^{-8.09E_{\text{w.e.}}} \quad (1)$$

where $i_{f,c}$ is the total continuous faradaic current, expressed in mμF/100 sec (1 mμF/100 sec = 0.965 μA) and $E_{\text{w.e.}}$ is the potential of the working electrode in volts *vs.* S.C.E. The second term on the right-hand side of eqn. (1) is only about half as large as the first at -1.6 V, and is negligible at less negative potentials, but it increases so much more rapidly as the potential becomes more negative that it constitutes nearly 95% of the total at -1.8 V.

The numerical coefficient of the exponent in the second term on the right-hand side of eqn. (1), which is equal to $-\alpha n_a$, corresponds to $\alpha n_a = 0.48$; both this value and the extrapolated exchange current density are in approximate agreement with those that characterize the reduction of water at mercury electrodes from dilute solutions of alkali metal hydroxides[3]. Hence it appears that the process predominating at potentials more negative than about -1.7 V *vs.* S.C.E. is the reduction of water. Then the process that predominates at potentials less negative than this can be only $HCN + e \rightarrow \frac{1}{2}H_2 + CN^-$. The value of αn_a (0.05) calculated for this process does not seem attractive, but neither does the alternative possibility that this is a double-layer effect, because of the extremely negative potentials involved.

Replicate measurements of $i_{f,c}$ in the range of potentials between -1.0 and -1.5 V *vs.* S.C.E. gave mean deviations of the order of $\pm$ 7%. This is much larger than the mean deviation of replicate values of $i_{f,c}$ for a single solution, and probably reflects small variations in the pH values (and therefore in the hydrogen cyanide concentrations) of different solutions.

The error incurred in a practical controlled-potential coulometric analysis by neglecting the continuous faradaic current is easily deduced from the following considerations. Assuming that the concentration of the substance being determined decreases with time in the usual exponential fashion (*i.e.*, that the current is not limited by a high cell resistance or any other extraneous factor), one has[4]

$$Q'_{\text{corr.}} = Q_{\text{corr.}}(1 - 10^{-\beta t}) = \frac{i^0}{2.3\beta}(1 - 10^{-\beta t}) \quad (2)$$

where β is the first-order rate constant of the electrolytic process and primes denote instantaneous values. It is tacitly assumed that the initial current, i^0, is large compared with $i_{f,c}$. Since

$$Q'_{f,c} = \int_0^t i_{f,c}\,dt = i_{f,c}t \quad (3)$$

and

$$\text{error} = \frac{Q'_{\text{corr.}} + Q'_{f,c}}{Q_{\text{corr.}}} - 1 \quad (4)$$

it follows at once that

$$\text{error} = -10^{-\beta t} + 2.3\,\beta t\,(i_{f,c.}/i^{\circ}) \qquad (5)$$

Some values calculated from eqn. (5) are plotted in Fig. 3, from which it is evident that neglect of the correction for the continuous faradaic current is justifiable only

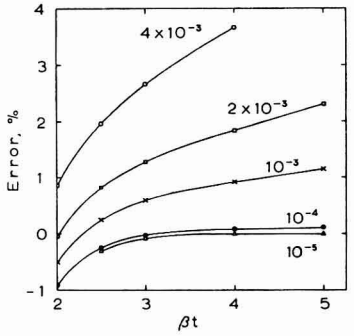

Fig. 3. Effect of the ratio $i_{f,c.}/i^{\circ}$, whose value is given beside each curve, on the error of a controlled-potential coulometric experiment, as calculated from eqn. (5).

if $i_{f,c.}/i^{\circ}$ is less than about 10^{-4}. The correction is best made by extrapolating the chronocoulogram to zero time, as is illustrated by curve Q of Fig. 1.

The kinetic current

Figure 2 shows that the steady final current obtained after exhaustive electrolysis of a cyanide solution containing manganese is larger than that obtained in the absence of manganese. The difference, which is termed the *kinetic* current, i_k, was determined by electrolyzing a pure 1 F sodium cyanide solution at each of three potentials (−1.50, −1.60, and −1.70 V *vs.* S.C.E.) on the plateau of the manganese(II) wave to obtain values of $i_{f,c.}$; then adding a known concentration of manganese(II) and again electrolyzing at the same potentials to obtain values of $(i_{f,c.} + i_k)$. Typical values of i_k, in μF/100 sec, were 0.315 ± 0.011 with 0.44 mF manganese, and 1.144 ± 0.004 with 7.25 mF manganese. Since these values were independent of working-electrode potential, they must reflect the rate of a chemical process occurring in the bulk of the solution: this is obviously the previously described[1] reaction between manganese(I) and hydrogen cyanide to regenerate manganese(II). As has previously been pointed out[5,6], the measurement of i_k is one of a very few techniques that permit the *direct* measurement of the rate of a chemical reaction.

The steady-state concentration of manganese(II) corresponding to the value of i_k in any experiment can be deduced from data on the relationship between the electrolysis current and the concentration of manganese(II) at the start of the electrolysis. The fact that a plot of log i *vs.* t is essentially linear for the first several hundred sec[7] permits i° to be obtained by a straightforward extrapolation. A number of experiments with solutions containing 0.1–1.5 mF manganese(II) gave $i^{\circ}/C^{\circ} = 44.8 \pm 3.9$ μF/100 sec/mmole /l. Hence, for example, the value of i_k cited above for an 0.44 mF manganese solution corresponds to a steady-state concentration of 0.0070 mF

manganese(II), so that reduction to the +1 state is only 98% complete under these conditions.

Figure 4 shows the manner in which the value of i_k varies with the concentration of manganese(I), and demonstrates conclusively that the chemical reaction

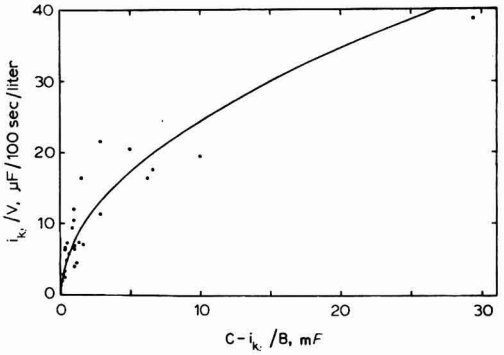

Fig. 4. Variation of the kinetic current with the concentration of manganese(I) in neutral 1 F sodium cyanide. Values of the manganese(I) concentration were obtained from the difference between the total concentration of manganese present (C) and the steady-state concentration of manganese(II) calculated from the kinetic current (equal to i_k/B, where B is the constant of proportionality relating the current for the reduction of manganese(II) to its concentration and is experimentally given by the ratio $i°/C°$).

responsible for i_k is not first-order with respect to manganese(I). The steady state is described by the equation

$$i_k/nV = k'[\mathrm{Mn(I)}]^a \tag{6}$$

where i_k is the kinetic current in mF/sec, n is 1 for the reduction of manganese(II) in neutral cyanide media, V is the volume of the solution in liters, k' is the appropriate rate constant, [Mn(I)] is the total concentration of manganese(I) in mmoles/l, and a is the order of the reaction with respect to manganese(I). Over the 300-fold range of concentrations shown in Fig. 4, the data are most accurately reproduced by the parameters $a = 1/2$ and $k' = 7.8 \cdot 10^{-5}$ mmole$^{1/2}$ l$^{-1/2}$sec^{-1}. The standard deviation of the latter value is $\pm$ 30%. Polarographic evidence[1] showed that the height of the manganese(II) wave is dependent not only on the concentration of the cyano complex but also on the pH; it therefore seems probable that the rather large uncertainty of k' is due to small variations in the pH values of the manganese(I) cyanide solutions. If, as is suggested by the polarographic data, the rate of regeneration of manganese(II) is proportional to the concentration of hydrogen cyanide, an uncertainty of $\pm$ 30% in the overall rate would correspond to an uncertainty of only about $\pm$ 0.12 pH unit.

The values of k' deduced from spectrophotometric ($5 \cdot 10^{-5}$ mmole$^{1/2}$ l$^{-1/2}$sec^{-1}) and polarographic ($3 \cdot 10^{-5}$ mmole$^{1/2}$ l$^{-1/2}$sec^{-1}) data[1] on the decomposition of manganese(I)-cyanide solutions are in acceptable agreement with this amperometric value. If it had been assumed that the reaction were first-order with respect to manganese(I), the calculated pseudo-first-order rate constants would have decreased uniformly from $30 \cdot 10^{-5}$ sec^{-1} (the spectrophotometric value) to $1.1 \cdot 10^{-5}$ sec^{-1} (the

mean of two amperometric values) as the concentration of manganese(I) increased from 0.03–30 mF.

This half-order dependence indicates that manganese(I) exists predominantly in the form of a dimeric species in cyanide solutions. This would be expected to be in equilibrium with a mononuclear species whose relative concentration would increase as the total concentration of manganese(I) decreases; this would account for the shift in the wavelength of maximum absorption by manganese(I) that is observed[1] as its concentration decreases from 0.04–0.02 mF. The experimental observations can be reproduced by the following mechanism:

$$(CN)_5\text{—Mn—O—Mn}(CN)_5^{10-} + H_2O = 2\ Mn(OH)(CN)_5^{5-};\ K = K_1 \tag{7}$$

$$Mn(OH)(CN)_5^{5-} + HCN \xrightarrow{k} Mn(CN)_6^{4-} + \tfrac{1}{2}\ H_2 + OH^- \tag{8}$$

$$Mn(CN)_6^{4-} + e = Mn(CN)_6^{5-} \tag{9}$$

$$2\ Mn(CN)_6^{5-} + H_2O = 2\ HCN + (CN)_5\text{Mn—O—Mn}(CN)_5^{10-};\ K = K_2 \tag{10}$$

If it is assumed that K_1 is small and that K_2 is large, then virtually all of the manganese(I) will be present in the form of the binuclear species unless the total concentration of manganese(I) is very low. Accordingly, the rate of reaction (8) will be given by

$$\frac{d[Mn(II)]}{dt} = k\ [Mn(OH)(CN)_5^{5-}][HCN] = k\ (K_1C/2)^{1/2}\ [HCN] \tag{11}$$

where k is the rate constant of the reaction described by eqn. (8) and C is the total concentration of manganese(I). The latter is obtained experimentally by subtracting the steady-state concentration of manganese(II), calculated from the values of i_k and $i°/C°$ for the experiment in question in the fashion described above, from the known total concentration of manganese present. The value of k' in eqn. (6) is evidently given by

$$k' = k\ (K_1/2)^{1/2}\ [HCN] = 2.4_6 \cdot 10^{-6}\ \text{mole}^{1/2}\text{l}^{-1/2}\text{sec}^{-1} \tag{12}$$

or, introducing the value of [HCN] appropriate to a neutral 1 F sodium cyanide solution,

$$k\ K_1^{1/2} = 9.5 \cdot 10^{-4}\text{l}^{1/2}\text{mole}^{-1/2}\text{sec}^{-1} \tag{13}$$

Crude estimates of the individual values of k and K_1 are made possible by the fact that the wavelength of maximum absorption for a 1 F sodium cyanide solution containing 3 mF manganese(I) was indistinguishable from that obtained with 0.04 mM manganese(I). Evidently it is only when the latter concentration is reached that the dissociation of the dimer begins to be detectable. On the other hand, the fact that the wavelength of maximum absorption is still shifting with concentration, in a solution containing 0.02 mF manganese(I), indicates that the dissociation of the dimer is still far from complete at that concentration. The approximation that

$$[Mn(OH)(CN)_5^{5-}]/[(CN)_5\text{Mn—O—Mn}(CN)_5^{10-}] = 0.2$$

when C = 0.03 mF can hardly be grossly in error. On this basis K_1 may be estimated to be approximately $5 \cdot 10^{-7}$ mole/l, whence k is calculated to be approximately 1 l mole^{-1}sec^{-1}.

The scatter of the points in Fig. 4 implies that corrections for the kinetic current in practical controlled-potential coulometric analysis should not be based on the use of an average value of k'. The sensitivity of the present data to small variations of pH

is certainly due in large part to the effect of pH on the concentration of hydrogen cyanide and thus on the rate of reaction (8). No doubt other systems will be found in which the chemical rate-determining step involves a reaction with water and has a rate independent of pH, or involves a protonated species whose concentration can be controlled much more closely than could the concentration of hydrogen cyanide in these experiments. Nevertheless, although the kinetic current should be much more reproducible in such systems, it is inherently dependent on a rate of mass transfer to the electrode surface and therefore susceptible to variations in stirring efficiency, temperature, and other factors that affect that rate.

Some time after the fundamental considerations underlying the application of amperometry at controlled potential to the study of reaction rates were first outlined[8], RECHNITZ[9] AND LAITINEN reported failure in an attempt to apply it to a study of the rate of the reduction of perchlorate ion by a reduced molybdenum species. However, it does not appear that they employed optimum stirring conditions, nor is it clear whether proper corrections for other processes (*e.g.*, the continuous faradaic current due to the reduction of hydrogen ion) were applied.

We have previously[2] outlined an algebraic treatment of the background current correction in the case in which i_k is proportional to the concentration of the reduced species. Somewhat different considerations are involved in the present case.

Neglecting the charging and faradaic impurity currents, and *assuming for the remainder of this subsection that there is no induced component of the electrolysis current*, we may consider that the total current at any instant is given by

$$i'_{\text{total}} = i'_{\text{corr.}} + i'_k + i'_{f,c} \tag{14}$$

where $i'_{\text{corr.}}$ may be considered to represent the current due to the reduction of manganese(II) present originally and never yet reduced, while i'_k represents the current due to the reduction of chemically regenerated manganese(II). With the aid of eqn. (6), the kinetic current at any instant can be represented by

$$i'_k = \mathscr{K}\{[\text{Mn(I)}]'/[\text{Mn(I)}]_\infty\}^{1/2} \tag{15}$$

where $\mathscr{K}$ is the appropriate constant of proportionality and $[\text{Mn(I)}]_\infty$ denotes the final steady-state concentration of manganese(I). If the reduction eventually became complete, this would be exactly equivalent to

$$i'_k = \mathscr{K}(Q'_{\text{corr.}}/Q_{\text{corr.}})^{1/2} \tag{16}$$

where $Q_{\text{corr.}}$ is equal to the number of microequivalents of manganese(II) present initially. Although, as was shown above, this condition is not quite fulfilled, the reduction is no less than 98% complete even with as little as 0.44 mF manganese, and because of the half-order dependence of the rate of reaction (8) on the total concentration of manganese(I) it is still more nearly complete at higher concentrations. Thus the use of eqn. (16) could not lead to an appreciable error except at extremely small concentrations of manganese. Writing eqn. (14) in integral form and combining with eqns. (2) and (16) gives

$$Q'_{\text{total}} = Q_{\text{corr.}}(1 - 10^{-\beta t}) + \int_0^t \mathscr{K}(1 - 10^{-\beta t})^{1/2}\mathrm{d}t + i_{f,c}t \tag{17}$$

Series expansion, retaining only the first two terms, and integration gives

$$\int_0^t i'_k\mathrm{d}t = \int_0^t \mathscr{K}(1 - 10^{-\beta t})^{1/2}\mathrm{d}t = \mathscr{K}\left(t - \frac{1}{4.61\,\beta}\right) \tag{18}$$

provided that βt is fairly large (*i.e.*, that the steady state has been reached). Combining this with eqn. (17) produces, finally,

$$Q_{corr.} = Q'_{total} - (\mathscr{K} + i_{f,c})t + \frac{\mathscr{K}}{4.61\,\beta} \qquad (19)$$

As is also true when i_k is proportional to the concentration of the reduced species[2], $Q_{corr.}$ cannot be obtained by a simple extrapolation of the final linear portion of the chronocoulogram to zero time; this would be tantamount to neglecting the last term on the right-hand side of eqn. (19). The preferable procedure is illustrated by the following typical example. A pure 1 *F* sodium cyanide solution was electrolyzed at −1.50 V *vs.* S.C.E. until a steady current (equal to $i_{f,c}$) was reached; this was found to be 0.17 μF/100 sec. An aliquot of a stock solution of manganese(II), containing 507.2 μmoles of this substance, was added, and the mixture was electrolyzed, first at −1.00 V to remove any trace of manganese(III) that might have been formed by air-oxidation, and then at −1.50 V to reduce the manganese to the +1 state. The current was measured at 50-sec intervals at the start of the latter electrolysis, and a plot of log $(i'_{total} - i_{f,c})$ *vs.* t was constructed for these data and found to give $\beta = 0.232/100$ sec. The electrolysis was then allowed to proceed for about 2 h more, until it was certain that the steady state had been reached. After a total of 8300 sec Q'_{total} was 687.98 μF and the final current (which is equal to $\mathscr{K} + i_{f,c}$) was 1.88_6 μF/100 sec. Hence $\mathscr{K}$ was 1.71_1 μF/100 sec, and substituting all these data into eqn. (19) gave

$$Q_{corr.} = 687.98 - (1.88_6)(83) + \frac{1.71_1}{(4.61)(0.232)} = 533.1\ \mu F$$

The manner in which the various components of Q'_{total} vary with time during a typical electrolysis is shown in Fig. 5.

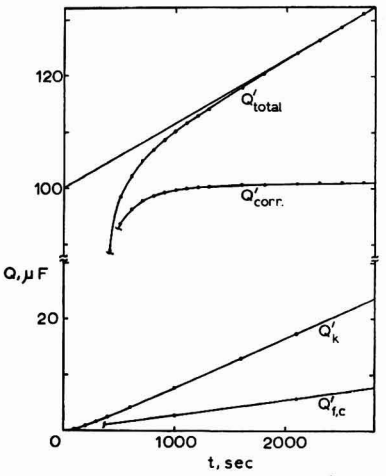

Fig. 5. Chronocoulograms showing the variations of Q'_{total}, $Q'_{f,c}$, Q'_k, and $Q'_{corr.}$ in a typical experiment in which a solution containing 100.1 μmoles of manganese(II) in 110 ml of neutral 1 *F* sodium cyanide was electrolyzed at −1.50 V *vs.* S.C.E. Six consecutive values of $Q_{corr.}$ at $2500 \leq t \leq 3500$ sec. gave, in mean, $101.12 \pm 0.01_5$ μF.

The induced current

The quantity of electricity obtained from the above calculation (533.1 μF) is several per cent larger than the quantity of manganese present (507.1 μmoles); numerous experiments with different concentrations of manganese showed that this is always the case. This excess consumption of electricity must reflect the occurrence of a side reaction that accompanies the electroreduction of manganese(II) (and that is therefore essentially complete by the time the steady state has been attained) but that results in the formation of hydrogen rather than of manganese(I). One possible mechanism for such a process involves the transient formation of a bridge structure such as

$$\text{electrode}-\text{HOH}-(\text{CN})\text{Mn}(\text{CN})_5^{4-}$$

When an electron is added to the hydrogen atom at the electrode surface, one of two things may happen. If the manganese complex remains bound for a length of time that suffices for the transfer of the electron through the bridging water molecule, the result is obviously the formation of $Mn(CN)_6^{5-}$. But if the hydrogen-cyanide bond breaks after an electron is transferred to the water molecule but before it is passed along to the manganese ion, the water molecule that has accepted the electron may break down into a hydrogen atom and a hydroxyl ion.

The frequency of this latter sequence of events must be proportional to the frequency with which electrons are transferred to the bridging water molecules [*i.e.*, to the overall rate of reduction of manganese(II)], so that the induced current at any instant, $i'_{i.c.}$, is given by

$$i'_i = b(i'_{corr.} + i'_k) \tag{20}$$

Together with eqns. (17) and (18), this gives, for long times,

$$\begin{aligned} Q'_{total} &= (1 + b)[Q'_{corr.} + \chi\left(t - \frac{1}{4.61\,\beta}\right) + i_{f,c}t \\ &= (1 + b)Q'_{corr.} + [(1 + b)\,\chi + i_{f,c}]t - \frac{(1 + b)\,\chi}{4.61\,\beta} \end{aligned} \tag{21}$$

Hence the steady-state current, which is equal to the slope of the chronocoulogram at long times, $(dQ'_{total}/dt)_\infty$, is given by

$$\left(\frac{dQ'_{total}}{dt}\right)_\infty = (1 + b)\,\chi + i_{f,c} \tag{22}$$

which, together with eqn. (21), yields

$$Q_{corr.} = \frac{1}{1 + b}\left\{Q'_{total} - \left(\frac{dQ'_{total}}{dt}\right)_\infty t + \frac{(dQ'_{total}/dt)_\infty - i_{f,c}}{4.61\,\beta}\right\} \tag{23}$$

in which all of the terms within braces can be measured experimentally. This permits the evaluation of b from data obtained with known amounts of manganese. As is shown in Fig. 6, the mean value of b was 0.03 $\pm$ 0.02, and there was no indication of any systematic trend when the quantity of manganese was varied from 10–500 μmoles (in about 100 ml). The value of b may be taken as the probability that the water–cyanide–manganese bridge will break in the midst of the electron-transfer process at -1.50 V *vs.* S.C.E. and that the electron will not be transferred back to the electrode.

Since this work was completed, the behavior of the induced current has been investigated[10] for a system in which it is much larger and hence much more amenable to precise measurement than is the case here. In the reduction of dimethylglyoxime the existence of the induced current was attributed to the possibility of reducing a

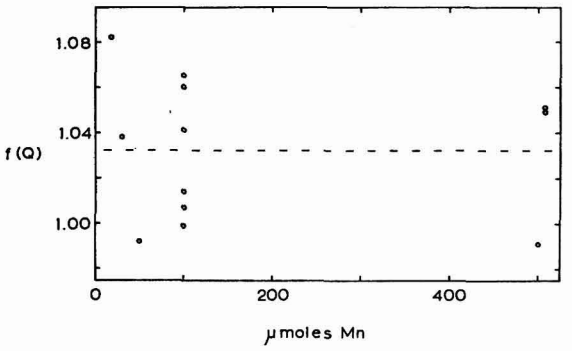

Fig. 6. Values of the function $f(Q) =$

$$\frac{1}{Q_{corr.}}\left\{Q'_{total} - \left(\frac{dQ'_{total}}{dt}\right)_{\infty} t + \frac{(dQ'_{total}/dt)_{\infty} - i_{f,c}}{4.61\,\beta}\right\}$$

[which, according to eqn. (23), is equal to $(1 + b)$] obtained with 10–500 μmoles of manganese in 100 ml of 1 F sodium cyanide at −1.50 V *vs.* S.C.E.

protonated intermediate in either of two ways: one yielding hydrogen and the other ultimately yielding 2,3-diaminobutane. This is mechanistically equivalent to postulating the existence of an electrode–hydrogen–nitrogen (or electrode–hydronium ion–nitrogen) bridge which may break after an electron has been transferred from the electrode into the bridge, but before it has been further transferred to the nitrogen atom. It was found that b increased exponentially with increasingly negative potential, though at a rate corresponding to an unexpectedly low value (0.11) of αn_a. Quite possibly this simply reflects an increasing polarization, and therefore a decreasing stability, of the hydrogen–nitrogen bond as the potential gradient near the electrode surface increases.

The fact that the value of b was essentially constant (at constant working-electrode potential) in the present work may be restated in a different form. Over a 50-fold range of quantities or concentrations of manganese, and despite the fact that the total quantity of electricity accumulated was always at least 20% larger than, and was occasionally as much as 3 times (in electrolyses allowed to proceed without attention for prolonged periods) the expected value, proper corrections for all of the components of the background current yielded results with a bias less than ± 0.5% and a precision of ± 2% (mean deviation).

SUMMARY

A plot of continuous faradaic current *vs.* working-electrode potential for the controlled-potential electrolysis of a neutral 1 F sodium cyanide solution at a large stirred mercury pool electrode consists of two portions, which correspond to the reductions of hydrogen cyanide and water. The final electrolysis current is increased

by the presence of manganese(I), and it is shown that this increase can be accounted for quantitatively by a mechanism involving the hydrolysis of the binuclear species $(CN)_5Mn—O—Mn(CN)_5^{10-}$ to give $Mn(OH)(CN)_5^{5-}$ ($K = ca.\ 5 \cdot 10^{-7}$) and the reaction of the latter ion with hydrogen cyanide ($k = ca.$ 1 $l/mole^{-1}sec^{-1}$) to give manganese(II) and hydrogen. Coulometric data show that the reduction of manganese(II) in a cyanide solution increases the rate of the simultaneous reduction of water, and this is interpreted on the basis of the probability of dissociation of the bridge structure electrode–HOH–$(CN)Mn(CN)_5^{4-}$ after an electron has been transferred from the electrode but before it has been transferred through the bridge to the manganese complex.

REFERENCES

1 S. A. MOROS AND L. MEITES, *J. Electroanal. Chem.*, 5 (1963) 90.
2 L. MEITES AND S. A. MOROS, *Anal. Chem.*, 31 (1959) 23.
3 R. PARSONS, *Handbook of Electrochemical Constants*, Butterworths, London, 1959, pp. 95–6.
4 W. M. MACNEVIN AND B. B. BAKER, *Anal. Chem.*, 24 (1952) 986.
5 L. MEITES, *Record Chem. Progr.*, 22 (1961) 81, 106.
6 J. M. MATSEN AND H. B. LINFORD, *Anal. Chem.*, 34 (1962) 142.
7 R. PARSONS, *Handbook of Electrochemical Constants*, Butterworths, London, 1959, Fig. 6a.
8 L. MEITES AND S. A. MOROS, *Paper presented before the Division of Analytical Chemistry at the 133rd National Meeting of the American Chemical Society, San Francisco, Calif., April, 1958.*
9 G. A. RECHNITZ AND H. A. LAITINEN, *Anal. Chem.*, 33 (1961) 1473.
10 M. SPRITZER AND L. MEITES, *Anal. Chim. Acta*, 26 (1962) 58.

FARADAIC ADMITTANCE, A DIFFUSION MODEL. II*

S. K. RANGARAJAN AND K. S. G. DOSS

Central Electrochemical Research Institute, Karaikudi (India)

(Received May 25th, 1962)

NOTATION

$C_i(x, t)$	Instantaneous concentration of the species i at a distance x from the electrode, ($i = O$ denotes that of oxidant, and $i = R$ that of reductant).
C_i°	Bulk concentration of species i.
D_{i_1}	Diffusion coefficient of species i in the first layer *i.e.*, adjacent to the electrode.
D_{i_2}	Diffusion coefficient of species i in the bulk.
ν_i	Thickness of the 'first' layer for species i.
D_i'	$\dfrac{\sqrt{D_{i_2}} - \sqrt{D_{i_1}}}{\sqrt{D_{i_2}} + \sqrt{D_{i_1}}}$.
$\bar{C}_i(x, p)$	Laplace transform of $C_i(x, t)$ is defined by $\mathscr{L}(C_i) = \bar{C}_i = p \int_0^\infty e^{-pt} C_i(x, t)\, dt.$
p	Transform variable.
θ	Phase angle between the alternating components of faradaic current $i(t) = I \cos(\omega t + \theta)$ and the electrode potential $v(t) = V \cos \omega t$.
a_i	$\nu_i \sqrt{2\omega / D_{i_1}}$.
i_o	Exchange current density.
β	$1 + (C_O^\circ \sqrt{D_{O_2}} / C_R^\circ \sqrt{D_{R_2}})$.
R_r, $1/\omega C_r$	Elements of the equivalent circuit for the classical model[1,2].
R_r' $1/\omega C_r'$	Elements of the equivalent circuit as derived for the perturbed diffusion model.

* This paper was presented at the Second Seminar on Electrochemistry held at the Central Electrochemical Research Institute, Karaikudi, 1960. For the first part of this series refer[6].

1. The classical theory of faradaic admittance[1,2,3,4] shows that the current voltage relationships obtained at the electrode–solution interface, can be simulated by a circuit comprising the resistance R_r and the capacitance C_r where

$$R_r = \frac{RT}{nF}\left\{\frac{1}{i_o} + \frac{1}{nF\sqrt{2\omega}}\left(\frac{1}{C_O^\circ\sqrt{D_{O_2}}} + \frac{1}{C_R^\circ\sqrt{D_{R_2}}}\right)\right\} \quad (1)$$

and

$$1/\omega C_r = \frac{RT}{n^2F^2}\left\{\frac{1}{\sqrt{2\omega}}\left(\frac{1}{C_O^\circ\sqrt{D_{O_2}}} + \frac{1}{C_R^\circ\sqrt{D_{R_2}}}\right)\right\} \quad (2)$$

R_r and C_r are the values of the circuit elements obtained after correcting for the capacity of the double-layer and the resistance of the cell.

The important assumptions underlying these conclusions are as follows:

(i) only small departures from the equilibrium are considered;

(ii) diffusion is the sole mode of mass transfer (*i.e.*, migration and convection effects are assumed negligible);

(iii) the rate-determining step *viz.*, Ox + n e $\rightleftarrows$ Red is not preceded, nor followed, by chemical reactions; and the specific adsorption of the reactants (or products) is absent.

Generally, any relaxation of the restrictions imposed by these assumptions results in different expressions for R_r and C_r.

For example, the diffusion equations governing the concentration distributions will have to be altered if migration effects in the diffuse layer are to be accounted for and consequently, the expressions for the elements of the equivalent circuit will be different. Or, if the reactants and/or products are specifically adsorbed, the quantitative formulations will have to be modified and so will the conclusions.

2. It is the purpose of the present paper to examine how a *perturbation in the diffusion model* will alter the conclusions as regards R_r and C_r. The main feature of this theoretical model is the assumption that there are two diffusion layers with different diffusion coefficients. Initially, there is no concentration variation with distance, but once the equilibrium state is disturbed by altering the electrode–solution potential, diffusion phenomena which become the sole mode of mass transfer, *cf.* assumption (ii), determine the concentration distributions of the reactive species. As the diffusion coefficients are different (or, as the diffusion phenomenon in the region adjacent to the electrode is *perturbed*), the diffusion equations have to be solved in the two regions $x \leqslant \nu_i$ and $x \geqslant \nu_i$, and fitted in at the boundary so as to avoid surface resistance at $x = \nu_i$.

The thicknesses ν_i ($i = O, R$) of the first layers, *viz.*, those nearer the electrode, can be assumed to be very small and the constant diffusion coefficients D_{i_1} in these regions, are different from those of the bulk D_{i_2}. Continuity of mass transfer is ensured at $x = \nu_i$ by equating the two fluxes

$$D_{i_1}\left(\frac{\partial C_i}{\partial x}\right)_{x=\nu_i-\varepsilon} \quad \text{and} \quad D_{i_2}\left(\frac{\partial C_i}{\partial x}\right)_{x=\nu_i+\varepsilon}$$

as $\varepsilon \to 0$. It may be mentioned that but for the perturbations in the diffusion phenomenon as outlined above, no changes are made in the assumptions (i) to (iii.) It will be of interest to find out how such a mathematical formulation can account

for the complex phenomena that may exist near the interface. With this in view, in a subsequent communication, a comparison will be made with the results obtained for the cases, where the effects of the diffuse double layer or of adsorption, are taken into account.

The conditions governing the concentration distributions $C_i(x, t)$ of the reactants may be expressed as

$$D_{i_1} \frac{\partial^2 C_i}{\partial x^2} = \frac{\partial C_i}{\partial t} \qquad (x \leqslant \nu_i) \tag{3}$$

$$D_{i_2} \frac{\partial^2 C_i}{\partial x^2} = \frac{\partial C_i}{\partial t} \qquad (x \geqslant \nu_i) \tag{4}$$

$$D_{i_1} \frac{\partial C_i}{\partial x}\Big)_{x=0} = \pm \frac{i(t)}{nFA} \tag{5}$$

(positive sign for oxidant and negative sign for reductant, net cathodic current being taken as positive)

$$C_i)_{x\to\infty} = C_i^\circ \tag{6}$$

$$C_i)_{t=0} = C_i^\circ \tag{7}$$

$$C_i)_{x=\nu_i-\varepsilon} = C_i)_{x=\nu_i+\varepsilon} \quad \varepsilon \to 0 \tag{8}$$

$$D_{i_1} \frac{\partial C_i}{\partial x}\Big)_{x=\nu_i-\varepsilon} = D_{i_2} \frac{\partial C_i}{\partial x}\Big)_{x=\nu_i+\varepsilon} \tag{9}$$

The solutions of eqns. (3) and (4) with the initial and boundary conditions (5) to (9), (see also Appendix I), are

$$\bar{C}_i(x, p) - C_i^\circ = \mp \frac{\bar{i}(p)}{nFA\sqrt{D_{i_1} p}} \exp\left(-\sqrt{p/D_{i_1}}\, x\right) \cdot \frac{1 - D_i' \exp\left[-2\sqrt{p/D_{i_1}}\,(\nu_i - x)\right]}{1 + D_i' \exp\left(-2\sqrt{p/D_{i_1}}\,\nu_i\right)} \tag{10}$$

where

$$D_i' = \frac{\sqrt{D_{i_2}} - \sqrt{D_{i_1}}}{\sqrt{D_{i_2}} + \sqrt{D_{i_1}}}$$

Two limiting cases, (a) and (b), are of interest in that the solutions for them have already been obtained independently[5,6].

(a) $D'_i \to 0$

It may easily be seen that

$$\bar{C}_i(x, p) - C_i^\circ \to -\frac{\bar{i}(p)}{nFA\sqrt{Dp}} \exp\left(\sqrt{p/D} \cdot x\right) \text{ if } D_{i_1} = D_{i_2} = D \text{ or } D_i' = 0\,, \tag{11}$$

and hence the present model degenerates into the familiar model[1], so that the expression for C_i coincides with the well known result already derived[5];

(b) $D_i' \to -1$; *i.e.*, $D_{i_1}/D_{i_2} \gg 1$.

One obtains in this case

$$\bar{C}_i(x,p) - C_i^\circ = -\frac{\bar{i}(p)}{nFA\sqrt{D_{i_1}p}} \left\{\frac{\text{Cosh}\,[\sqrt{p/D_{i_1}}\,(x-\nu_i)]}{\text{Sinh}\,(\sqrt{p/D_{i_1}}\,\nu_i)}\right\} \tag{12}$$

so that

$$\bar{C}_i(o,p) - C_i^\circ = -\frac{\bar{i}(p)}{nFA\sqrt{D_{i_1}p}}\,\text{Coth}\,(\sqrt{p/D_{i_1}}\,\nu_i)$$

It may be verified that the same expression will result, if one assumes the conditions

$$D_{i_1}\left(\frac{\partial C_i}{\partial x}\right)_{x=0} = \pm\frac{i(t)}{nFA}$$

and

$$D_{i_1}\left(\frac{\partial C_i}{\partial x}\right)_{x=\nu_i} = 0$$

as well as (3) and (7). Such a model is discussed elsewhere[6].

A formal series expression can be derived for $C_i(x,t)$, and, in particular, it is proved that $C_i(0,t)$, the concentration of the species i (O or R) at the interface, is given as, (Appendix II),

$$\mp\frac{1}{nFA\sqrt{D_{i_1}}}\sum_{n=0}^{\infty} C_n \int_0^t \frac{i(t-\tau)}{\sqrt{\pi\tau}}\exp\left(-\nu_i^2 n^2/D_{i_1}\tau\right)d\tau$$

where

$$C_0 = 1 \text{ and } C_n = 2(-D_i')^n,\ n = 1, 2, 3, \ldots$$

$$C_i(o,t) - C_i^\circ = \mp\frac{1}{nAF\sqrt{D_{i_1}}}\int_0^t \frac{i(t-\tau)}{\sqrt{\pi\tau}}\,d\tau \mp\frac{2}{nAF\sqrt{D_{i_1}}}\sum_{1}^{\infty}(-D_i')^n\int_0^t\frac{i(t-\tau)}{\sqrt{\pi\tau}}\exp\left(-\nu_i^2n^2/D_{i_1}\tau\right)d\tau \tag{13}$$

which

$$\to \mp\frac{1}{nAF\sqrt{D_i}}\int_0^t\frac{i(t-\tau)}{\sqrt{\pi\tau}}\,d\tau \text{ if } D_{i_1} = D_{i_2} = D_i \text{ (i.e., } D' \to 0)$$

When the net current $i(t)$ is sinusoidal, say, of the form $I\cos(\omega t+\theta)$, where θ is the phase angle between the alternating components of the current and the potential, $V\cos\omega t$, the steady component of the interfacial concentrations assumes the form $\delta C_i \sin(\omega t+\theta+\phi_i)$ where

$$\delta C_i = \mp\frac{I}{nAF\sqrt{D_{i_1}\omega}}\sqrt{\frac{e^{2a_i}+D'^2-2D'e^{a_i}\cos a_i}{e^{2a_i}+D'^2+2D'e^{a_i}\cos a_i}}$$

and

$$\tan\phi_i = \frac{e^{2a_i}-D_i'^2+2D_i'e^{a_i}\cos a_i}{e^{2a_i}-D_i^2-2D_i'e^{a_i}\cos a_i} \tag{14}$$

$$a_i = \nu_i\sqrt{2\omega/D_{i_1}}$$

(Note: $\delta C_i \to \mp I/nAF\sqrt{D_{i_1}\omega}$ and $\phi_i \to \pi/4$ if $D_i' \to 0$, as it should be[5]).

Particular cases

$v_i \to \infty$ such that $v_i\sqrt{\omega/D_{i_1}} \gg 1$, $\delta C_i \to \mp I/nAF\sqrt{D_{i_1}\omega}$, which means that the layer adjacent to the electrode surface controls the mass transfer phenomena. It can be easily seen to be so, since the inequality $v_i\sqrt{\omega/D_{i_1}} \gg 1$ implies that the thickness of the first layer is much greater than that of the diffusion layer ($\sim\sqrt{D_{i_1}/\omega}$).

In the limit $v_i \to 0$ (such that $v_i\sqrt{\omega/D_{i_1}} \ll 1$), $\delta C_i \to \mp I/nAF\sqrt{D_{i_2}\omega}$ (whatever be D_{i_1}) and $\phi_i \to \pi/4$, which would be the result for the *unperturbed* model — wherein the same diffusion coefficient had been assumed throughout the interval $(0, \infty)$ for x.

An approximation

Viewed as a perturbation, the dimensionless parameter $v_i\sqrt{2\omega/D_{i_1}}$ (which is a measure of the perturbation), can be assumed to take small values, *i.e.*, it can be assumed that $v_i\sqrt{\omega/D_{i_1}} < 1$ such that $(v_i\sqrt{\omega/D_{i_1}})^2$ and higher powers can be neglected. It can be easily proved that

$$\delta C_i = \mp \frac{I}{nAF\sqrt{D_{i_2}\omega}}\left[1 + \frac{a_i}{2}\left(\sqrt{\frac{D_{i_2}}{D_{i_1}}} - \sqrt{\frac{D_{i_1}}{D_{i_2}}}\right)\right] \text{ and } \tan\phi_i = 1 + a_i\left(\sqrt{\frac{D_{i_2}}{D_{i_1}}} - \sqrt{\frac{D_{i_1}}{D_{i_2}}}\right) \quad (15)$$

The electrode–solution potential, v, the net cathodic current $i(t)$, and the interfacial concentration $C_i(0, t)$ are related by the rate equation

$$i(t) = i_0\left\{\frac{C_O(0,t)}{C_O^\circ}\exp(-\alpha nFv/RT) - \frac{C_R(0,t)}{C_R^\circ}\exp[(1-\alpha)nFv/RT]\right\}$$

Linearising the exponentials and rewriting, we obtain

$$i(t) = i_0\left\{\frac{C_O(0,t)}{C_O^\circ} - \frac{C_R(0,t)}{C_R^\circ} - \frac{nFv}{RT}\right\} \quad (16)$$

With $i(t) = I\cos(\omega t + \theta)$, $v(t) = V\cos\omega t$ and the values of $C_i(0, t)$, as derived in eqns. (13) and (15), substituted in (16), the resulting equation will be

$$\frac{I\cos(\omega t+\theta)}{i_0} = -\left\{\frac{I}{nAFC_O^\circ\sqrt{D_{O_2}\omega}}\left[1 + \frac{a_O}{2}\left(\sqrt{\frac{D_{O_2}}{D_{O_1}}} - \sqrt{\frac{D_{O_1}}{D_{O_2}}}\right)\right]\sin(\omega t+\theta+\phi_O)\right.$$

$$\left. + \frac{I}{nAFC_R^\circ\sqrt{D_{R_2}\omega}}\left[1 + \frac{a_R}{2}\left(\sqrt{\frac{D_{R_2}}{D_{R_1}}} - \sqrt{\frac{D_{R_1}}{D_{R_2}}}\right)\right]\sin(\omega t+\theta+\phi_R) + \frac{nFV\cos\omega t}{RT}\right\} \quad (17)$$

(The negative sign accompanying the terms in the right hand side is due to the convention C_{11} being chosen[7]). Thus one can obtain the I–V relationship, and an equation for the phase angle between the alternating components of the faradaic current and the electrode potential. In particular, the situation existing adjacent to the electrode–solution interface can be simulated by an equivalent circuit comprising a resistance R_r' and a capacitance C_r' in series, provided the applied field is so small that $(nFV/RT)^2 \ll 1$.

The expressions for R_r' and $1/\omega C_r'$ as derived for this model can easily be proved to be

$$R_r' = R_r + \frac{RT}{n^2F^2}\left[\frac{v_O}{C_O^\circ}\left(\frac{1}{D_{O_1}} - \frac{1}{D_{O_2}}\right) + \frac{v_R}{C_R^\circ}\left(\frac{1}{D_{R_2}} - \frac{1}{D_{R_1}}\right)\right]$$

and

$$1/\omega C_r' = 1/\omega C_r$$

where

$$R_r = \frac{RT}{nF}\left[\frac{1}{i_O} + \frac{1}{nF\sqrt{2\omega}}\left(\frac{1}{C_O^\circ\sqrt{D_{O_2}}} + \frac{1}{C_R^\circ\sqrt{D_{R_2}}}\right)\right]$$

and

$$1/\omega C_r = \frac{RT}{n^2F^2}\left[\frac{1}{\sqrt{2\omega}}\left(\frac{1}{C_O^\circ\sqrt{D_{O_2}}} + \frac{1}{C_R^\circ\sqrt{D_{R_2}}}\right)\right]$$

It may be observed that R_r and $1/\omega C_r$ are the same as those obtained for the *unperturbed* model[1,2,3,4] (*i.e.*, where $D_{i_1} = D_{i_2}$).

Hence, to the first order in the parameter $v_0\sqrt{\omega/D_{i_1}}$, it is seen that the effect of a variation in the diffusion coefficient near the electrode surface is to alter the value of the resistance by a quantity *which is independent of frequency*, whereas $1/\omega C_r$ remains unaffected.

It has been proved for the classical case (*i.e.*, $D_{i_1} = D_{i_2}$):

(a) that a plot of R_r *vs.* $1/\sqrt{\omega}$ will be a straight line whose intercept is inversely proportional to the exchange current density;

(b) that the plot of $1/\omega C_r$ *vs.* $1/\sqrt{\omega}$ will be a straight line passing through the origin;

(c) $(R_r - 1/\omega C_r)$ is equal to RT/nFi_O;

(d) $\cot\theta = \omega R_r C_r = 1 + (nFC_O/\beta i_O)\sqrt{2\omega D_{O_2}}$ where $\beta = 1 + C_O^\circ\sqrt{D_{O_2}}/C_R^\circ\sqrt{D_{R_2}}$ so that according to this classical model, it is *a priori impossible* for $\cot\theta$ to be $\leqslant 1$, so that θ is always $\leqslant \pi/4$.

It may be noted that, according to the present model:

(a) the plot of R_r' *vs.* $1/\sqrt{\omega}$ is a straight line, but the intercept is no longer $= RT/nFi_O$;

(b) the graphs $1/\omega C_r'$ *vs.* $1/\sqrt{\omega}$ will still be a straight line and, practically, the change in the model has no effect on this;

(c) $R_r' - 1/\omega C_r'$ cannot be a measure of $1/i_O$ since $(R_r' - 1/\omega C_r') - RT/nFi_O$ is generally different from zero and may be positive or negative;

(d) the expression for $\cot\theta = \omega R_r' C_r'$ is:

$$1 + \frac{nFC_O^\circ}{\beta i_O}\sqrt{2\omega D_{O_2}} + \frac{C_O^\circ\sqrt{2\omega D_{O_2}}}{\beta}\left[\frac{v_O\left(\frac{D_{O_2}}{D_{O_1}} - 1\right)}{C_O^\circ D_{O_2}} + \frac{v_R\left(\frac{D_{R_2}}{D_{R_1}} - 1\right)}{C_R^\circ D_{R_2}}\right]$$

so that the slope of the straight line $\cot\theta$ *vs.* $1/\sqrt{\omega}$ is not proportional to $1/K_s$, and the slope can be positive or negative. Hence, theoretically, there is the possibility of θ attaining a value greater than 45°.

CONCLUSIONS

Consequences that follow from the assumption that the diffusion coefficient near the electrode surface is different from that of the bulk are discussed by solving the diffusion equation with the appropriate boundary conditions. It is shown that, under certain conditions:

(a) the phase angle between the alternating components of the faradaic current and the voltage can be greater than $\pi/4$, say, for example when $i_O \to \infty$ and $D_{O_1} \gg D_{O_2}$;
(b) a parallel shift is expected for a plot of R_r' against $1/\sqrt{\omega}$ for not very high frequencies; at high frequencies, non-linearity in the behaviour is to be expected;
(c) for not very high frequencies $1/\omega C_r'$ is not different from $1/\omega C_r$, whereas for high frequencies the graph $1/\omega C_r'$ *vs.* $1/\sqrt{\omega}$ ceases to be a straight line.

SUMMARY

Consequences of the assumption that there are two diffusion layers (o, ν_i) and (ν_i, ∞) across the electrode-bulk region (with different diffusion coefficients) are discussed. The elements of the equivalent circuit which will follow from such a model are compared with those of the classical model[1,2].

APPENDIX I

To obtain the variation with time of the interfacial concentration, the partial differential equation

$$D_{i_1} \frac{\partial^2 C_i}{\partial x^2} = \frac{\partial C_i}{\partial t}$$

is to be solved in the region $x \leqslant \nu_i$ with the following conditions:

$$\text{(a)} \quad D_{i_2} \frac{\partial^2 C_i}{\partial x^2} = \frac{\partial C_i}{\partial t} \qquad x \geqslant \nu_i$$

$$\text{(b)} \quad C_i(x, t) \to C_i^{\circ} \qquad \text{as } x \to \infty$$

$$\text{(c)} \quad [C_i(x, t)]_{x=a-\varepsilon} \to [C_i(x, t)]_{x=a+\varepsilon} \qquad \text{as } \varepsilon \to 0$$

$$\text{(d)} \quad D_{i_1} \frac{\partial C_i}{\partial x}\Big)_{x=a-\varepsilon} \to D_{i_2} \frac{\partial C_i}{\partial x}\Big)_{x=a+\varepsilon} \qquad \text{as } \varepsilon \to 0$$

$$\text{(e)} \quad D_{i_1} \frac{\partial C_i}{\partial x}\Big)_{x=0} = \pm \frac{i(t)}{nFA}$$

(positive sign for $i = O$; negative sign for $i = R$; $i(t)$ = net cathodic current)

$$\text{(f)} \quad C_i(x, 0) = C_i^{\circ}$$

Denoting the Laplace Transform of $C_i(x, t)$ as $\mathscr{L}[C_i(x, t)] = \bar{C}_i(x, p)$, the equations to be solved become,

$$D_{i_1} \frac{\mathrm{d}^2 \bar{C}_i}{\mathrm{d}x^2} - p(\bar{C}_i - \bar{C}_i^{\circ}) = 0 \qquad 0 \leqslant x \leqslant \nu_i$$

$$D_{i_2} \frac{\mathrm{d}^2 \bar{C}_i}{\mathrm{d}x^2} - p(\bar{C}_i - \bar{C}_i^{\circ}) = 0 \qquad x \geqslant \nu_i$$

The solutions of which assume the form,

$$\bar{C}_i(x, p) - C_i^{\circ} = A_1 \exp(\sqrt{p/D_{i_1}}\, x) + B_1 \exp(-\sqrt{p/D_{i_1}}\, x) \qquad x \leqslant \nu_i$$

$$= A_2 \exp(\sqrt{p/D_{i_2}}\, x) + B_2 \exp(-\sqrt{p/D_{i_2}}\, x) \qquad x > \nu_i$$

The boundary condition (b) gives $A_2 = 0$. Using (c) and (d), we obtain

$$A_1 \exp(\sqrt{p/D_{i_1}}\, v_i) + B_1 \exp(-\sqrt{p/D_{i_1}}\, v_i) = B_2 \exp(-\sqrt{p/D_{i_2}}\, v_i)$$

and

$$\sqrt{\frac{D_{i_1}}{D_{i_2}}}\,[A_1 \exp(\sqrt{p/D_{i_1}}\, v_i) - B_1 \exp(-\sqrt{p/D_{i_1}}\, v_i)] = -B_2 \exp(-\sqrt{p/D_{i_2}}\, v_i)$$

Thus it may be seen that,

$$A_1\left(1 + \sqrt{\frac{D_{i_1}}{D_{i_2}}}\right)\exp(\sqrt{p/D_{i_1}}\, v_i) + B_1\left(1 - \sqrt{\frac{D_{i_1}}{D_{i_2}}}\right)\exp(-\sqrt{p/D_{i_1}}\, v_i) = 0$$

or

$$A_1\left(\frac{\sqrt{D_{i_2}} + \sqrt{D_{i_1}}}{\sqrt{D_{i_2}} - \sqrt{D_{i_1}}}\right)\exp(2\sqrt{p/D_{i_1}}\, v_i) = -B_1 \qquad \text{A(1)}$$

By virtue of condition (e)

$$A_1 - B_1 = \pm \frac{\bar{i}(p)}{nFA\sqrt{D_{i_1} p}} \qquad \text{A(2)}$$

so that A_1 and B_1 can be solved from A(1) and A(2).

$$A_1 = \pm \frac{i(p)}{nFA\sqrt{D_{i_1} p}} \cdot \frac{D'}{D' + \exp(2\sqrt{p/D_{i_1}}\, v_i)}$$

where, for brevity, D' has been written for

$$\frac{\sqrt{D_{i_2}} - \sqrt{D_{i_1}}}{\sqrt{D_{i_2}} + \sqrt{D_{i_1}}}$$

and

$$B_1 = \mp \frac{i(p)}{nFA\sqrt{D_{i_1} p}} \cdot \frac{\exp(2\sqrt{p/D_{i_1}}\, v_i)}{D' + \exp(2\sqrt{p/D_{i_1}}\, v_i)}$$

The transform of the interfacial concentration is, therefore,

$$C_i^\circ + A_1 + B_1 = \mp \frac{\bar{i}(p)}{nFA\sqrt{D_{i_1} p}} \cdot \frac{1 - D' \exp(-2\sqrt{p/D_{i_1}}\, v_i)}{1 + D' \exp(-2\sqrt{p/D_{i_1}}\, v_i)} + C_i^\circ$$

In general,

$$\bar{C}_i(x, p) - C_i^\circ = A_1 \exp(\sqrt{p/D_{i_1}}\, x) + B_1 \exp(-\sqrt{p/D_{i_1}}\, x)$$

$$= \exp(-\sqrt{p/D_{i_1}}\, x)\left[\mp \frac{\bar{i}(p)}{nFA\sqrt{D_{i_1} p}}\right]\left\{\frac{1 - D' \exp[-2\sqrt{p/D_{i_1}}\,(v_i - x)]}{1 + D' \exp(-2\sqrt{p/D_{i_1}}\, v_i)}\right\} \qquad \text{A(3)}$$

$$\bar{C}_i(0, p) - C_i^\circ = \mp \frac{\bar{i}(p)}{nFA\sqrt{D_{i_1} p}} \cdot \frac{1 - \exp[-(2\sqrt{p/D_{i_1}}\, v_i + \gamma)]}{1 + \exp[-(2\sqrt{p/D_{i_1}}\, v_i + \gamma)]} \quad \text{if} \quad D_{i_1} < D_{i_2}$$

$$= \mp \frac{\bar{i}(p)}{nFA\sqrt{D_{i_1}p}} \cdot \frac{1 + \exp[-2(\sqrt{p/D_{i_1}}\nu_i + \gamma)]}{1 - \exp[-2(\sqrt{p/D_{i_1}}\nu_i + \gamma)]} \quad \text{if} \quad D_{i_1} > D_{i_2} \qquad \text{A(4)}$$

where $\exp(-2\gamma)$ is written for D' (if $D_{i_1} < D_{i_2}$) and for $-D'$ (if $D_{i_1} > D_{i_2}$).

APPENDIX II

To obtain the inverse transform of $\bar{C}_i(x, p)$, one may use the operational relationships,

$$p^{\frac{1}{2}} \tanh(p^{\frac{1}{2}} + \alpha) = \mathscr{L}\{e^{\alpha^2 t}[\theta_2(\alpha t/i\pi t) + \hat{\theta}_2(\alpha t/i\pi t)] - 1/\sqrt{\pi t}\} \qquad \text{B(1)}$$

$$p^{\frac{1}{2}} \coth(p^{\frac{1}{2}} + \alpha) = \mathscr{L}\{e^{\alpha^2 t}[\theta_3(\alpha t/i\pi t) + \hat{\theta}_3(\alpha t/i\pi t)] - 1/\sqrt{\pi t}\} \qquad \text{B(2)}$$

$$\frac{\bar{f}_1(p)\bar{f}_2(p)}{p} = \mathscr{L}\left\{\int_0^t f_1(\tau) f_2(t - \tau)\, d\tau\right\} \qquad \text{B(3)}$$

and

$$\bar{f}_1(\beta p) = \mathscr{L}[f_1(t/\beta)] \qquad \text{B(4)}$$

In particular, only $C_i(o, t)$ is of interest to us, and so $C_i(o, t)$ $(i = O, R)$ are expressed in terms of Theta functions and modified Theta functions which are defined by

$$\theta_2(\nu/\tau) = (-i\tau)^{-\frac{1}{2}} \sum_{n=-\infty}^{\infty} (-1)^n \exp[-i\pi(\nu + n)^2/\tau]$$

$$\theta_3(\nu/\tau) = (-i\tau)^{-\frac{1}{2}} \sum_{n=-\infty}^{\infty} \exp[-i\pi(\nu + n)^2/\tau]$$

$$\hat{\theta}_2(\nu/\tau) = (-i\tau)^{-\frac{1}{2}} \left[\sum_{n=0}^{\infty} (-1)^n \exp[-i\pi(\nu + n)^2/\tau] - \sum_{n=-1}^{-\infty} (-1)^n \exp[-i\pi(\nu + n)^2/\tau]\right] \qquad \text{B(5)}$$

and

$$\hat{\theta}_3(\nu/\tau) = (-i\tau)^{-\frac{1}{2}} \left[\sum_{n=0}^{\infty} \exp[-i\pi(\nu + n)^2/\tau] - \sum_{n=-1}^{-\infty} \exp[-i\pi(\nu + n)^2/\tau]\right] \qquad \text{B(6)}$$

Since

$$\bar{C}_i(o, p) - C_i^\circ = \mp \frac{\bar{i}(p)}{nFA\sqrt{D_{i_1}p}} \coth(\nu_i\sqrt{p/D_{i_1}} + \gamma) \quad (\text{for } D_{i_1} > D_{i_2})$$

and

$$= \mp \frac{\bar{i}(p)}{nFA\sqrt{D_{i_1}p}} \tanh(\nu_i\sqrt{p/D_{i_1}} + \gamma) \quad (\text{for } D_{i_1} < D_{i_2})$$

with

$$\exp(-2\gamma) = D' \ (\text{for } D_{i_1} < D_{i_2})$$
$$= -D' \ (\text{for } D_{i_1} > D_{i_2}) \quad (\text{Refer to A(4), Appendix I.})$$

With the help of B(1) to B(4), we may conclude that

$$C_i(o, t) - C_i^\circ = \mp \frac{1}{nAF\sqrt{D_{i_1}}} \int_0^t i(t - \tau)\phi(\tau)\, d\tau$$

where

$$\phi(t) = \frac{\nu_i}{\sqrt{D_{i_1}}} e^{\nu^2 D_{i_1} t/\nu_i^2} \left[\theta_3\left(\frac{\gamma D_{i_1} t/\nu_i^2}{i\pi D_{i_1} t/\nu_i^2}\right) + \theta_3\left(\frac{\gamma D_{i_1} t/\nu_i^2}{i\pi D_{i_1} t/\nu_i^2}\right)\right] - 1/\sqrt{\pi t} \qquad \text{B(7)}$$

for $D_{i_1} > D_{i_2}$, and a similar expression for $D_{i_1} < D_{i_2}$ substituting θ_2 for θ_3 in B(7).

Alternatively, one may use the operational rule that if

$$\lambda(x) = \sum_{n=0}^{\infty} C_n x^n \quad (|x| < \varrho),$$

$$\mathscr{L}\left\{\frac{U(t)}{\sqrt{\pi t}} \sum_{n=0}^{\infty} C_n \exp\left[(-n^2/4)t\right]\right\} = \sqrt{p}\ \lambda\left[\exp\left(-\sqrt{p}\right)\right] \qquad \text{B(8)}$$

($U(t)$, is Heaviside's unit step function), which with B(3) yields

$$(nFA\sqrt{D_{i_1}})\ \ (C_i(0,t) - C_i^0) = \sum_{n=0}^{\infty} C_n \int_0^t i(t-\tau)\ \frac{\exp\left(-a^2 n^2/D_{i_1}\tau\right)}{\sqrt{\pi\tau}}\, d\tau \qquad \text{B(9)}$$

where

$$\frac{1 - D' \exp\left(-2\sqrt{p/D_{i_1}}\,\nu_i\right)}{1 + D' \exp\left(-2\sqrt{p/D_{i_1}}\,\nu_i\right)} = \sum_{n=0}^{\infty} C_n \exp\left(-2n\sqrt{p/D_{i_1}}\,\nu_i\right)$$

Using B(5), the solutions as given by B(7) and B(9) can be proved to be identical.

REFERENCES

1 J. E. B. RANDLES, *Discussions Faraday Soc.*, 1 (1947) 11.
2 B. V. ERSHLER, *ibid.*, 1 (1947) 269.
3 D. C. GRAHAME, *J. Electrochem. Soc.*, 99 (1952), 370 c.
4 P. DELAHAY, *New Instrumental Methods in Electrochemistry*, Interscience Publishers Inc., New York, 1954.
5 S. K. RANGARAJAN, *J. Electroanal. Chem.*, 1 (1960) 396.
6 S. K. RANGARAJAN AND K. S. G. DOSS, *J. Electroanal. Chem.*, 4 (1962) 237.
7 S. K. RANGARAJAN AND K. S. G. DOSS, *Electrochim. Acta*, 7 (1962) 201.

A POLAROGRAPHIC STUDY OF INDIUM THIOCYANATE COMPLEXES

T. P. RADHAKRISHNAN AND A. K. SUNDARAM

Analytical Division, Atomic Energy Establishment, Trombay, Bombay (India)

(Received June 12th, 1962)

INTRODUCTION

Trivalent indium forms thiocyanate complexes in aqueous solution. SUNDEN[1] has investigated the lower complexes, $In(SCN)^{2+}$, $In(SCN)_2^-$ and $In(SCN)_3$ potentiometrically using an indium electrode. Evidence for the formation of the anionic complex $In(SCN)_4^-$, has been obtained by the distribution method[2]. The purpose of our study was to determine the stability constants of the thiocyanate complexes of indium from the polarographic data.

EXPERIMENTAL

Apparatus

Current–voltage measurements were made on a manual set-up using a H-type cell in conjunction with a saturated calomel electrode as the reference electrode. The experiments were carried out at 30 $\pm$ 0.1° with air-free solutions. Average currents were measured and the diffusion currents were corrected for the residual currents. The half-wave potentials were obtained by plotting $\log(i/i_d - i)$ against $E_{d.e.}$ (*vs.* S.C.E. and corrected for the iR drop) in steps of 5 mV along the rising part of the curve. The capillary used in these measurements had the following characteristics: $m = 1.33$ mg sec^{-1}, $t = 3.7$ sec in 0.1 N KCl at -0.7 V *vs.* S.C.E.

Reagents

Ammonium thiocyanate (E. Merck, G.R.) was used without further purification. Other chemicals were of analytical grade. The indium perchlorate stock solution was obtained from indium metal. A known weight of the metal (B.D.H., 99.9%) was dissolved in nitric acid. After removing the excess acid, the nitrate was converted to the perchlorate by repeated fuming with perchloric acid. Sufficient perchloric acid was added to the residue to prevent hydrolysis and the solution diluted to the desired volume. Total indium in the solution was estimated by titration with EDTA[3]. Gelatin, at a concentration of $1 \cdot 10^{-3}$% in the final solution, was found satisfactory as the maximum suppressor.

RESULTS AND DISCUSSION

Experiments were carried out with $5.1 \cdot 10^{-4}$ M indium and 0.1 M perchloric acid. The concentration of ammonium thiocyanate was varied from $2 \cdot 10^{-2}$ to 1.2 M keep-

ing the ionic strength at 2.0 by the addition of requisite amounts of sodium perchlorate. The evidence for the reversibility of the polarographic reduction of indium in thiocyanate medium was obtained from the following experimental facts: (i) the temperature coefficient for the diffusion current was 1% per degree and that for the half-wave potential was +1.5 mV per degree; (ii) the plots of $\log(i/i_d - i)$ against $E_{d.e.}$ gave good straight lines with the slope equal to 20 ± 2 mV.

The half-wave potential for the reduction of the aquo-indic ion was determined by extrapolation of the values obtained at lower concentrations of ammonium thiocyanate. A value of −0.4833 V *vs.* S.C.E. was obtained. This is in good agreement with the value of −0.485 reported by COZZI AND VIVARELLI[4], who used indium-amalgam electrodes for measuring the half-wave potentials for progressively smaller concentrations of different supporting electrolytes.

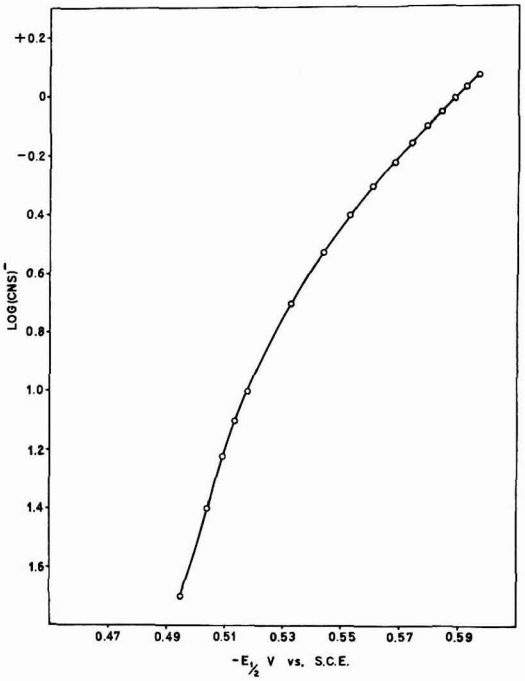

Fig. 1. $E_{1/2}$ as a function of thiocyanate concentration.

The plot of the half-wave potentials against log(SCN^-) was a curve (Fig. 1). The formation constants were calculated by the method of DE FORD AND HUME[5] using the general form of the equations

$$F_0(X) = \text{antilog } \{0.435\, nF/RT[(E_{1/2})_s - (E_{1/2})_c] + \log I_s/I_c\} \quad (1)$$

$$F_1(X) = \frac{[F_0(X) - K_0/f_s]}{C_X f_X} \quad (2)$$

$$F_2(X) = \frac{[F_1(X) - K_1/f_{MX}]}{C_X f_X} \quad (3)$$

TABLE I

ANALYSIS OF $F_j(X)$ FUNCTION

$HClO_4 = 0.1\ M$; In $= 5.1 \cdot 10^{-4}\ M$; ionic strength $= 2.0$; $(E_{1/2})_s = -0.4833$ *vs.* S.C.E.; $(i_d)_s = 3.55\ \mu A$.

NH₄SCN (*M*)	$E_{1/2}$ *vs.*S.C.E. (*V*)	i_d (μA)	$F_0(X) \cdot 10^{-2}$	$F_1(X) \cdot 10^{-1}$	$F_2(X) \cdot 10^{-2}$	$F_3(X) \cdot 10^{-2}$	$F_4(X) \cdot 10^{-2}$	$F_5(X) \cdot 10^{-2}$	$F_6(X) \cdot 10^{-2}$
0.02	0.4955	3.69	0.0392	14.6	—	—	—	—	—
0.04	0.5042	3.69	0.1067	24.2	30.5	—	—	—	—
0.06	0.5094	3.69	0.1942	30.7	31.2	—	—	—	—
0.08	0.5135	3.73	0.3080	37.3	31.6	194.5	244.1	—	—
0.1	0.5176	3.75	0.4911	48.1	36.1	201.1	261.0	—	—
0.2	0.5330	3.76	2.884	143.7	65.9	249.3	371.3	—	—
0.3	0.5435	3.76	9.638	320.9	102.9	289.9	383.1	—	—
0.4	0.5527	3.76	27.8	694.8	170.7	386.7	529.3	898.2	620.6
0.5	0.5605	3.76	68.23	1364.4	270.5	508.9	667.9	995.8	691.7
0.6	0.5670	3.77	143.80	2396.5	397.4	635.7	767.8	996.4	577.3
0.7	0.5735	3.82	300.00	4285.6	610.5	849.3	963.3	1133.3	690.4
0.8	0.5790	3.82	565.00	7062.4	881.3	1081.6	1133.3	1204.1	692.6
0.9	0.5840	3.82	1005.00	11166.6	1239.4	1359.3	1315.9	1273.2	692.5
1.0	0.5885	3.86	1669.00	16689.9	1667.8	1651.8	1476.8	1306.8	656.8
1.1	0.5925	3.86	2646.00	24054.5	2185.7	1972.4	1634.0	1330.9	619.0
1.2	0.5968	3.86	4341.00	36174.9	3013.6	2497.9	1935.8	1471.5	684.6

K_j values: $K_0 = 1$; $K_1 = 1.2 \cdot 10^2$; $K_2 = 1.6 \cdot 10^3$; $K_3 = 1.75 \cdot 10^4$; $K_4 = 1.7 \cdot 10^4$; $K_5 = 6.5 \cdot 10^4$; $K_6 = 6.9 \cdot 10^4$.

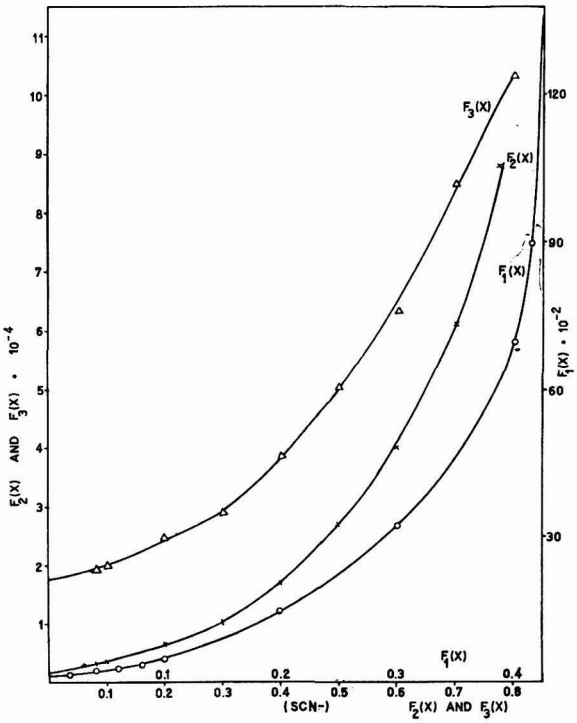

Fig. 2. Plot of $F_1(X)$, $F_2(X)$ and $F_3(X)$ as a function of thiocyanate concentration.

where the subscripts s and c refer to the aquated ion and the complex respectively and I_s/I_c is the ratio of the diffusion current constants. K_0 and K_1 are the formation constants of the zero complex and the complex containing one ligand. C_X denotes the concentration of the complexing agent and the f's represent the activity coefficients. The experimentally determined values of the half-wave potential and the diffusion current, together with the $F_j(X)$ values calculated from eqns. (1), (2) and (3) assuming f_X as unity, are given in Table I. The overall formation constants given in Table I

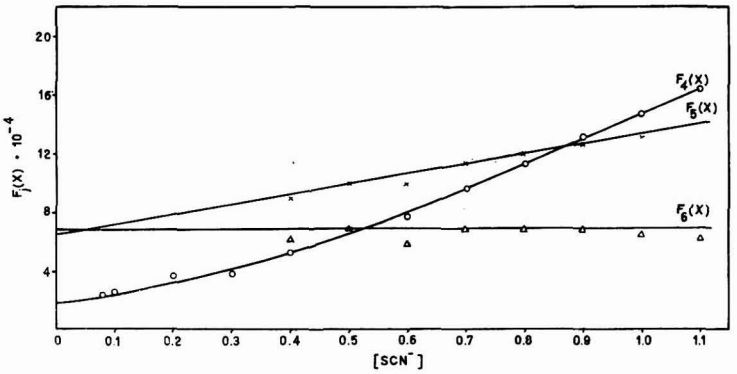

Fig. 3. Plot of $F_4(X)$, $F_5(X)$ and $F_6(X)$ as a function of thiocyanate concentration.

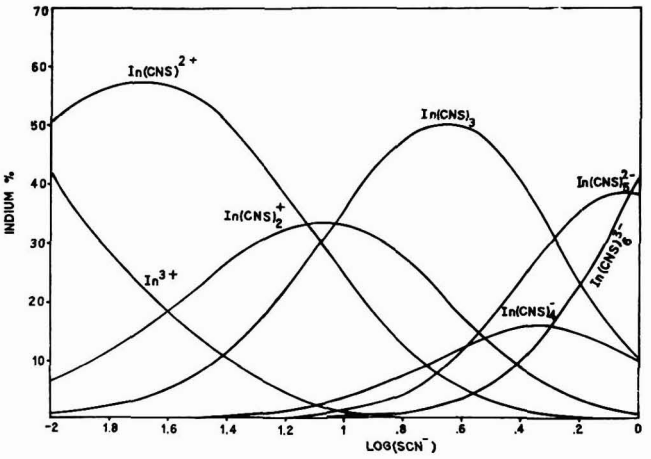

Fig. 4. Percentage of indium in various forms as a function of free thiocyanate concentration.

were obtained by a graphical extrapolation (Figs. 2 and 3) of the $F_j(X)$ functions to zero ligand concentration. The probable error of each constant is estimated to be $\pm$ 15%. The overall formation constants for the complex ion $In(SCN)^{2+}$, $In(SCN)_2^+$, $In(SCN)_3$, $In(SCN)_4^-$, $In(SCN)_5^{2-}$ and $In(SCN)_6^{3-}$ are $1.2 \cdot 10^2$, $1.6 \cdot 10^3$, $1.75 \cdot 10^4$, $1.7 \cdot 10^4$, $6.5 \cdot 10^4$ and $6.9 \cdot 10^4$. The first three stepwise constants reported by SUNDEN

(*loc. cit.*) are log $k_1 = 2.58$, log $k_2 = 1.02$ and log $k_3 = 1.03$. The values obtained here for the same constants are 2.08, 1.25 and 1.04 respectively.

Figure 4 gives the distribution of indium, in per-cent, present as the cationic or anionic form, as a function of the logarithm of the thiocyanate concentration.

ACKNOWLEDGEMENTS

The authors wish to thank Dr. V. T. ATHAVALE, Head, Analytical Division, A.E.E.T., for his kind interest and encouragement.

SUMMARY

The variation of the half-wave potential of indic ion as a function of ammonium thiocyanate concentration has been studied at an ionic strength of 2.0 in $HClO_4$–$NaClO_4$ medium. The results are interpreted on the basis of complex formation of indium with thiocyanate. The overall constants for the six complex ions have been estimated.

REFERENCES

1 N. SUNDEN, *Svensk. Kem. Tidskr.*, 66 (1954) 50.
2 F. AUERBACH AND H. PECK, *Arb. Kaiser. Gesundh.*, 38 (1911) 243.
3 F. J. WELCHER, *The Analytical Uses of Ethylenediaminetetraacetic acid*, D. van Nostrand Company, London and Inc., New York, p. 179.
4 D. COZZI AND S. VIVARELLI, *Z. Elektrochem.*, 58 (1954) 907.
5 D. D. DE FORD AND D. N. HUME, *J. Am. Chem. Soc.*, 73 (1957) 5321.

ETUDE THERMODYNAMIQUE DE LA DISSOCIATION DE L'ACIDE GLUTAMIQUE

J. LLOPIS ET D. ORDONEZ

Instituto de Química Física, "Rocasolano", C.S.I.C., Madrid (Espagne)

(Reçu le 18 juin, 1962)

Malgré l'importance biochimique de cet acide aminé, on ne dispose pas d'information sur la variation de ses constantes macroscopiques de dissociation en fonction de la température et, en conséquence, des magnitudes thermodynamiques dépendent de ce processus d'ionisation.

C'est pour ce motif que nous avons déterminé ces constantes de dissociation de l'acide glutamique (pK_1,pK_2,pK_3), dans un intervalle de températures de 5–50°, par la méthode des f.e.m. de cellules sans union liquide. On trouvera dans ce travail les résultats obtenus.

TECHNIQUE EXPÉRIMENTALE

La détermination des constantes de dissociation d'un acide faible, par la méthode tensiométrique, s'effectue en employant des cellules sans union liquide du type

$$Pt,H_2 \,/\, AH\ (M_1),\ NaA\ (M_2),\ NaCl\ (M_3) \,/\, AgCl,Ag \,/\, Pt \qquad (1)$$

qui contient des ions H^+, provenant de l'acide faible, et des ions Cl^- provenant du NaCl, chacune avec deux électrodes réversibles correspondant à ces mêmes ions. La tension chimique (ou force électromotrice) de cette cellule est donc

$$E = E^\circ - \frac{RT}{F} \ln M_{H^+} M_{Cl^-} - \frac{RT}{F} \ln \gamma_{H^+} \gamma_{Cl^-} \qquad (2)$$

Dans le cas de l'acide glutamique, on obtient une détermination plus adéquates de la première constante d'ionisation acide K_1, avec une cellule du type

$$Pt,H_2 \,/\, Ac.Glut.\ (M_1),\ HCl\ (M_2) \,/\, AgCl,\ Ag \,/\, Pt \qquad (3)$$

où la molalité $M_1 \simeq M_2$. Tandis qu'on détermine la seconde et troisième constantes d'ionisation au moyen de cellules du type

$$Pt,\ H_2 \,/\, Ac.\ Glut.\ (M_1),\ NaOH\ (M_2),\ NaCl\ (M_3) \,/\, AgCl,Ag \,/\, Pt \qquad (4)$$

où $M_1 \simeq 3/2\ M_2$ dans le cas de K_2, et $M_1 \simeq 2/3\ M_2$ dans le cas de K_3.

Préparation des électrodes

(a) Electrodes d'hydrogène. Les électrodes d'hydrogène employées dans ce but ont été préparées selon les prescriptions de BATES[1].

(b) Electrodes de AgCl,Ag. IVES ET JANZ[2] ont donné récemment une étude assez ample de la préparation de ces électrodes. Celles que nous avons utilisées correspondent au type appelé „électrolytique". Pour leur vérification, on dispose de 2 électrodes de H_2 et 5 électrodes de AgCl,Ag, et l'on effectue les mesures tensiométriques des 10 cellules possibles, avec une solution de HCl $\simeq$ 0.05 *N*. La déviation standard de la moyenne de ces 10 déterminations est habituellement de 0.03 mV.

Description de la cellule

La cellule employée a la forme d'un H, (Fig. 1), avec un robinet qui sépare les deux compartiments. La disposition de cette cellule permet d'utiliser un bain d'eau dans le thermostat.

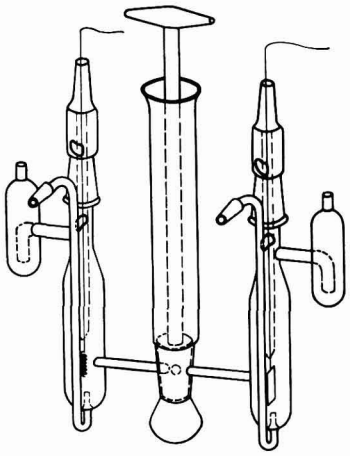

Fig. 1. Schéma de la cellule de mesure.

Contrôle de la température

Les mesures de température ont été réalisées avec une precision de $\pm$ 0.02°. En général, les températures étudiées sont comprises entre 0 et 50°.

Mesures électriques

L'ensemble expérimental permet d'effectuer des mesures avec une précision de 0.01 mV.

Vérification de la technique expérimentale

Pour vérifier la technique nous avons réalisé une série de six expériences, en employant comme électrolyte des solutions de HCl, de molalités comprises entre 0.1–0.01 *M*. Ces mesures nous ont permis de déterminer $E°$, pour une valeur donnée de la température, et comparer les résultats obtenus avec ceux qui ont été publiés jusqu'à présent. La cellule dont on a mesuré la tension chimique (ou f.e.m.) est la suivante:

$$Pt,H_2/HCl\ (M)\ /\ AgCl,Ag/Pt \qquad (5)$$

On corrige les valeurs mesurées de la E, pour ce qui concerne l'électrode de H_2, à la pression normale (760 mm)[3]. Pour réaliser l'extrapolation qui conduit à la détermination de $E°$, nous représentons en fonction de M l'expression

$$E' \equiv E° + 2\phi \log M - 2\phi S_f\sqrt{\Gamma} = E° - 2\phi BM \qquad (6)$$

Les valeurs des constantes ϕ et S_f, ainsi que la notation employée, ont été empruntées à l'ouvrage de HARNED ET OWEN[3] ou à la nomenclature élaborée par le C.I.T.C.E.

Dans la représentation des valeurs de E' en fonction de M, on obtient des lignes droites, ce qui rend l'extrapolation beaucoup plus sûre et conduit à la valeur de $E°$, à 25°

$$E° = +0.2222_5 \text{ V}$$

qui coïncide d'une manière satisfaisante avec les résultats obtenus par de nombreux chercheurs. De plus, on observe aussi, avec cette série d'expériences, que non seulement la valeur de $E°$ mais aussi les valeurs de E', pour toutes les valeurs de M, coïncident d'une manière satisfaisante avec les résultats obtenus par d'autres auteurs. On peut déduire de tout cela, que la précision que nous avons obtenue est suffisante.

Préparation et pureté des produits employés

(a) Acide chlorhydrique. On prépare une solution — 1 N avec HCl Merck, pure pour analyse. On titre six fois avec du borax et quatre avec du Na_2CO_3, obtenant ainsi la concentration c en mol/l, à 20°. Le matériel employé dans ce travail a été préalablement calibré.

(b) Chlorure sodique. On a recristallisé deux fois le produit Probus, dans de l'eau de conductivité. On a précipité le NaCl dans une solution concentrée de HCl, on a introduit le sel dans un tube de verre et on y a fait le vide (10^{-2} mm). On y a fait passer ensuite un courant de N_2 sec, pour en enlever le HCl et la vapeur d'eau. Finalement, on a chauffé le sel dans un creuset de Pt à 400°, pendant 6 h.

(c) Hydroxide sodique. On a préparé la solution de NaOH — 1 N par dilution d'une solution saturée, décantée et claire. On l'a gardée dans une bouteille fermée, avec les précautions nécessaires pour éviter l'action de CO_2. On l'a titrée avec du HCl, en employant de la phénolphtaleine et du méthyl-orange comme indicateurs.

(d) Acide glutamique. On a employé l'acide $l(+)$-glutamique préparé par la maison T. Schuchardt (München). La pureté a été vérifiée en déterminant l'azote par le micro-Kjeldahl. La moyenne de six déterminations a été de 9.53% tandis que la valeur théorique est de 9.52% de N_2. La rotation optique, mesurée dans une dissolution d'acide nitrique, à 20°, a été de $[\alpha]_D^{20°} = 30.0_7$, tandis que la valeur des tables[4] est de 29.9°.

Préparation des solutions à mesurer

Pour déterminer la première constante de dissociation on emploie une série de solutions qui contiennent de l'acide glutamique, du HCl et de l'H_2O. Pour déterminer la seconde et la troisième constantes de dissociation on emploie une série de solutions qui contiennent de l'acide glutamique, du NaCl, du NaOH et de l'H_2O. La préparation de ces dernières s'effectue dans une cage de manipulation, dans laquelle il y a une surpression de N_2, sec et exempt de CO_2, pour éviter la carbonatation du NaOH.

L'H_2O employée a été préalablement distillée et ensuite bouillie et mise à refroidir dans l'interieur de la cage même.

DÉTERMINATION DE LA PREMIÈRE CONSTANTE DE DISSOCIATION

Exposé théorique

Dans la cellule (3), l'équation qui représente la quantité total d'acide aminé, sous les quatre formes sous lesquelles il peut se trouver, est la suivante:

$$T_A = M_{H_2AH^+} + M_{HAH^\pm} + M_{HA^-} + M_{A^{2-}} \tag{7}$$

L'équation qui exprime la neutralité électrique de la solution sera:

$$M_{H_2AH^+} + M_{H^+} = M_{Cl^-} + M_{HA^-} + M_{OH^-} + 2M_{A^{2-}} \tag{8}$$

et la première constante d'équilibre de dissociation sera donnée par:

$$K_1 = \frac{M_{H^+}M_{HAH^\pm}}{M_{H_2AH^+}} \cdot \frac{\gamma_{H^+}\gamma_{HAH^\pm}}{\gamma_{H_2AH^+}} \tag{9}$$

On peut obtenir à partir de ces éqns., vu que les concentrations $M_{A^{2-}}$ et M_{OH^-} sont négligeables en milieu acide, l'expression pour M_{H^+}, qui combinée avec l'expression (2) relative à la f.e.m. de la cellule, permet d'obtenir l'expression:

$$pK_1' \equiv pK_1 - \log \frac{\gamma_{H_2AH^+}}{\gamma_{H^+}\gamma_{HAH^\pm}} = \frac{E - E^\circ}{\phi} + \log M_{Cl^-} + \log \gamma_{H^+}\gamma_{Cl^-} + \log \frac{M_{Cl^-} - M_{H^+} + M_{HA^-}}{T_A - M_{Cl^-} + M_{H^+} + 2M_{HA^-}} \tag{10}$$

Si l'on attribue une valeur approchée à K_2, on peut obtenir les valeurs de M_{HA^-} en employant l'expression:

$$M_{HA^-} = \frac{K_2'(T_A + M_{H^+} - M_{Cl^-})}{M_{H^+} + 2K_2'} \tag{11}$$

expression à partir de laquelle on calcule le dernier terme de (10).

La force ionique pour ces déterminations sera:

$$\mu \equiv \tfrac{1}{2} \Sigma M_i Z_i^2 \simeq M_{HCl} + \tfrac{1}{2}M_{HA^-} \tag{12}$$

On trouve les valeurs de pK_1 par extrapolation à $\mu = 0$, des représentations de pK'_1 en fonction de μ. On peut faire dans l'éqn. (10) les deux approximations suivantes, en ce qui concerne le terme $\log \gamma_{H^+}\gamma_{Cl^-}$

$$\log \gamma_{H^+}\gamma_{Cl^-} = 2 \log \gamma_{\pm(HCl)} \tag{13}$$

$$\log \gamma_{H^+}\gamma_{Cl^-} = -2S_f (2d_0\mu)^{1/2} \tag{14}$$

où d_0 est la densité de l'eau à la température en question. A partir de celles-ci, en représentant les pK_1' en fonction de μ on obtient, pour des solutions très diluées, deux lignes droites de pente différente qui coupe l'ordonnée au même point, ce qui rend ces extrapolations plus sûres.

TABLE I

Molalités		*E observées et corrigées à 1 atm H_2*									*E interpolée*		
Ac. Glut.	*HCl*	*5°*	*10°*	*15°*	*20°*	*25°*	*30°*	*35°*	*40°*	*45°*	E_{25}	$a10^6$	$-b10^8$
0.09670_0	0.10000_0	—	—	0.38787_7	0.38766_6	0.38692_2	0.38616_6	0.38544_4	0.38466_6	0.38371_1	0.38689_9	—125	130
0.07089_9	0.06975_5	0.40487_7	0.40433_3	0.40348_8	0.40299_9	0.40216_6	0.40157_7	0.40119_9	0.40035_5	0.39998_8	0.40242_2	—286	557
0.04834_4	0.05000_0	0.41430_0	0.41494_4	0.41489_9	0.41494_4	0.41509_9	0.41498_8	0.41463_3	0.41428_8	0.41357_7	0.41507_7	— 19	265
0.03970_0	0.03908_8	0.42210_0	0.42266_6	0.42335_5	0.42380_0	0.42445_5	0.42474_4	0.42454_4	0.42437_7	0.42406_6	0.42433_3	54	327
0.03394_4	0.03511_1	0.42612_2	0.42711_1	0.42815_5	0.42900_0	0.42936_6	0.42951_1	0.42960_0	0.42951_1	0.42953_3	0.42930_0	33	635
0.01871_1	0.01845_5	0.44938_8	0.45060_0	0.45150_0	0.45268_8	0.45355_5	0.45423_3	0.45480_0	0.45508_8	0.45534_4	0.45351_1	151	290
0.01300_0	0.01344_4	0.46162_2	0.46315_5	0.46427_7	0.46565_5	0.46748_8	0.46856_6	0.46942_2	0.46979_9	0.47046_6	0.46724_4	229	313
0.00899_9	0.00886_6	0.47670_0	0.47859_9	0.48018_8	0.48186_6	0.48355_5	0.48478_8	0.48567_7	0.48651_1	0.48717_7	0.48340_0	265	375

Résultats expérimentaux

Pour une composition donnée de l'électrolyte, on a déterminé les f.e.m., tous les 5° dans l'intervalle de 5–45°. Les mesures se font dans les 48 h. Le premier jour l'on mesure à 25°, et l'on descend jusqu'à 5°, en vérifiant à la fin des mesures la valeur de la f.e.m. à 25°. Le lendemain on mesure de 20°–45° et l'on descend à nouveau à 25° pour vérifier la stabilité des électrodes. On utilise une ou deux électrodes de H_2 et six de AgCl,Ag. On corrige toutes les mesures vis-à-vis de la pression, et on déduit la moyenne des valeurs de E_x que l'on obtient de cette façon. Ces valeurs de E peuvent être représentées en fonction de la température par l'éqn.:

$$E = E_{25} + a(t - 25) + b(t - 25)^2 \qquad (15)$$

et les valeurs des paramètres se déterminent par la méthode des minima carrés. Dans la Table I on peut voir les valeurs de E à différentes concentrations de l'électrolyte

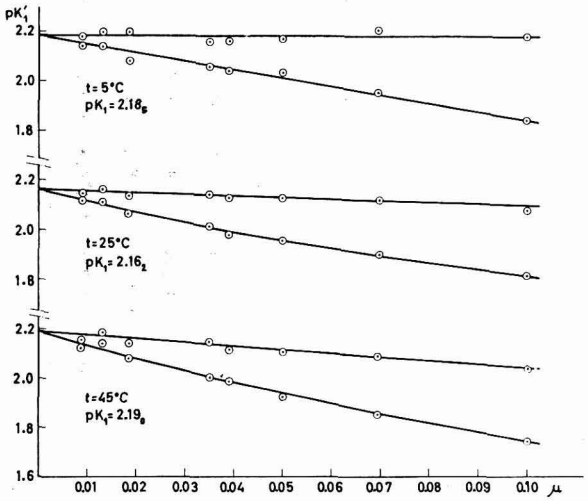

Fig. 2. Variation de pK_1' en fonction de la force ionique.

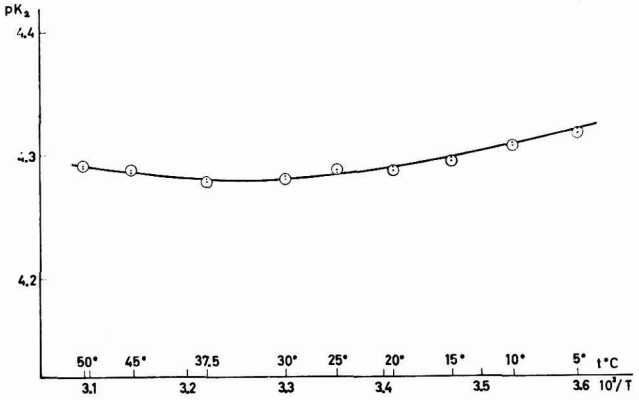

Fig. 3. Représentation des valeurs des pK_1 en fonction de $1/T$.

et à différentes températures. De même, on y réunit aussi les valeurs de E_{25}, a et b.

On calcule les valeurs de pK_1' en employant les expressions (10), (11), (13) et (14), et les valeurs de E° et ϕ dépendent de la température. La variation de pK_1' en fonction de μ à 5, 25 et 45° a été représentée dans la Fig. 2. Les extrapolations à $\mu = 0$ permettent de déterminer les valeurs correspondantes de pK_1. On représente les valeurs obtenues de cette façon dans la Fig. 3 en fonction de $1/T$.

Fonctions thermodynamiques ΔG_1°, ΔH_1°, et ΔS_1°

On peut représenter les valeurs trouvées de pK_1 en fonction de la température en appliquant la formule:

$$pK_1 = \frac{1961.6}{T} - 9.22_7 + 1.91_9 \cdot 10^{-2}T \qquad (16)$$

On a tracé la courbe interpolée dans la Fig. 3 avec les valeurs calculées à partir de cette expression.

On peut également ajuster une expression du type trouvé par HARNED ET EMBREE[5] et l'on obtient la meilleure interpolation avec l'expression suivante:

$$pK_1 = 2.16_4 + 6.5 \cdot 10^{-2}\,(t - 23.9)^2 \qquad (17)$$

Les valeurs de pK_1 à différentes températures, calculées en employant cette expression, sont données dans la Table II.

TABLE II

t°	5	10	15	20	25	30	35	40	45
pK_1(exptl.)	2.18$_5$	2.17$_8$	2.16$_9$	2.17$_4$	2.16$_2$	2.16$_5$	2.18$_0$	2.17$_8$	2.19$_0$
pK_1(calc. 16)	2.18$_9$	2.17$_8$	2.17$_0$	2.16$_4$	2.16$_5$	2.16$_7$	2.17$_3$	2.18$_1$	2.19$_1$
pK_1(calc. 17)	2.18$_9$	2.17$_8$	2.17$_0$	2.16$_5$	2.16$_5$	2.16$_6$	2.17$_2$	2.18$_0$	2.19$_1$
ΔG_1° cal mol^{-1}	2784	2820	2859	2903	2950	3004	3061	3123	3189
ΔH_1° cal mol^{-1}	949	703	452	197	—62	—326	—594	—867	—144
ΔS_1° cal mol^{-1} deg^{-1}	—6.6	—7.5	—8.4	—9.2	—10.1	—11.0	—11.9	—12.7	—13.6

Pour les variations des fonctions thermodynamiques on a les expressions suivantes:

$$\Delta G_1^\circ = 7738 - 42.22_0T + 8.77_7 \cdot 10^{-2}T^2 \qquad (18)$$

$$\Delta H_1^\circ = 7738 - 8.77_7 \cdot 10^{-2}T^2 \qquad (19)$$

$$\Delta S_1^\circ = 42.22_0 - 17.55 \cdot 10^{-2}T \qquad (20)$$

DÉTERMINATION DE LA SECONDE CONSTANTE DE DISSOCIATION

Exposé théorique

Pour cette détermination on emploie la cellule (4). La deuxième constante d'ionisation est donnée par

$$K_2 = \frac{M_{H^+}M_{HA^-}}{M_{HAH^\pm}} \cdot \frac{\gamma_{H^+}\gamma_{HA^-}}{\gamma_{HAH^\pm}} \qquad (21)$$

et l'éqn. qui exprime la neutralité électrique est:

$$M_{H_2AH^+} + M_{H^+} + M_{Na^+} = M_{HA^-} + M_{OH^-} + M_{Cl^-} + 2M_{A^{2-}} \qquad (22)$$

d'où l'on tire l'expression:

$$pK_2' \equiv pK_2 - \log \frac{\gamma_{HAH^{\pm}}}{\gamma_{H^+}\gamma_{HA^-}} = \frac{E - E^\circ}{\phi} + \log M_{Cl^-} + \log \gamma_{Cl^-}\gamma_{H^+} + \log \frac{T_A - M_{NaOH} - M_{H^+} + 2M_{H_2AH^+}}{M_{NaOH} + M_{H^+} + M_{H_2AH^+}} \quad (23)$$

où les concentrations $M_{A^{2-}}$ et M_{OH^-} ont été négligées et où l'on a considéré la concentration M_{Na} égale à celle de M_{NaOH}, vu que la M_{Na^+} du NaCl est compensée par une quantité équivalente de M_{Cl^-}. On trouve les valeurs de $M_{H_2AH^+}$ au moyen de la relation:

$$M_{H_2AH} = \frac{M_H(T_A - M_{H^+} - M_{NaOH})}{K_1 + 2M_{H^+}} \quad (24)$$

ce qui permet de calculer le dernier terme de (23).

La force ionique est dans ces expériences

$$\mu \simeq M_{NaOH} + M_{NaCl} \quad (25)$$

On trouve les valeurs de pK_2 par extrapolation à $\mu = 0$ dans les représentations de pK_2' en fonction de μ. On introduit dans l'éqn. (23) les deux approximations (13) et (14), pour ce qui concerne le terme $\log \gamma_{H^+}\gamma_{Cl^-}$, en prenant dans ce cas comme valeurs de $\gamma_{\pm(HCl)}$ les valeurs correspondant aux mélanges de HCl et NaCl[6].

Résultats expérimentaux

On a déterminé dans tous les cas les f.e.m. dans l'intervalle de 5–50°. Les détails des expériences sont semblables à ceux des expériences antérieures. Les valeurs de E s'ajustent à une éqn. du type (15), par la méthode des minima carrés. Dans la Table III on peut voir les valeurs de E pour différentes compositions de l'électrolyte et à différentes températures et l'on y réunit aussi les valeurs de E_{25}, a et b.

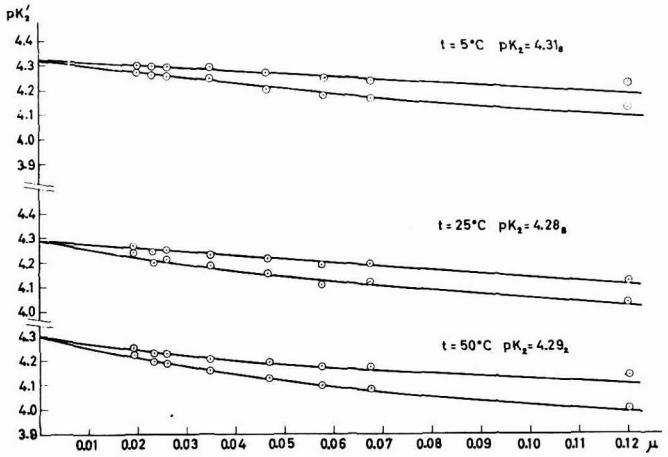

Fig. 4. Variation de pK_2' en fonction de la force ionique.

TABLE III

Molalités			*E observées et corrigées à 1 atm H_2*									*E interpolée*		
Ac. Glut.	*NaOH*	*NaCl*	5°	10°	15°	20°	25°	30°	37,5°	45°	50°	E_{25}	$a10^6$	$-b10^8$
0.09655_5	0.0692_0	0.0507_3	0.5748_9	0.5768_1	0.5787_8	0.5808_1	0.5827_6	0.5850_5	0.5884_6	0.5917_0	0.5940_0	0.5828_9	421	— 99
0.0543_6	0.0389_7	0.0285_7	0.5861_1	0.5888_7	0.5915_1	0.5941_8	0.5977_3	0.6000_2	0.6037_3	0.6070_4	0.6097_0	0.5973_8	542	220
0.0465_0	0.0333_0	0.0244_0	0.5891_6	0.5921_2	0.5947_5	0.5974_3	0.6002_0	0.6028_5	0.6070_3	0.6107_6	0.6131_3	0.6002_1	538	68
0.0375_5	0.0269_1	0.0197_3	0.5955_1	0.5981_9	0.6006_9	0.6031_3	0.6066_8	0.6094_2	0.6134_7	0.6168_0	0.6196_8	0.6064_4	545	62
0.0280_7	0.0201_1	0.0147_5	0.6024_5	0.6053_3	0.6079_5	0.6108_6	0.6141_3	0.6170_1	0.6210_3	0.6248_9	0.6276_0	0.6139_8	567	84
0.0209_0	0.0150_0	0.0110_0	0.6091_0	0.6122_5	0.6154_2	0.6186_6	0.6222_1	0.6253_4	0.6296_6	0.6333_5	0.6365_1	0.6220_4	620	184
0.0187_5	0.0134_4	0.0098_5	0.6110_7	0.6143_1	0.6173_3	0.6205_5	0.6239_4	0.6275_0	0.6317_8	0.6359_2	0.6391_0	0.6239_7	630	108
0.0158_6	0.0111_1	0.0081_3	0.6158_8	0.6191_2	0.6224_4	0.6257_6	0.6301_2	0.6330_8	0.6376_7	0.6418_5	0.6450_8	0.6295_9	663	185

La variation de pK_2' en fonction de μ à 5, 25 et 50° a été représentée dans la Fig. 4, ainsi que les valeurs de pK_2, obtenues dans les extrapolations, en fonction de $1/T$ dans la Fig. 5.

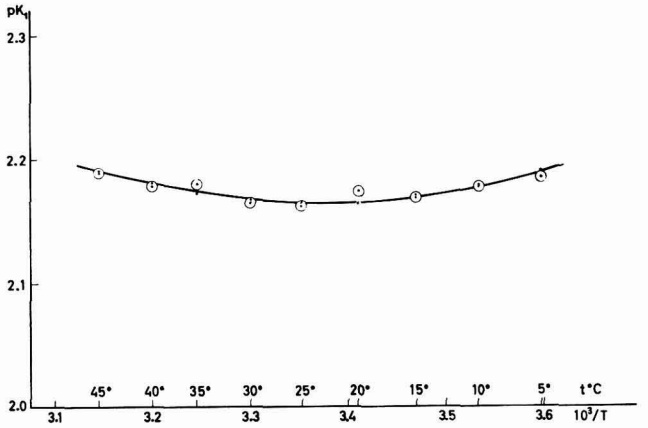

Fig. 5. Représentation des valeurs des pK_2 en fonction de $1/T$.

Fonctions thermodynamiques

La variation de pK_2 avec la température est donnée par les expressions:

$$pK_2 = \frac{1278.8}{T} - 4.020 + 1.347 \cdot 10^{-2}T \tag{26}$$

ou bien

$$pK_2 = 4.281 + 4.7 \cdot 10^{-2}(t - 35.0)^2 \tag{27}$$

On a pu tracer la courbe représentée dans la Fig. 5 grâce aux valeurs calculées à partir de l'expression (26).

On a pour les variations des fonctions thermodynamiques

$$\Delta G_2^\circ = 5849 - 18.389T + 6.16 \cdot 10^{-2}T^2 \tag{28}$$

$$\Delta H_2^\circ = 5849 - 6.16 \cdot 10^{-2}T^2 \tag{29}$$

$$\Delta S_2^\circ = 18.39 - 12.32 \cdot 10^{-2}T \tag{30}$$

La Table IV rassemble, pour différentes températures, les valeurs expérimentales de pK_2 et les valeurs calculées à partir de l'expression (26) ou (27). De même on y voit les valeurs correspondantes de ΔG_2°, ΔH_2° et ΔS_2°, calculées à partir de ces dernières expressions.

TABLE IV

t°	5	10	15	20	25	30	37.5	45	50
pK_2 (exptl.)	4.318	4.308	4.296	4.287	4.288	4.280	4.278	4.289	4.292
pK_2 (calc. 26)	4.323	4.310	4.298	4.290	4.286	4.283	4.280	4.285	4.290
pK_2 (calc. 27)	4.323	4.310	4.299	4.291	4.286	4.282	4.281	4.286	4.291
ΔG_2° cal mol^{-1}	5500	5580	5565	5752	5842	5935	6081	6233	6339
ΔH_2° cal mol^{-1}	1085	912	722	558	375	265	—94	—384	—581
ΔS_2° cal mol^{-1} deg^{-1}	—15.9	—16.5	—17.2	—17.7	—18.3	—18.7	—19.9	—20.8	—21.4

DÉTERMINATION DE LA TROISIÈME CONSTANTE DE DISSOCIATION

Exposé théorique

L'expression de la troisième constante est:

$$K_3 = \frac{M_{H^+} M_{A^{2-}}}{M_{HA^-}} \frac{\gamma_{H^+}\gamma_{A^{2-}}}{\gamma_{HA^-}} \tag{31}$$

et l'équation de la neutralité électrique sera:

$$M_{Na^+} + M_{H^+} = M_{HA^-} + M_{OH^-} + 2M_{A^{2-}} \tag{32}$$

où M_{H^+} peut être négligé, vu que les solutions employées sont alcalines et où M_{Na^+} représente la quantité de Na^+ qui provient du NaOH.

Si l'on combine ces deux expressions avec celle qui donne la quantité totale d'acide aminé (7) et celle qui exprime les f.e.m. d'une cellule de ce type (4), on obtient l'expression suivante:

$$pK_3 = \frac{E - E^\circ}{\phi} + \log M_{Cl^-} + \log \frac{2T_A - M_{NaOH} + M_{OH^-}}{M_{NaOH} - T_A - M_{OH^-}} + \log \frac{\gamma_{Cl^-}\gamma_{AH^-}}{\gamma_{A^{2-}}} \tag{33}$$

Dans les conditions dans lesquelles on opère pour déterminer la troisième constante on a:

$$\mu \simeq 2M_{NaOH} + M_{NaCl} - T_A \tag{34}$$

et dans l'expression (33) on peut supprimer M_{OH^-}, qui est relativement petite à côté de $(2T_A - M_{NaOH})$ et $(M_{NaOH} - T_A)$.

Le dernier terme peut être remplacé par $2S_f(2d_0\mu)^{1/2} - B\mu$ et alors on aura:

$$pK_3' \equiv pK_3 + B_\mu = \frac{E - E^\circ}{\phi} + \log M_{Cl^-} + \log \frac{2T_A - M_{NaOH}}{M_{NaOH} - T_A} + 2S_f(2d_0\mu)^{1/2} \tag{35}$$

La représentation de pK_3' en fonction de μ permet d'obtenir les valeurs de pK_3 par extrapolation à $\mu = 0$.

Résultats expérimentaux

La mise au point de la cellule pour les mesures de f.e.m. est semblable à celle qui a été décrite pour les autres constantes d'ionisation. On a réalisé les déterminations dans l'intervalle de 5–50° et dans tous les cas on a ajusté les valeurs de E à une équation du type (15), par la méthode des minima carrés. La Table V rassemble les résultats obtenus.

On représente la variation de pK_3' en fonction de T, à 5, 25 et 50° dans la Fig. 6 et les valeurs extrapolées de pK_3 ont été représentées dans la Fig. 7 en fonction de $1/T$.

Fonctions thermodynamiques

On observe dans la Fig. 7 que la dispersion des points expérimentaux, de la ligne droite, est parfaitement justifiée par les erreurs de mesure. Aussi nous avons omis toute courbature dans cette représentation et nous acceptons que la variation de pK_3 en fonction de la température sera décrite par l'expression:

$$pK_3 = \frac{2094.0}{T} + 2.347 \tag{36}$$

TABLE V

Molalités			*E observées et corrigées à 1 atm H_2*									*E interpolée*		
Ac. Glut.	*NaOH*	*NaCl*	*5°*	*10°*	*15°*	*20°*	*25°*	*30°*	*37.5°*	*45°*	*50°*	E_{25}	$a10^6$	$-b10^8$
0.05039	0.07675	0.01513	0.86656	0.86823	0.86948	0.87067	0.87170	0.87269	0.87322	0.87465	0.87504	0.87127	288	355
0.03039	0.04628	0.00913	0.88050	0.88251	0.88449	0.88643	0.88841	0.88980	0.89114	0.89300	0.89390	0.88808	240	271
0.02582	0.03934	0.00776	0.88727	0.88927	0.89113	0.89286	0.89415	0.89488	0.89595	0.89720	0.89793	0.89390	247	382
0.02255	0.03434	0.00677	0.88995	0.89180	0.89365	0.89570	0.89722	0.89853	0.90008	0.90111	0.90235	0.89715	260	300
0.01890	0.02880	0.00568	0.89613	0.89817	0.90008	0.90181	0.90299	—	0.90490	0.90565	0.90620	0.90291	289	353
0.01415	0.02156	0.00427	0.90270	0.90520	0.90754	0.90945	0.91089	0.91221	0.91330	0.91375	0.91440	0.91086	300	552
0.01175	0.01789	0.00352	0.90610	0.90864	0.91136	0.91375	0.91538	0.91655	0.91775	0.91900	0.91973	0.91513	325	464

Dans la même Fig. on représente les valeurs de pK_3 pour l'acide aspartique[7] et il est évident que dans ce cas cette considération est aussi valide.

On peut calculer à partir de (36) les valeurs de $\Delta G_3°$, $\Delta H_3°$ et $\Delta S_3°$ et l'ensemble des valeurs calculées est donné dans la Table VI.

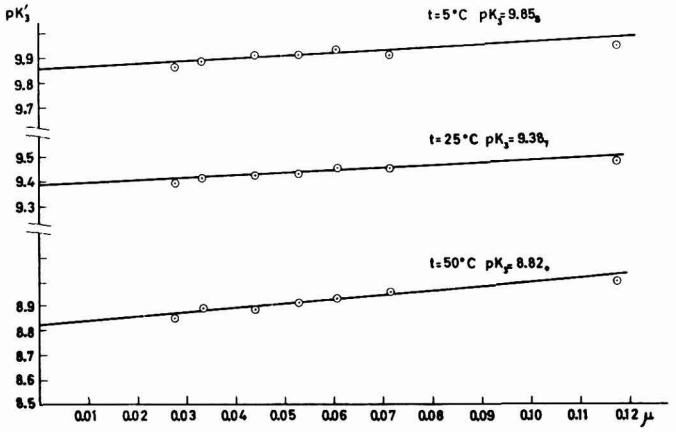

Fig. 6. Variation de pK_3' en fonction de la force ionique.

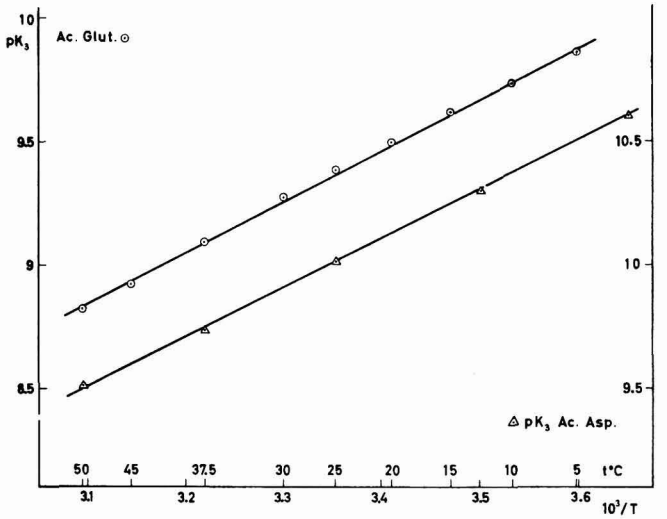

Fig. 7. Représentation des valeurs des pK_3 pour les acides aspartique et glutamique en fonction de $1/T$.

TABLE VI

$t°$	5	10	15	20	25	30	37.5	45	50
pK_3 (exptl.)	9.85$_3$	9.73$_1$	9.62$_6$	9.49$_7$	9.38$_7$	9.27$_0$	9.09$_3$	8.92$_3$	8.82$_0$
pK_3 (calc. 36)	9.87$_6$	9.74$_4$	9.61$_6$	9.49$_1$	9.37$_1$	9.29$_6$	9.08$_9$	8.93$_0$	8.82$_8$
$\Delta G_3°$ cal mol^{-1}	12563	12618	12617	12724	12777	12888	12913	12993	13046
$\Delta H_3°$ cal mol^{-1}	9578	9578	9578	9578	9578	9578	9578	9578	9578
$\Delta S_3°$ cal mol^{-1} deg^{-1}	—10.7	—10.7	—10.7	—10.7	—10.7	—10.7	—10.7	—10.7	—10.7

DISCUSSION

Les valeurs des constantes de dissociation de l'acide glutamique obtenues dans ce travail, à la température de 25°, sont les suivantes:

$$pK_1 = 2.165 \qquad pK_2 = 4.286 \qquad pK_3 = 9.371$$

Parmi les résultats publiés jusqu'à présent[8-11] ceux qui méritent le plus de confiance sont ceux de NEUBERGER[10], pour avoir essayé d'extrapoler à dilution infinie. Les valeurs que donne cet auteur sont les suivantes:

$$pK_1 = 2.155 \qquad pK_2 = 4.324 \qquad pK_3 = 9.960$$

La concordance qu'il y a entre les deux premières constantes est assez satisfaisante, mais les valeurs de pK_3 sont assez différentes.

Dans les mesures réalisées par NEUBERGER, on a utilisé des cellules avec union liquide, ce qui diminue assez la confiance dans ses résultats. De plus, les expressions employées pour l'extrapolation à $\mu = 0$, conduisent à des représentations de pK_3' en fonction de μ avec pente excessive à l'origine, ce qui donne des valeurs extrapolées par excès.

Etude comparative des constantes de dissociation de l'acide glutamique et d'autres acides aminés de la série homologue

La série homologue à laquelle appartient l'acide glutamique est celle des acides α-amino-n-dicarboxyliques

$$\underset{2}{HOOC}—(CH_2)_n—CH(\underset{3}{NH_2})—\underset{1}{COOH} \qquad (n = 0,1,2. \ldots)$$

Le premier de la série est l'acide amino-malonique et suivent les acides aspartique et glutamique. Les constantes de dissociation de l'acide aminomalonique ont été peu étudiées[12,13] et les détails expérimentaux publiées ne permettent pas d'apprécier la garantie qu'on peut leur accorder. Les constantes de l'acide aspartique ont été déterminées par SMITH ET SMITH[7], au moyen d'une technique minucieuse, semble-t-il,

TABLE VII

$t = 20°$

Acide aminé	pK_1	pK_2	pK_3	*References*
HOOC—CH(NH_2)—COOH Ac. aminomalonique	—	3.32 (pG_2')	9.83 (pG_3')	12 13
HOOC—CH_2—CH(NH_2)—COOH Ac. aspartique	2.03	3.92	10.15	7
HOOC—CH_2—CH_2—CH(NH_2)—COOH Ac. glutamique	2.164	4.290	9.491	Ce travail

$t = 25°$

Acide aminé	pK_1	$\Delta H_1°$	$\Delta S_1°$	pK_2	$\Delta H_2°$	$\Delta S_2°$	pK_3	$\Delta H_3°$	$\Delta S_3°$	*References*
Ac. aspartique	1.995 2.01	1783 —	—3.1 —	3.910 3.90	1110 —	—14.2 —	10.01 9.84	9025 —	—15.5 —	7 7a
Ac. glutamique	2.165	—62	—10.1	4.286	375	—18.3	9.371	9578	—10.7	Ce travail

et dans un ample intervalle de températures. Nous emploierons pour l'acide glutamique dans cette discussion les données que nous venons d'exposer dans la partie expérimentale de ce travail. Dans la Table VII on réunit les résultats obtenus, pour deux valeurs de la température, 20 et 25°, et pour cette dernière température on indique en plus les valeurs de $\Delta H°$ et $\Delta S°$, correspondant à chacune des ionisations.

Dans la série homologue des α-amino acides normaux $CH_3—(CH_2)_n—CH(NH_2)—COOH$, on voit que $pK_1 \simeq 2.3$ et $pK_2 \simeq 9.8$, et que l'influence de la chaine alkyde est très petite dans l'ionisation de ces acides aminés. Par contre, dans la série homologue des amino-acides qui ont leurs groupes fonctionnels aux extrémités de la chaine, $H_2N—(CH_2)_n—COOH$, on observe que pK_1 augmente, en tendant vers la valeur correspondant aux acides gras, $pK \simeq 4.9$, tandis que pK_2 tend vers la valeur correspondant aux amines aliphatiques, $pK \simeq 10.8$.

Pour les acides α-amino-dicarboxyliques on peut seulement en première approximation attribuer les valeurs de pK_1, pK_2 et pK_3 aux ionisations des groupes 1, 2 et 3, dans la formule générale, mentionnée plus haut, de ces acides aminés. La discussion complète de leur ionisation exige la connaissance des constantes microscopiques correspondantes[15].

Dans cette série des acides aminés la valeur du pK_1 dépendera de la position α du groupe ammonium 3 par rapport au groupe carboxyle 1. A mesure qu'augmente la chaine sa valeur tendra vers la valeur caractéristique des acides aminés en α ($pK \simeq 2.3$). L'influence du groupe carboxyle 2 se manifeste par un accroissement supplémentaire de la force du premier et cette influence diminue en passant de l'acide aspartique à l'acide glutamique.

La valeur de pK_2 tendra vers celle de l'acide gras correspondant ($pK \simeq 4.9$). L'influence du groupe $—NH_3^+$ se manifestera par une acidité plus forte du groupe carboxyle 2, en comparaison avec celle de l'acide *n*-dicarboxylique correspondant. C'est que nous pouvons constater avec les acides aminomalonique ($pK_2 \simeq 3.20$) et malonique ($pK_2 \simeq 5.70$), les acides aspartique ($pK_2 \simeq 3.90$) et succinique ($pK_2 \simeq 5.64$) et les acides glutamique ($pK_2 \simeq 4.29$) et glutarique ($pK_2 \simeq 5.50$)[16-18].

Finalement, pour ce qui concerne la troisième ionisation, il faudra tenir compte de l'effet des deux carboxyles ionisés sur le groupe ionisé $—NH_3^+$. On peut tenir compte de ces effets au moyen de la relation empirique de EDSALL ET BLANCHARD[19], avec les paramètres employés par GREENSTEIN[20]. Pour l'ionisation de ce groupe on a

$$pK = 10.72 - \Sigma \frac{0.9}{d_i} \qquad (36)$$

TABLE VIII

Substance	*Formule*	*pK (calc.)*	*pK (exptl.)*
α-Alanine	$CH_3—CH(^+NH_3)—COO^-$	9.8	9.87
Ac. aminomalonique	$^-OOC—CH(^+NH_3)—COO^-$	8.9	9.8
Ac. α-aminobutirique	$CH_3—CH_2—CH(^+NH_3)—COO^-$	9.8	9.83
β-Alanine	$^-OOC—CH_2—CH_2(^+NH_3)$	10.3	10.24
Ac. aspartique	$^-OOC—CH_2—CH(^+NH_3)—COO^-$	9.4	9.84 10.00
Ac. α-aminovalerianique	$CH_3—(CH_2)_2—CH(^+NH_3)—COO^-$	9.8	9.81
Ac. γ-aminobutirique	$^-OOC—(CH_2)_2—CH_2(^+NH_3)$	10.4	10.56
Ac. glutamique	$^-OOC—(CH_2)_2—CH(^+NH_3)—COO^-$	9.5	9.37

où d_i vaut 1, 2, 3. . . ., selon que le groupe qui influence le groupe dissocié, se trouve en position α, β, γ . . . . etc., par rapport à ce dernier. Dans la Table VIII on expose les valeurs de pK qu'on a calculées ainsi, en même temps que les valeurs expérimentales. La concordance est acceptable pour toutes les substances étudiées, sauf pour les acides aminomalonique et aspartique.

Malheureusement, les valeurs expérimentales de l'acide amino malonique offrent très peu de garantie et ne nous permettent pas d'accorder notre confiance aux considérations que nous pourrions faire sur ce premier terme de la série. Néanmoins, il faut faire observer que la valeur expérimentale révèle une acidité moindre pour le groupe $-NH_3^+$ que la valeur calculée. Ce fait est moins remarquable, mais encore évident, dans le cas de l'acide aspartique et ne se présente plus dans le cas de l'acide glutamique.

Pour expliquer ce fait on peut supposer que, dans le cas de l'acide aspartique la configuration moléculaire prédominant est celle qui présente un rapprochement du groupe carboxyle 2 au groupe ammonium 3; ce qui augmente l'effet électrostatique sur ce dernier. GANE ET INGOLD[18], entre autres, ont déjà admis des rapprochements de cette nature entre les groupes ionisables, dans le cas des acides alkyl-dicarboxyliques.

Etude critique des valeurs des $\Delta H°$ et $\Delta S°$ à 25° pour l'ionisation de l'acide glutamique

Dans l'ionisation des acides carboxyliques les valeurs de $\Delta H°$ sont relativament petites, de l'ordre de 2 kcal/mol et beaucoup sont plus petites que 1 kcal/mol. On observe ces ordres de grandeurs dans le cas de $\Delta H_1°$ et $\Delta H_2°$ correspondant aux acides glutamique et aspartique (Table VII). Les valeurs de $\Delta H_3°$ pour l'ionisation du groupe ammonium sont de l'ordre de 10–12 kcal/mol. Pour les acides α-amino-mono-carboxyliques, les valeurs de cette enthalpie d'ionisation varient peu autour de 10.7 kcal/mol et pour les deux acides α-amino-dicarboxyliques étudiées les valeurs obtenues sont un peu plus petites $\simeq$ 9 kcal/mol.

Sous certains aspects les considérations sur l'entropie d'ionisation $\Delta S°$ sont plus édifiantes. L'ionisation d'un acide carboxylique est en général:

$$R-COOH + H_2O \rightleftharpoons R-COO^- + H_3O^+ \qquad (37)$$

liée à une valeur négative de l'entropie $\Delta S°$, car dans la réaction deux ions se sont formés, lorsqu'il n'y en avait aucun auparavant, et la solvatation de ces ions sera accompagnée d'une diminution marquée de l'entropie. On a dans l'ionisation des acides gras $\Delta S° \simeq -23$ cal/mol deg et on obtient dans l'ionisation des acides dicarboxyliques des valeurs encore plus négatives pour l'entropie $\Delta S°$.

Dans le cas des acides α-amino-mono-carboxyliques la présence du groupe $-NH_3^+$ neutralise l'interaction électrostatique du groupe $-COO^-$ sur les dipoles qui l'entourent et la valeur de $\Delta S_1°$ pour l'ionisation du groupe carboxyle, quoique négative, est beaucoup plus petite, $\Delta S_1° \simeq -9$ cal/mol deg.

Dans l'ionisation du groupe ammonium

$$R-NH_3^+ + H_2O \rightleftharpoons R-NH_2 + H_3O^+ \qquad (38)$$

c'est un transfert d'un proton de l'ion ammonium à la molécule d'eau qui a lieu seulement. Les variations d'entropie sont beaucoup plus petites que dans le cas antérieur. Pour les ions alkyl-ammonium elle est de l'ordre de $\Delta S° \simeq -4$ cal/mol deg.

Pour les α-amino acides monocarboxyliques, les valeurs de cette entropie sont

beaucoup plus négatives ($\Delta S_2° \simeq -9$) à cause de l'interaction du groupe $-COO^-$ voisin. Dans la série des acides aminés normaux, où les groupes aminé et carboxyle sont aux extrémités de la chaine normale aliphatique, on observe qu'à mesure qu'augmente la chaine les valeurs de $\Delta S_1°$ deviennent plus négatives et tendent vers la valeur caractéristique de l'ionisation du groupe $-COOH$ des acides gras ($\Delta S° \simeq -22$), tandis que celles de $\Delta S_2°$ deviennent moins négatives et tendent vers la valeur caractéristique de l'ion alkyl-ammonium ($\Delta S° \simeq -4$).

Pour les α-amino acides dicarboxyliques que nous considérons (Table VIII) maintenant, on observe que $\Delta S_1°$ est négatif, mais petit, dans le cas de l'acide aspartique, et il est de l'ordre des acides α-aminés normaux dans le cas de l'acide glutamique. Les valeurs de $\Delta S_2°$ sont, tant dans le cas de l'acide aspartique que dans celui de l'acide glutamique, plus négatives que les $\Delta S_1°$, comme il fallait s'y attendre vu qu'il s'agit de la deuxième ionisation d'acides dicarboxyliques.

Mais ce qui est le plus surprenant, c'est que l'on a trouvé, dans le cas de la troisième ionisation, une valeur très négative de l'entropie d'ionisation pour l'acide aspartique ($\Delta S_3° = -15.5$), tandis que pour l'acide glutamique on ne trouve qu'une valeur à peine plus négative que celle des acides α-aminés normaux ($\Delta S_3° = -10.7$).

On peut comprendre ce comportement si nous admettons l'hypothèse, dont nous avons parlé plus haut, où, dans le cas de l'acide aspartique, le groupe $-COO^-(2)$ se trouve assez près du groupe $-NH_3^+$, neutralisant l'effet électrostatique de ce dernier. A cause de cela, la réaction d'ionisation conduira à une espèce de libération du proton et le comportement du $-NH_3^+$, dans ces conditions, se rapprochera de celui de l'ionisation d'un groupe neutre. Dans le cas de l'acide glutamique ce fait serait moins marquant, à cause de la plus grande distance qui séparé le deuxième $-COO^-$ du groupe $-NH_3^+$.

SUMMARY

The ionization constants of glutamic acid have been measured at several temperatures from 5–50°, using e.m.f. measurements of cells without liquid junctions. The results were analyzed in terms of the Harned–Robinson equation and values of $\Delta G°$, $\Delta H°$ and $\Delta S°$ for the ionization process were determined. The eqns. for ionization constants as a function of temperature are as follows:

$$pK_1 = \frac{1961.6}{T} + 9.227 + 1.919 \cdot 10^{-2}T$$

$$pK_2 = \frac{1278.8}{T} + 4.020 + 1.347 \cdot 10^{-2}T$$

$$pK_3 = \frac{2094.0}{T} + 2.347$$

The results were interpreted in terms of inductive and electrostatic effects and are discussed in relation to those obtained for aspartic acid.

BIBLIOGRAPHIE

[1] R. G. BATES, *Electrometric pH Determinations*, John Wiley and Sons, Inc., New York, 1954, p. 166.

[2] D. J. G. IVES ET G. J. JANZ, *Reference Electrodes*, Academic Press, New York and London, 1961, p. 206.

[3] H. S. HARNED ET B. B. OWEN, *The Physical Chemistry of Electrolytic Solutions*, Reinhold, New York, 1943, p. 116.
[4] *International Critical Tables*, VII, p. 377.
[5] H. S. HARNED ET N. D. EMBREE, *J. Am. Chem. Soc.*, 56 (1934) 1050.
[6] H. S. HARNED ET B. B. OWEN, *The Physical Chemistry of Electrolytic Solutions*, Reinhold, New York, 1943, p. 467.
[7] E. R. B. SMITH ET P. K. SMITH, *J. Biol. Chem.*, 90 (1942) 165.
[7a] A. C. BATCHELDER ET C. L. A. SCHMIDT, *J. Phys. Chem.*, 44 (1940) 893.
[8] S. MYAMOTO ET C. L. A. SCHMIDT, *J. Biol. Chem.*, 146 (1931) 187.
[9] E. J. COHN ET J. T. EDSALL, *Proteins, Aminoacids and Peptides*, Reinhold, New York, 1943, p. 85.
[10] A. NEUBERGER, *Biochem. J.*, 30 (1936) 2085.
[11] M. LEVY ET D. E. SILBERMAN, *J. Biol. Chem.*, 118 (1937) 723.
[12] O. LUTZ, *Ber.*, 35 (1902) 2549.
[13] G. SCHWARZENBACH, E. KAMPITSCH ET R. STEINER, *Helv. Chim. Acta*, 28 (1945) 1133.
[14] C. K. INGOLD, *Structure and Mechanism in Organic Chemistry*, Cornell University Press, Ithaca, N.Y., 1953, p. 734.
[15] T. L. HILL, *J. Phys. Chem.*, 48 (1944) 101.
[16] W. J. HAMER, J. O. BURTON ET S. F. ACREE, *J. Res. Natl., Bur. Std.* 24 (1940) 269.
[17] B. D. PINCHING ET R. G. BATES, *J. Res. Natl. Bur. Std.*, 45 (1950) 322,444.
[18] R. GANE ET C. K. INGOLD, *J. Chem. Soc.*, (1931) 2153.
[19] J. T. EDSALL ET M. H. BLANCHARD, *J. Am. Chem. Soc.*, 55 (1933) 2337.
[20] J. P. GREENSTEIN, *J. Biol. Chem.*, 96 (1932) 499.

POLAROGRAPHIC STUDIES ON THE INTERACTION OF COPPER WITH TRANSFUSION GELATIN

WAHID U. MALIK AND SALAHUDDIN

Chemical Laboratories, Aligarh Muslim University, Aligarh (India)

(Received February 24th, 1962)

The marked decrease in the diffusion current of metal ions in the presence of increasing amounts of gelatin[1] was ascribed by KOLTHOFF AND LINGANE[2] to probable metal–protein complex formation. Alternatively, it was pointed out that such effects may be caused by viscosity[2] or adsorption[3]. TANFORD[4,5,6] had also shown conclusively that a decrease in the limiting current of metal ions with increasing concentration of serum albumin was due to combination of metal with the protein, and that adsorption[6] phenomena could only be operative at lower pH values.

Application of polarographic methods to the study of metal–protein interaction has so far received very little attention, due to the involved nature of the reduction at the dropping mercury electrode, especially that due to formation of a catalytic wave. It was, therefore, appropriate to choose a protein where the latter effect could be eliminated. Since the cysteine and cystine contents of gelatin are negligible, this was selected for polarographic studies. The present investigation deals with complexes formed by copper ions with transfusion gelatin (of known molecular weight) in the higher pH range. Some of the results in the lower pH range have also been included, although the binding here is too weak to give useful quantitative results.

EXPERIMENTAL

Transfusion gelatin[7] (concentration 6%, mol. wt. = 75,000), supplied by the Director, National Chemical Laboratories, Poona, India, was used throughout these investi gations.

Copper sulphate (A.R.) was dissolved in water which had been doubly distilled in all-glass apparatus. Ammonia–ammonium chloride buffers were prepared from one *M* solutions of ammonia and ammonium chloride. The pH of the buffer solutions was measured by means of a Beckman pH Meter, Model G, using glass electrodes.

Polarographic measurements were carried out using a Fisher Electropode in conjunction with a Multiflux Galvanometer Type MG F_2. An H–shaped polarographic cell as recommended by TANFORD[8] was found suitable for deaeration of the protein solution without denaturation. Nitrogen, purified by passing it through a solution of chromous chloride and alkaline pyrogallol, was passed to ensure an inert atmosphere. Triply distilled mercury was used for the dropping mercury electrode. The cell was immersed in a water thermostat (Townson Mercer Co., Croydon) maintained at 20° $\pm$ 1°. The following sets of solutions were prepared.

(i) Varying concentrations of the protein (0.5, 0.75, 1.25, 1.75 and 2%) were taken in 50 cc conical flasks and 4.5 cc of 0.005 M Cu^{2+} solution were added. The total volume was made up to 12 cc by adding the requisite volume of water and 1.8 cc of 1 M ammonia–1 M ammonium chloride buffer (to make the total ionic strength = 0.15). The results, in the form of a graph of protein concentration (%) against $i_d/(i_d)_0$, where

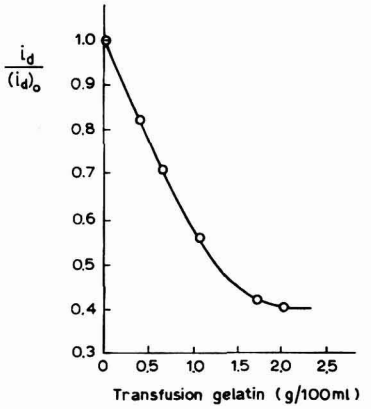

Fig. 1. Effect of protein concentration on diffusion current.

TABLE IA

CONCENTRATION OF Cu^{2+}, $1.87 \cdot 10^{-3}$ M; pH, 9.4

Concn. of protein (%)	i_d $(4 \cdot 10^{-8} A)$	$(i_d)_0$ $(4 \cdot 10^{-8} A)$	$\frac{i_d}{(i_d)_0}$	C_b	O_M
0.50	18	15	0.83	0.529	7.9
0.75	18	13	0.72	0.865	8.6
1.25	18	10.5	0.58	1.30	7.8
1.75	18	7.5	0.41	1.83	7.8
2.00	18	7.2	0.40	1.81	7

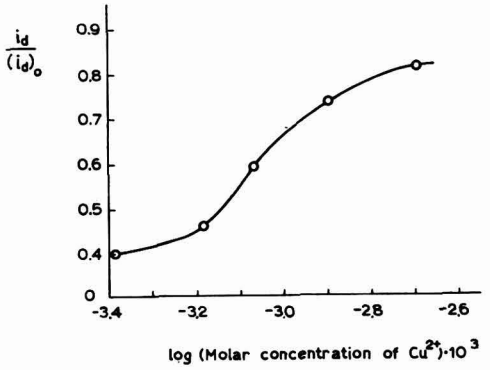

Fig. 2. Effect of copper concentration on diffusion current depression.

i_d and $(i_d)_0$ are the diffusion currents of the metal ion, in the presence and absence of the protein, respectively, as given in Fig. 1, (Table IA).

(ii) 1 cc gelatin, 1.8 cc buffer (pH 9.4) and varying concentrations of Cu^{2+} ion *viz.*, 0.4166, 0.6249, 0.8332, 1.249 and $1.874 \cdot 10^{-3}$ *M* Cu^{2+} were used, keeping the total volume to 12 cc as before. Figure 2 shows the variation of $i_d/(i_d)_0$ with the logarithm of copper concentration, (Table IB).

TABLE IB

CONCENTRATION OF THE PROTEIN, 0.5%; pH 9.4

Concn. of $Cu^{2+} \cdot 10^{-3}$ *M*	i_d $(4 \cdot 10^{-8}$ *A*$)$	i_d $(4 \cdot 10^{-8}$ *A*$)$	$\frac{i_d}{(i_d)_0}$	C_b	O_M
1.87	18	15	0.83	0.529	7.9
1.249	12	9	0.75	0.52	7.8
0.833	8	4.8	0.60	0.55	8.3
0.6249	6	2.8	0.46	0.56	8.4
0.520	5	1.9	0.38	0.53	8.05

(iii) Similarly, 1.5 cc of 0.005 *M* Cu^{2+} solution, 1 cc protein and 1.8 cc buffer of different pH's (from pH 2.65–11) were taken and the volume was made up to 12 cc. The curve shown in Fig. 3 represents $i_d/(i_d)_0$ as a function of pH, (Table IC).

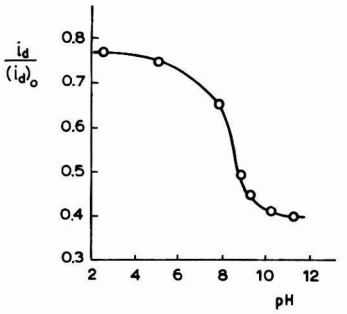

Fig. 3. Effect of pH on diffusion current depression.

TABLE IC

CONCENTRATION OF THE PROTEIN, 0.5%; CONCENTRATION OF Cu^{2+}, $0.6249 \cdot 10^{-3}$ *M*

pH	i_d $(4 \cdot 10^{-8}$ *A*$)$	$(i_d)_0$ $(4 \cdot 10^{-8}$ *A*$)$	$\frac{i_d}{(i_d)_0}$	C_b	O_M
11	6	2.4	0.40	0.624	9.3
10	6	2.4	0.40	0.624	9.3
9.4	6	2.8	0.46	0.56	8.4
8.9	6	3.0	0.50	0.52	7.8
5.1	6	4.5	0.75	0.26	3.9
2.65	6	4.8	0.77	0.239	3.58

In all, fifty polarograms were traced. Typical ones are shown in Fig. 4. The reversibility of the waves was tested by TOMES[9] method.

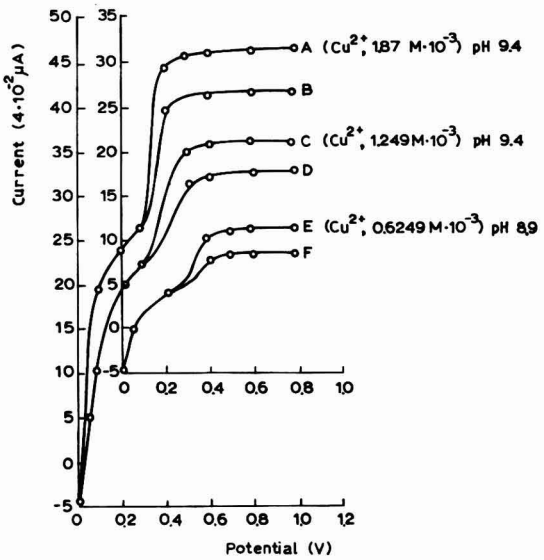

Fig. 4. Polarograms. A, C and E for copper alone; B for 0.5% protein + $1.87 \cdot 10^{-3}$ *M* Cu^{2+}; D for 0.5% protein + $1.249 \cdot 10^{-3}$ *M* Cu^{2+}; and F for 0.5% protein + $0.6249 \cdot 10^{-3}$ *M* Cu^{2+}.

DISCUSSION

The usual polarographic method for the study of metal complexes from the shift in half-wave potential of the metal ion[10] failed to give precise information regarding the metal–protein interaction because of very small variations in $E_{1/2}$ values (of the order of 0.01 V). TANFORD'S method, with all its limitations could, however, be advantageously employed. Since the copper–gelatin complex (violet in colour) is formed only at higher pH ranges, the adsorption effects usually encountered could be assumed to exert the minimum influence and the decrease in the ratio $i_d/(i_d)_0$ can be safely taken as a measure of the extent of metal ion complexed with the protein. Furthermore, the decrease in the diffusion current can not be solely ascribed to viscosity effects, since no perceptible change in this property can be expected without the denaturation of the protein—a condition which was uniformly maintained throughout these investigations.

The decrease in the $i_d/(i_d)_0$ values at pH 9.4 as determined experimentally and illustrated in Figs. 1 and 2 (for sets (i) and (ii)) provides enough information regarding the binding of Cu^{2+} with transfusion gelatin. From TANFORD'S equation

$$\frac{i_d}{(i_d)_0} = \frac{C + kC_b}{C_0}$$

where C and C_b are the concentrations of free and bound copper, C_0, its total concentration and k a constant which can be evaluated from the limiting value of i_d (k for sets (i) and (ii) being 0.40, see Figs. 1 and 2), the amount of bound copper can be found. Taking the molecular weight of transfusion gelatin to be 75,000, the amount

of metal bound (V_M) per mole of the protein could be determined. The results are summarised in Tables I A and I B. From these, the value of V_M is seen to be approximately eight at pH 9.4.

Polarographic measurements carried out at different pH's (Fig. 3) show that the value of V_M ranges between 7.8–9.3 for the pH range 8.9–11, while at the lower pH range (2.65–5.1), V_M is approximately four. These results are significant since they show that the amino groups of transfusion gelatin bind copper ions more strongly the carboxyl groups.

The formation constant for the complex formed between Cu^{2+} and amino groups of the protein could be determined by using the simple equation of SCATCHARD[11].

$$K = \frac{V_M}{(n - V_{H^+} - V_M)C}$$

where V_{H^+} and V_M are the active sites covered by hydrogen ions and metal ions respectively, and n is the total number of such sites in the protein molecule. K is the formation constant. Inserting the values of n, V_M, C and V_{H^+} (as determined by separate experiments on the hydrogen ion equilibria of transfusion gelatin) the value of log K at pH 9.4 is found to be 3.91, whereas the value log K for carboxyl groups is small (*viz.* 2.1) showing weak interaction between Cu^{2+} and the carboxyl groups of the protein. This work is being continued.

ACKNOWLEDGEMENTS

Thanks are due to Dr. A.R. KIDWAI for providing facilities and for his keen interest during the progress of this work and also to the C.S.I.R., Government of India, for the award of a fellowship to one of us (S). We also wish to express thanks to Dr. JAGGANATHAN, Assistant Director, Biochemistry Division, National Chemical Laboratories, Poona (India), for the supply of transfusion gelatin.

SUMMARY

The influence of the protein concentration, metal ion concentration and pH on the $i_d/(i_d)_0$ values was studied by carrying out polarographic measurements in mixtures of cupric sulphate and transfusion gelatin. It was found that a decrease in the value took place with increase in protein concentration and pH, while the same behaviour was observed with decreasing concentration of Cu^{2+}. The latter effect has been attributed to the binding of Cu^{2+} with transfusion gelatin. Evaluation of log K showed that the copper is more strongly bound to the amino than to the carboxyl group.

REFERENCES

1 J. K. TAYLOR AND R. E. SMITH, *Anal. Chem.*, 22 (1950) 495.
2 I. M. KOLTHOFF AND J. J. LINGANE, *Polarography*, Interscience Publishers Inc., New York, N.Y., 1952, p. 397.
3 K. WIESNER, *Collection Czechoslov. Chem. Communs.*, 12 (1947) 594.
4 C. TANFORD, *J. Am. Chem. Soc.*, 73 (1951) 2066.
5 C. TANFORD, *ibid.*, 74 (1952) 211.
6 C. TANFORD, *ibid.*, 74 (1952) 6036.
7 S. L. KALRA, G. SINGH AND M. RAM, *Indian J. Med. Research*, 46 (1958) 171.
8 C. TANFORD AND J. EPSTEIN, *Anal. Chem.*, 23 (1951) 802.
9 J. TOMES, *Collection Czechoslov. Chem. Communs.*, 9 (1937) 12.
10 I. M. KOLTHOFF AND J. J. LINGANE, *Polarography*, Interscience Publishers Inc., New York, N.Y., 1952, p. 214.
11 G. SCATCHARD, *Ann. N.Y. Acad. Sci.*, 51 (1949) 660.

OPERATIONAL AMPLIFIER CIRCUITS FOR CONTROLLED POTENTIAL CYCLIC VOLTAMMETRY. II

JOHN R. ALDEN,* JAMES Q. CHAMBERS AND RALPH N. ADAMS

Department of Chemistry, University of Kansas, Lawrence, Kan. (U.S.A.)

(Received May 22nd, 1962)

We wish to describe as briefly as is possible several practical, inexpensive, operational amplifier (OA) circuits that are particularly useful in single sweep and cyclic voltammetry at stationary electrodes. Specific adaptations of OA's to electroanalytical instrumentation were made some time ago by BOOMAN and coworkers[1] and DEFORD[2] among others. Highly finished polarographic instruments have been designed by KELLY and coworkers[3,4]. No claim is made for originality of circuit design in the instruments described herein. They are functional, devoid of multipurpose appendages, and specifically oriented towards solid electrode applications. Their reliability has been proven by continuous operation for several years in a variety of modern electroanalytical operations. The units function satisfactorily with aqueous or non-aqueous electrochemical systems.

The instruments consist of the basic OA potentiostat coupled with a cyclic voltage scanning input. Two forms of cyclic scanner are described, a mechanical or motor driven unit, and an OA integrator network which is more versatile. We are convinced of the utility of cyclic voltammetry and, since any cyclic unit can be used for single sweep operation, we see no purpose in building single sweep polarographs as such.

A. OPERATIONAL AMPLIFIER POTENTIOSTAT AND POWER SUPPLY

Figure 1 shows the heart of the instrument, the potentiostat. The "E Amplifier" maintains the desired potential between the reference (*Ref.*) and controlled (*Cont.*) electrodes. The "I Amplifier" maintains the controlled electrode at amplifier ground potential while providing an output voltage proportional to the current. The recorder output signal (current measurement) is designed for either 5 or 10 mV span recorders. The voltage between the yellow and green scanning potential jacks is the same polarity and magnitude as the voltage applied between the controlled electrode (green binding post) and reference electrode (yellow binding post).

The potentiostat can be used with fixed input voltage for recording current–time curves at constant potential in linear diffusion studies. Alternately, by connecting a resistor between *Cont.* and *Ref.*, a constant current becomes available between *Ref.* and the auxiliary electrode (*Aux*); *i.e.*, chronopotentiometry can be carried out.

* Electronics Associate, Department of Chemistry.

For these cases where the input voltage is constant, we have found it desirable to stabilize the E amplifier with the K2-PA unit (it is desirable to have the I amplifier stabilized with its K2-P unit at all times).

When, however, the potentiostat is coupled with the scanning unit to carry out controlled potential voltammetry, the K2-PA in the E amplifier should be replaced

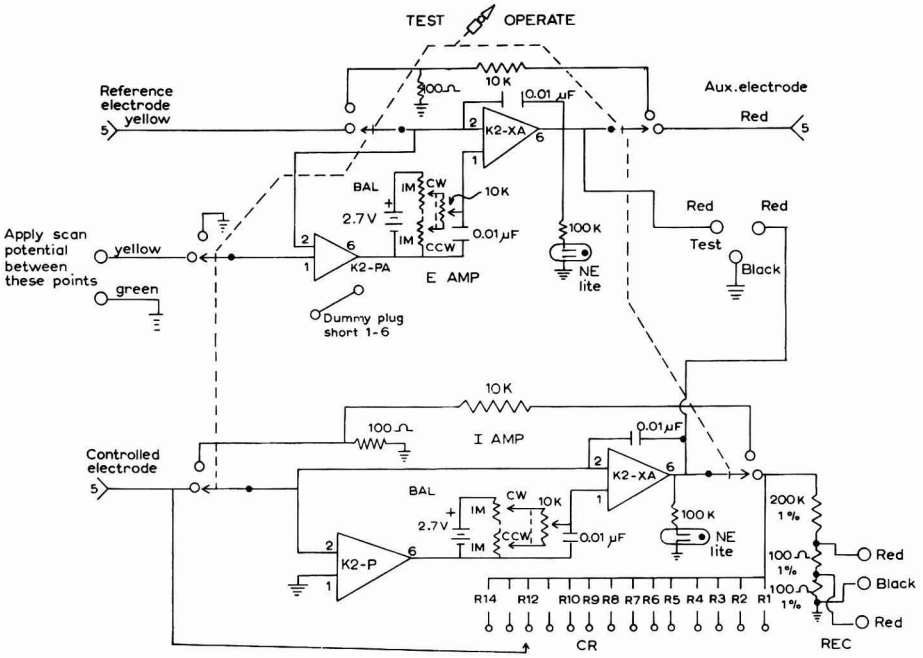

Fig. 1. Operational amplifier potentiostat: BAL, amplifier balance adjusts, coarse 1 M, fine 10 K; TEST, test jacks for amplifier balancing; CR, current range switch with following 1% precision resistors and corresponding full scale current ranges: R1, 10 M, 1 μA; R 2, 5 M, 2 μA; R 3, 2 M, 5 μA; R 4, 1.428 M, 7 μA; R 5, 1.0 M, 10 μA; R 6, 667 K, 15 μA; R 7, 500 K, 20 μA; R 8, 333 K, 30 μA; R 9, 200 K, 50 μA; R 10, 133 K, 75 μA; R 11, 100 K, 100 μA; R 12, 50 K, 200 μA; R 13, 20 K, 500 μA; R 14, 10 K, 1 mA; E AMP, voltage amplifier, Philbrick K2-XA, optional K2-PA and associated balance network; I AMP, current amplifier, K2-XA, K-2P and associated balance network; REC, recorder output for 5 or 10 mV recorders; 5 ⋋, 5-way binding posts; O, banana jacks.

by the dummy plug which shorts pins 1 and 6 of the K2-PA socket. With the K2-PA removed, the input impedance from whatever type scanning unit is used may be quite large (50–100 kΩ) and the sweep frequency can also be quite high. If the K2-PA is not removed, the source impedance from the scanner must be less than about 500 Ω to avoid introducing 60 cycle ripple caused by the chopper stabilizer. While there are many other ways to circumvent this problem, the simple removal of the K2-PA for scanning operations has been found quite satisfactory. (Clearly if one plans to do only potential sweep operations, the K2-PA is unnecessary and could be left completely out of the circuit.) The errors in unstabilized operation should be less than 2–3 mV for the normal time intervals used in scanning.

In the test position, the amplifiers are balanced by adjusting the individual balance pots to approximate zero voltage at the test jack positions. In the test position,

the amplifiers are connected with a gain of 100, so an ordinary multimeter can be used for balancing.

An excellent discussion of OAP's is contained in the new instrumentation text by BAIR[5].

The power supply for the potentiostat (which also powers the triangular wave generator of Fig. 4) can be a Philbrick R-100 B, which will power at least 3 potentiostats or similar devices. Alternately, one can build a power supply similar to the Philbrick R-100 A, which is no longer commercially available.

B. CYCLIC SCANNING UNIT

The utility of cyclic voltammetry using pen and ink recording with sweep rates of *ca.* 0.2–10 V/min for investigating complex organic electrode reactions at solid electrodes has been discussed[6]. The cyclic scanning voltage is a relatively slowly varying isosceles triangle which can be conveniently generated either by motor driven slide wires or electronic integrator networks.

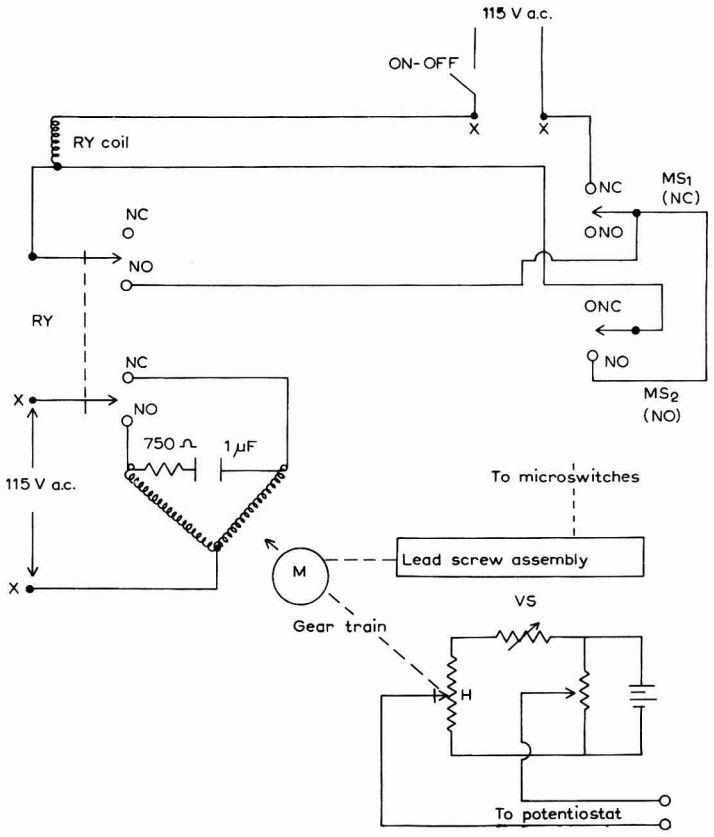

Fig. 2. Electromechanical triangular wave generator: M, reversible, synchronous motor, typical, Bristol 830-8D, 115 V, 60 cycles, 10 rev./min, 8 watt; RY, relay, typical, Guardian Electric G 57400, 115 V, 60 cycles, DPDT; MS_1 and MS_2, microswitches, typical 2HBT-1; Gear train, coupling to scanning helipot, hand adjustable for sweep rates; VS, voltage sweep unit, arranged as desired; H, 10 turn, 0.1% linearity helipot or equivalent.

1. Electromechanical triangular wave generator

Figure 2 shows the electrical connections of the motor driven unit. The synchronous motor drives a 10-turn helipot which provides the sweep voltage. The motor is coupled through variable gear ratios (hand adjustment) to a lead screw assembly (Servomechanisms, Inc.) which then engages micro switches at both ends of its travel. The micro switches and latching relay provide the motor reversing action. The micro switches are adjustable for varying the sweep width (voltage range). Figure 3 is a diagram of the mechanical layout of the scanner. Surprisingly little lag

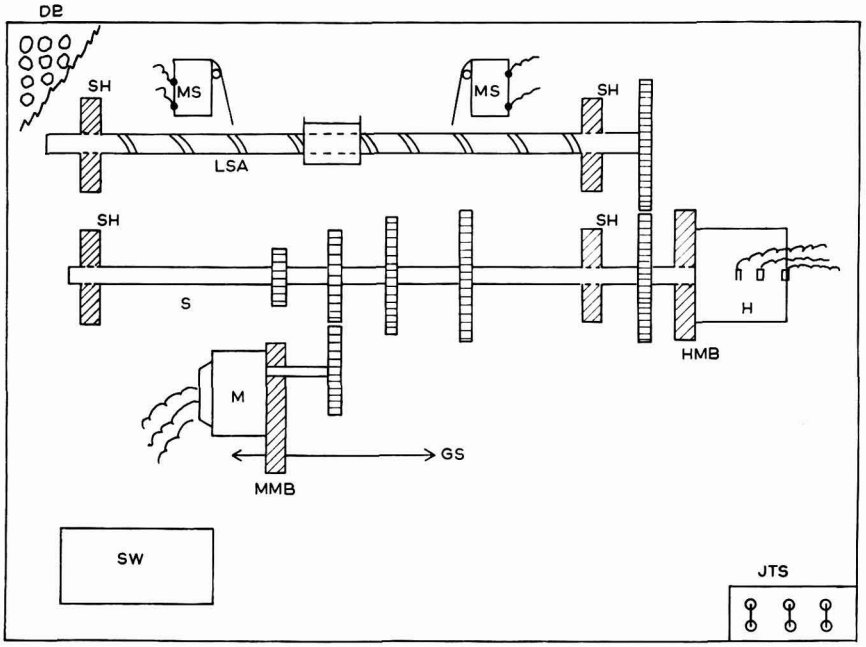

Fig. 3. Mechanical layout of motor driven triangular wave scanner: DB, drilled board, typical "Servoboard", Servo Corp. of America (masonite Pegboard having 3/16 in. holes on 1/2 in. centers, available from Country Workshop, Newark, N. J., can be used and all adjustable shaft hangers, etc, fit this Pegboard well); SH, shaft hangers; MS, micro switches, adjustable positions; H, helipot; HMB, helipot mounting block; M, motor; MMB, motor mounting block; GS, gear shift, MMB adjusted manually along gear train; LSA, lead screw assembly, typical 0.5 in. travel per rev. (Servomechanisms, Inc.); S, 1/4 in. diam. stainless steel shaft; JTS, Jones terminal strip; All gears were common brass spur gears (Boston Gear, Co.); All batteries, wiring, etc. not shown is below DB or on dial plates at the side.

exists in the reversal and the unit functions very well for moderate sweep rates. Sweep rates are very simply adjusted by the total span voltage applied to the helipot with intermediate adjustments via the gear couplings. Sweep rates between 0.2 V and 9 V/min have been used successfully. Undoubtedly many other electromechanical triangular wave scanning devices can be designed.

2. OA integrator triangular wave generator

The integrator network is more versatile, providing span width, sweep rate ad-

justment, etc., by mere dial changes. Figure 4 details the circuit. The scanner is coupled to the potentiostat via the yellow and green output terminals indicated in the upper right corner of Fig. 4. Sweep rates up to *ca.* 15 V/min are available. The various panel adjustments are indicated in the legend of Fig. 4. The push button controls initiate scan and allow manual reversal when desired. In adjusting the 100 K helipots for scan limits, the "+ limit" (cathodic limit) should not be allowed to become negative with respect to the "— limit" setting.

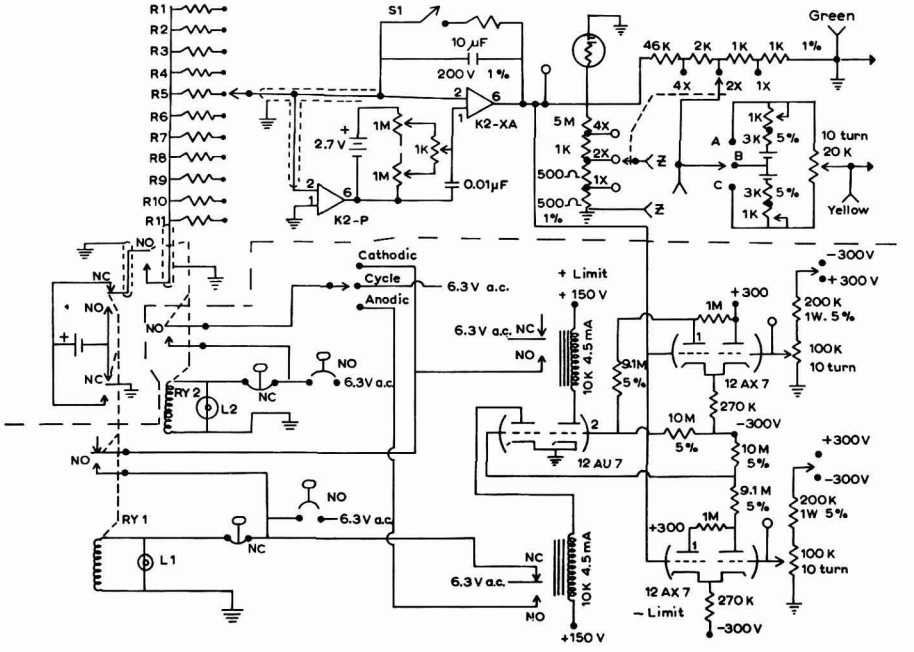

Fig. 4. OA Triangular wave generator: S1, SPST toggle switch; operate to initiate sweep after starting conditions are preset on relays RY1 and RY2, etc.; RY1 and RY2, 6.3 V as 3PDT relays; RY1 for direction of sweep, when L1 on, sweep is cathodic going; RY2, sweep operating relay, when L2 is on, sweep is operative; R1–R11, sweep rate resistors, all 1%, 1 watt: R1, 804K; R2, 402K; R3, 268K; R4, 201K; R5, 161K; R6, 107K; R7, 80.6K; R8, 64.5K; R9, 54K; R10, 46K; R11, 40.33K; Z,Z, output to 5 mV recorder.

The + 150 V supply for the cycling relays is not shown on Fig. 4. This power supply is a single half-wave rectifier with capacitor filter (50 μF) using a Stancor PA 8421 power transformer or equivalent. A standard 150–500 mA silicon diode serves as the rectifier. Since this supply is completely non-critical it is not included in the circuit.

In the output bias circuit (voltage source for the 20 K, 10-turn potentiometer in the upper right of Fig. 4), a voltage of 1.000 V should be adjusted between points (A–B) and (B–C).

While there is no question that the all-electronic scanner has greater versatility, the breadboard style electromechanical device is more easily constructed and used by workers who are beginning to use the apparatus. Excellent results have been obtained with both scanning units.

C. RECORDING EQUIPMENT

X–Y recording is by far the most satisfactory means of recording cyclic polarograms. If conventional X–time or strip chart recording is used, one must fold the paper over to compare forward and reverse scans (while inconvenient, there is nothing inherently wrong with such a procedure). If only single sweep operation is used, then X–time recording is satisfactory. Nominal pen response of at least 1-sec should be available on the recorder. A variety of X–Y recorders are commercially available. The Moseley Model 3 (which also has an X–time provision) has proven very satisfactory.

ACKNOWLEDGEMENTS

This work was supported by the Atomic Energy Commission through contract AT(11-1)-686 and by the Air Force through Air Force Office of Scientific Research.

REFERENCES

1 G. L. BOOMAN, *Anal. Chem.*, 29 (1957) 221; 31 (1959) 10.
2 D. D. DEFORD, *Abstracts, 133rd* A.C.S. *Meeting, San Francisco, 1958.*
3 M. T. KELLY, H. C. JONES AND D. J. FISHER, *Anal. Chem.*, 31 (1959) 1475.
4 M. T. KELLY, D. J. FISHER AND H. C. JONES, *ibid.*, 32 (1960) 1262.
5 E. J. BAIR, *Introduction to Chemical Instrumentation*, McGraw-Hill Book Co., N.Y., 1962.
6 G. GALUS, H. Y. LEE AND R. N. ADAMS, *J. Electroanal. Chem.*, 5 (1963) 17.

A TIME-DELAY CIRCUIT FOR POLAROGRAPHY

U. H. NARAYANAN AND K. R. VENKATACHALAM

Central Electrochemical Research Institute, Karaikudi (India)

(Received May 7th, 1962)

In recent years, polarography has assumed great importance both in the field of analytical chemistry and in the study of electrode processes. Variations in the polarographic current during the life of the mercury drop are due to changes in polarisation as well as to changes in the area of the drop. Furthermore, the current is a composite value of both faradaic and charging currents. It would simplify the application of the theory if the current could be measured at a certain well-defined moment in the life of the drop, as this would help in obtaining a value for the almost pure faradaic current corresponding to a particular drop area.

An instrument has therefore been designed which will switch the polarographic current into the measuring device at a predetermined phase in the life of the mercury drop. Advantage is taken of the pulse produced by the detachment of the mercury drop to trigger the time-delay circuit[1]. It is also possible to obtain the trigger pulse by using a special cell in conjunction with photocells, at the time when the mercury detaches itself from the capillary[2]. The required time delay can be obtained by a number of methods. One of the methods employed is to cascade two monostable

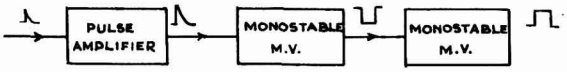

Fig. 1. Block diagram of the time-delay circuit.

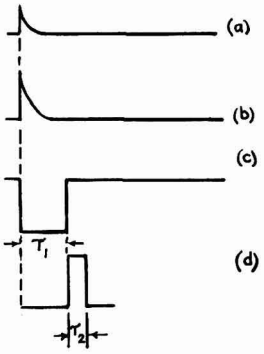

Fig. 2. Wave forms of the time-delay unit: (a), trigger pulse of the polarographic cell; (b), amplified trigger pulse; (c), output pulse from the first monostable multivibrator.

multivibrators (Fig. 1) triggered initially by an amplified pulse from the polarographic cell. The second multivibrator is triggered by the rising voltage of the first multivibrator. The pulse width, τ_1, of the first multivibrator gives the required time delay (with reference to the instant when the mercury detaches itself from the capillary) after which the polarographic current is switched to the measuring device for a time τ_2, *i.e.* the duration of the pulse width of the second multivibrator (Fig. 2).

Although the above method was tried successfully, there were certain inherent drawbacks, such as irreproducibility, in achieving precise, large time delays, presumably due to considerable imperfections in the components employed.

An instrument based on a Dekatron Scaler as the time-delay unit was developed and any predetermined delay could be obtained by employing an auxiliary stable audio-oscillator. A diagrammatic scheme of the apparatus is given in Fig. 3. Basic time reference is provided by the pulse produced when the mercury detaches itself from the capillary at time $t = t_0$. This pulse, after suitable amplification by the pulse amplifier (Fig. 4) triggers an Eccles–Jordon bistable multivibrator with the result that the previously conducting tube is cut off. The cut-off tube is made to conduct, thereby producing gate voltage at the plates of the tubes. The switching of the tube from one state to the other occurs very rapidly because of the regenerative feedback between the tubes. The gating voltage opens the first gate for the output of the audio-oscillator whose frequency determines the time delay required.

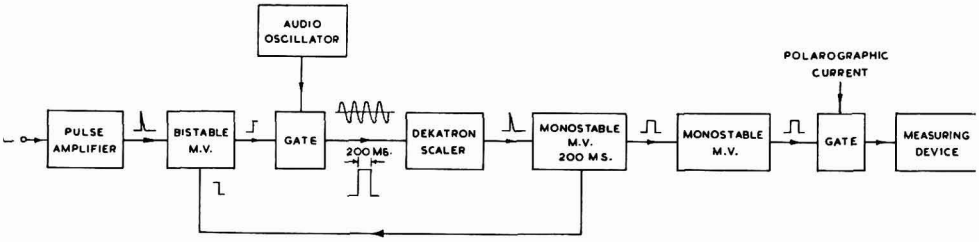

Fig. 3. Block diagram of the time-delay circuit.

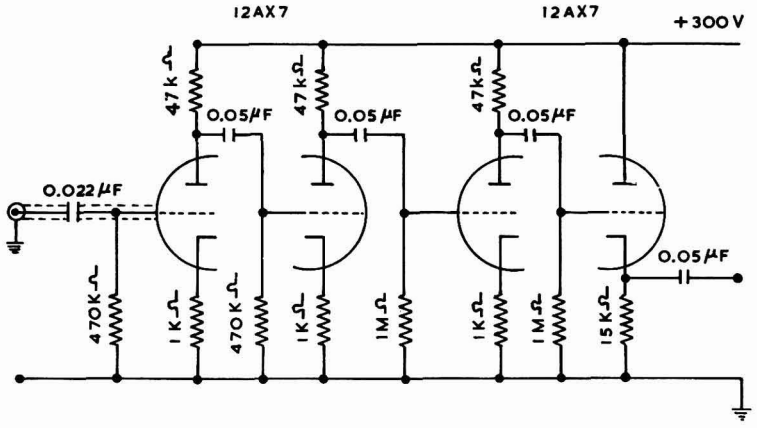

Fig. 4. Pulse amplifier.

The waves from the oscillator which pass through the time operated gate (Fig. 5) are counted by a series of decade counters using Dekatron tubes. The scaler used for the delay unit produces one pulse for every thousand waves received. If the time delay required is 3 sec, the frequency of the oscillator is set to 1000/3 = 333.3 c/sec. The precision of the instrument is limited only by the reliability, stability, and calibration

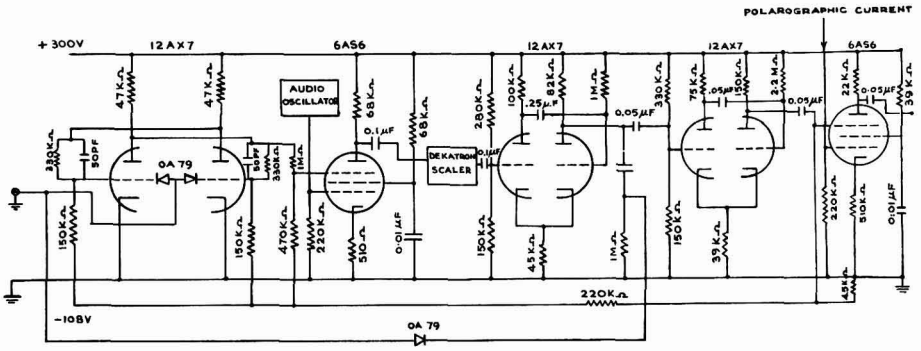

Fig. 5. Time-delay unit.

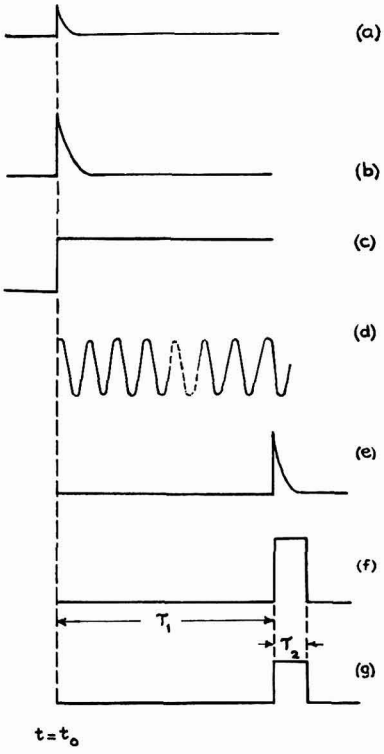

Fig. 6. Wave forms of the time-delay unit: (a), trigger pulse from the polarograph; (b), amplified trigger pulse; (c), gating pulse from the bistable multivibrator; (d), audio-oscillator output passing to the Dekatron scaler through the first gate; (e), trigger pulse to monostable multivibrator; (f), gating pulse to operate the second gate; (g), return pulse to close the first gate.

of the audio-oscillator used. The output pulse from the scaler, triggers a cathode-coupled, monostable multivibrator which produces a square pulse of a predetermined width (*i.e.* equal to the period during which the polarographic current is to be switched on to the measuring device through the second successive gate). The gating pulse is also fed back in order to restore the bistable multivibrator to the original state, thereby closing the first gate for the oscillator output to enter the scaler. The wave forms are indicated in Fig. 6.

ACKNOWLEDGEMENT

The authors are grateful to Professor K. S. G. Doss, Director, Central Electrochemical Research Institute, Karaikudi, for his kind interest in this work.

REFERENCES

1 G. C. Barker, and I. L. Jenkins, *Analyst*, 77 (1952) 685.
2 J. Glickstan, S. Rankowitz, C. Auerbach and H. L. Finston, *Advances in Polarography, (Proc. II. International Congress on Polarography, Cambridge, 1959)*, Vol. 1, Pergamon Press Ltd., London, 1960, p. 187.

Book Reviews

The Principles of Electrochemistry, by D. A. MAC INNES, Dover Publications, N.Y., 1961, 478 pages, $ 2.35.

The first edition of this book appeared in 1939. It has now been republished with only minor additions, so that the whole treatment is very old-fashioned and outmoded.

From the title, it is clear that this book is concerned mainly with the basic principles of electrochemistry, with the exception of four topics which cannot be considered to be basic principles *i.e.* pH, potentiometric titrations, the use of conductance for various physico-chemical investigations, and the passivity of metals. Other very important basic topics are, however, completely ignored, *e.g.* electro-chemical kinetics are not considered, and hydrogen overvoltage, the only kinetic topic treated, is only superficially dealt with. The material is treated in a rather disorganized way, *e.g.* conductance is dealt with in chapter 3, in connection with the classical theory of dissociation, and then again in chapter 18, after some theory and after galvanic cells, in connection with inter-ionic theory of electrolytes. Basic concepts of this electrical quantity are thus divided between two different, and separate, chapters.

The most autstanding defect of this book is the lack of modernity: Volta and Galvani potentials are not mentioned at all; the fact that the so called EMF is actually measured as a difference of potentials between two electrodes, and hence its sign depends on the order of the phases in a galvanic cell is also ignored, and other similar omissions could be given. Concepts essential for a sound understanding of electrochemistry could be ignored in 1939, but such is not the case in 1962. In addition, some errors were overlooked in the manuscript, *e.g.* de lack of distinction between a differential and finite quantity (see eqns. 10, 13 and 14, p. 103). The enumeration of defects could continue, but this is enough to give an idea of the general level of this book. It is the opinion of the reviewer that this book cannot be given to students to introduce them to electrochemistry. Also, it cannot be used as a reference source because all the references are twenty years old, or even more, and because nearly all the numerical material is old and superceeded.

GIULIO MILAZZO, Istituto Superiore di Sanità, Rome

Inorganic Chemistry of Qualitative Analysis, by A. F. CLIFFORD, Prentice-Hall, Inc., Englewood Cliffs, N.J., 1961, xvii + 515 pages, 68 figs., 102 tables, $ 6.95.

It is difficult to offer a better description of the present state of qualitative analysis than that given by Clifford: "It has long been recognized by instructors of undergraduate chemistry that there is little need to teach qualitative analysis for its own sake. Actual analyses are very seldom, carried out in this manner any longer. It is nevertheless true that the classical analytical scheme is one of the best vehicles ever devised for teaching the systematics of inorganic chemistry". His present work is an excellent treatise, dealing with a possible system which could be evolved for qualitative analysis as a didactical possibility for the consolidation of the terms of inorganic chemistry proper. One of the many advantages offered by his book is that it also includes a practical part summarizing the teaching experiences of the author.

In the introductory chapters, the structure of matter, some important terms such as ionic radius, atomic distance, intramolecular electron distribution, dipole moment, electronegativity, solubility, equilibrium reactions occurring in solutions, reaction rate, heterogeneous equilibria, solubility function, various factors affecting solubility, etc. are explained to the reader. At the same time, the correctness of the terms explained is supported by a great number of experimental data. The fundamental explanations are followed by descriptions of the investigations of flame colours, and practical qualitative analysis of alkali and alkaline earth metals.

Qualitative analysis of class 1(a) of the Fresenius system is introduced by a study of halides and oxides insoluble in acids. In the part dealing with sulphides insoluble in acids (insolubility in weak acids and bases is also considered), the method of separating the elements of classes (b) and 2 of the Fresenius system by thioacetamide is presented. Subsequently, an entire chapter

is devoted to polybasic acids and bases, and the application of their equilibrium conditions in calculations is described very clearly. A chapter summarizing insoluble hydroxides and sulphides insoluble in alkalies follows. However, before discussing practical procedures, the author deals in detail with hydrolysis, and with its quantitative aspects.

The chapters on simultaneous equilibria and amphotery are excellent. A complete system of detection of metal ions is presented in connection with amphotery proper.

The structure of molecules (including that of complex compounds) is treated by the author in a most meritable way. However, this is the sole chapter in CLIFFORD's book where one has the feeling that perhaps a more detailed text would be necessary. Since the author emphasizes in his foreword that the book represents only part of a system of education, the above-mentioned deficiency is only valid for some methods of teaching theoretical chemistry.

With elements having negative oxidation states, redox equilibria are treated. In this connection, reactions suitable for detecting various anions are described.

After presenting the fundamental terms of electrochemistry, oxidation states of the elements are investigated, and then the qualitative analysis of platinum metals is discussed.

A separate chapter is devoted by CLIFFORD to studies of reaction kinetics. Important fundamental terms are discussed well, and both the simple and more complicated kinetics are illustrated by some excellently chosen examples. The overpotentials of hydrogen and oxygen are also treated here.

The last chapter of the book points out a few anomalies occurring in the periodic system which can be easily interpreted.

The 14 chapters in the appendix consist of some tables and a few calculated examples.

As an educational aid, the book by CLIFFORD is a masterpiece of its kind. The value of the book lies in the fact that it is written in an excellent style, and guides the reader through the fundamental terms of chemistry. It is particularly useful for university students because summarizing questions are included at the end of each chapter, which enable the reader to repeat the contents of the chapter concerned easily.

E. PUNGOR, The University, Budapest

J. Electroanal. Chem., 5 (1963) 162–163

Chromatographische Methoden in der analytischen und präparativen anorganischen Chemie, (unter besonderer Berücksichtigung der Ionenauscher, Die Chemische Analyse, Vol. 46, by Priv. Doz. Dr. E. BLASIUS, Ferdinand Enke Verlag, Stuttgart, 1958, xx + 370 pages, 139 illustrations and 40 tables, D.M. 99.

This book deals with inorganic chromatography in all its aspects, including the theoretical physical chemistry of the processes involved. A long chapter is devoted to equilibrium processes, ion exchange equilibria etc., and another to a thorough discussion of the theories of chromatographic elution. The mechanism of adsorption and the ion–solvent–adsorbent interactions are also dealt with in detail. Adsorption, ion exchange and partition methods are treated separately, with a wealth of information concerning the techniques and materials used. Separations are usually listed in well organised tables. Electrophoretic methods in porous media and ion exchange membranes are discussed in the last two chapters.

This volume is by far the most complete reference book in the German language, and it will retain its usefulness for many years to come.

M. LEDERER, Consiglio Nazionale Delle Ricerche, Rome

J. Electroanal. Chem., 5 (1963) 163

Infrared Methods, Principles and Applications, by G. K. T. CONN AND D. G. AVERY, Academic Press Inc., N.Y., 1960, viii + 203 pages, $ 6.50.

This book is intended to cover experimental methods and techniques used in infrared spectroscopy. Although the subject has been developing continuously for more than sixty years, this is the first book giving a comprehensive and compact treatment of technical aspects of infrared spectroscopy.

J. Electroanal. Chem., 5 (1963) 163–164

The first section of this book is divided into five chapters, each of which is concerned with a single part of a spectrograph. Chapter I gives a survey of the sources of infrared radiation, with particular emphasis on the near infrared region. The performances and limitations of the most popular sources, *e.g.* Nernst Glower and Globar Road are illustrated in detail. Chapter II is an exhaustive description of optical components *i.e.* prisms, windows, cells, filters etc. Although little space is devoted to special devices, such as low or high temperature cells or beam polarizers, sufficient references are given to original papers. Chapter III gives a detailed summary of the various types of detectors, and their principles of operation, design and sensitivity. Chapter IV deals with electronic amplifiers, and describes some useful types adaptable to different detectors. Finally, chapter V illustrates the basic principles and practical design of dispersive systems and gives an extremely useful discussion of optical factors affecting the performance of spectrographs.

The second section is divided into four chapters dealing with practical applications of the principles discussed in the first section. Thus, chapter VI describes practical calibration of detectors, chapter VII describes a simple monochromator. Chapter VIII gives a survey of instruments for gas analysis and plant control, and chapter IX covers the basic principles of radiation pyrometry.

Useful tables of radiant power and photon densities emitted by black bodies at various temperatures, and of refractive indices of prism materials at different wavelengths, are included.

Probably the only criticism that can be made of the book is the little attention paid to commercial instruments. Such instruments are so widely used, and play such an important role in molecular spectroscopy, that a detailed analysis of their relative performances by such experts as Drs. CONN AND AVERY would have been of great help to practical spectroscopists.

The authors were able not only to assemble much technical information in a relatively limited space, but also to amalgamate the contents by continuous critical discussion. In this respect the chapter on dispersive systems is unique in the literature.

Thus, anyone who encounters technical problems in infrared spectroscopy in his research will find this book of the greatest value.

S. CALIFANO

J. Electroanal. Chem., 5 (1963) 163–164

A Textbook of Quantitative Inorganic Analysis, Including Elementary Instrumental Analysis, 3rd edn., by A. J. VOGEL, Longmans, Green & Co., Ltd., London, 1961, xxx + 1216 pages, £3 10s.

This edition of VOGEL's well-known book is the 17th impression of a text first published in 1939. Since then it has been revised twice, to cope with new analytical methods. This well-established text book has maintained its wide-spread use by generations of students.

This third edition has been enlarged by some chapters devoted to instrumental analysis although this term can sometimes be misleading. In fact, every analysis, including those made by classical methods, is "instrumental", because all use some indicating apparatus, *e.g.*, gravimetric analysis uses the balance, and volumetric analysis uses the burette. A preferable term might be "physico-chemical" analysis.

The completely new chapters describe complexometric and coulometric titration, ion exchange and chromatographic methods, fluorimetric, nephelometric and turbidimetric analysis, emission spectrography and flame photometry, solvent extraction, and high frequency titrations. Besides these new techniques, the treatment of gravimetric and volumetric analysis has been much improved, and the same can be said for the physico-chemical methods already treated in the preceding edition. This book is an excellent laboratory guide for students beginning quantitative analysis, particularly because the apparatus and methods are described in sufficient detail. Perhaps the theory could be extended in a future edition, without unduly increasing the size of the book, while maintaining its high standard. To give two examples: (1), the theoretical basis of fixed and homologous pairs, which is fundamental for understanding spectrographic analysis, is hardly mentioned; (2), theoretical inter-dependence of the electrical quantities that can be used in high frequency titrations, and the shape of the analytical diagrams, are not mentioned. Similar remarks could be made for other methods, but, in spite of these criticisms, this book is worth while for many analysts, particularly because of the abundance of practical detail, and the instructions for "do-it-yourself" devices.

G. MILAZZO, Istituto Superiore di Sanità, Rome

CONTENTS

Original papers

ELSEVIER PUBLISHING COMPANY, AMSTERDAM

Printed in The Netherlands by

NEDERLANDSE BOEKDRUK INRICHTING N.V., 'S-HERTOGENBOSCH